

Award Number:
W81XWH-08-1-0232

Á
TITLE:
Modulation of Beta-catenin activity with PKD1 in Prostate Cancer

Á
PRINCIPAL INVESTIGATOR:
Meena Jaggi, PhD

Á
CONTRACTING ORGANIZATION:
Sanford Research
Sioux Falls, SD 57105

REPORT DATE: N*ã↔→ÁGCF€

TYPE OF REPORT:
Annual

PREPARED FOR: U.S. Army Medical Research and Materiel Command
Fort Detrick, Maryland 21702-5012

DISTRIBUTION STATEMENT:

x Approved for public release; distribution unlimited

The views, opinions and/or findings contained in this report are those of the author(s) and should not be construed as an official Department of the Army position, policy or decision unless so designated by other documentation.

REPORT DOCUMENTATION PAGE			<i>Form Approved</i> OMB No. 0704-0188		
Public reporting burden for this collection of information is estimated to average 1 hour per response, including the time for reviewing instructions, searching existing data sources, gathering and maintaining the data needed, and completing and reviewing this collection of information. Send comments regarding this burden estimate or any other aspect of this collection of information, including suggestions for reducing this burden to Department of Defense, Washington Headquarters Services, Directorate for Information Operations and Reports (0704-0188), 1215 Jefferson Davis Highway, Suite 1204, Arlington, VA 22202-4302. Respondents should be aware that notwithstanding any other provision of law, no person shall be subject to any penalty for failing to comply with a collection of information if it does not display a currently valid OMB control number. PLEASE DO NOT RETURN YOUR FORM TO THE ABOVE ADDRESS.					
1. REPORT DATE (DD-MM-YYYY) 30-04-2010		2. REPORT TYPE Annual		3. DATES COVERED (From - To) 4/01/2009 - 3/31/2010	
4. TITLE AND SUBTITLE Modulation of Beta-catenin activity with PKD1 in Prostate Cancer			5a. CONTRACT NUMBER W81XWH-08-1-0232		
			5b. GRANT NUMBER		
			5c. PROGRAM ELEMENT NUMBER		
6. AUTHOR(S) Jaggi, Meena Chauhan, Subhash C. Go ckr"o ggpcQci i kB wuf Qf w			5d. PROJECT NUMBER		
			5e. TASK NUMBER		
			5f. WORK UNIT NUMBER		
7. PERFORMING ORGANIZATION NAME(S) AND ADDRESS(ES) Sanford Research 1100 E. 21 st Street, Suite 700 Sioux Falls, SD 57105			8. PERFORMING ORGANIZATION REPORT NUMBER		
9. SPONSORING / MONITORING AGENCY NAME(S) AND ADDRESS(ES) US Army Medical Research Acquisition Activity 820 Chandler Street Fort Detrick, MD 21702-5014			10. SPONSOR/MONITOR'S ACRONYM(S) USAMRAA		
			11. SPONSOR/MONITOR'S REPORT NUMBER(S)		
12. DISTRIBUTION / AVAILABILITY STATEMENT Approved for public release; distribution unlimited					
13. SUPPLEMENTARY NOTES					
14. ABSTRACT During the 2009-10 funding cycle we have made significant progress on our project. We have published six papers and seven abstracts. In addition to publications, we have obtained grants from the state (Governor's 2010 initiative), NIH (NCI RO1) and pharmaceutical industries (Merck Pharmaceuticals, Investigator Initiated Grant). In this study cycle, we attempted to isolate stable C4-2 cell lines transfected with PKD1 mutant constructs in order to identify the domains involved in interaction and modulation of β -catenin activity. While we had difficult time generating and isolating stably transfected cell lines, we used transiently transfected C4-2 cell lines to investigate the effect of PKD mutants on the various aspects of cellular functions including cell proliferation, colony formation and motility. The results from these experiments are presented below and provide promising results for further investigation. However, due to the low efficiency of transient transfection of C4-2 cells, we have decided to generate stably transfected C4-2 cell lines using retro-viral mediated transfection system to obtain reliable results. The retroviral system is a well established technique that yields much higher efficiency of generation of stable transfect compared to cationic-lipid mediated transfection. We, in collaboration with Dr. Chauhan, have also developed a xenograft mouse model system with the highly metastatic C4-2 cell lines. We have also discovered a new method of PKD1 activation by a dietary compound curcumin, results were presented at the AACR 2010 meeting. Our work related to curcumin pre-treatment strategy of cancer cells induces chemo/radiosensitivity in cancer cells has been published. Based on clinical implications of this novel strategy, this paper was selected for press release.					
15. SUBJECT TERMS None provided.					
16. SECURITY CLASSIFICATION OF:			17. LIMITATION OF ABSTRACT UU	18. NUMBER OF PAGES 139	19a. NAME OF RESPONSIBLE PERSON USAMRMC
a. REPORT U	b. ABSTRACT U	c. THIS PAGE U			19b. TELEPHONE NUMBER (include area code)

Table of Contents

	<u>Page</u>
Introduction.....	5
Body.....	7-15
Key Research Accomplishments.....	15-16
Reportable Outcomes.....	16
Conclusion.....	17
References.....	18
Appendices.....	18

INTRODUCTION:

Understanding the basic biology of prostate cancer will provide us with additional critical information necessary to improve existing treatments or to find newer treatments for patients suffering from prostate cancer. While several genetic alterations play specific functions in a cell, some of these genes can have multiple functions. One such gene encodes a protein called β -catenin, which plays a dual role in cancer cells by: a) playing a role in cellular adhesion via another protein called E-cadherin, and b) playing a role in causing cellular division through a set of proteins which cause cells to divide abnormally. In addition to these proteins which β -catenin is already known to associate with, we have discovered a new interaction with a protein called protein kinase D1 (PKD1) in prostate cancer cells. Unraveling this complex interaction of β -catenin with PKD1 in prostate cancer cells may hold the key to understanding the role of a single important protein in causing unregulated cellular division and loss of cellular adhesion – the two fundamental hallmarks of a cancer cell. We have previously made two important discoveries in this field: a) PKD1 levels are lower in advanced prostate cancer which are associated with more aggressive types of cancer, and b) PKD1 interacts with another important protein in cancer cells, β -catenin. These preliminary discoveries in prostate cancer have led us to put forth the current proposal. Our major objective in this proposal is to understand the consequences of binding of PKD1 to β -catenin in tumor development and to study the exact alteration of these proteins in human prostate cancer tissues.

Understanding the details of how cancer causing proteins communicate with each other in a cell will help us intervene in the disease process more effectively. To this end, we propose to study the effect of β -catenin and PKD1 interaction on the cancer cell. We plan to achieve these goals by increasing PKD1 activity in the cell by use of a drug called Bryostatin1, which has already been used in clinical trials in various types of cancers. During 2008-09 funding period we made considerable progress on our grant proposal and published one paper in *Molecular Cancer Therapeutics*. Our research findings were considered for highlight and appeared on cover page (cover illustration, MCT September 2008, volume 7). In brief, we investigated the effect of bryostatin on PKD1 expression, β -catenin transcription, cell proliferation, and cellular aggregation. In this study we examined the effect of Bryostatin 1 treatment on PKD1 activation, β -catenin translocation and transcription activity and malignant phenotype of prostate cancer cells. Activation of PKD1 with Bryostatin 1 leads to colocalization of the cytoplasmic pool of β -catenin with PKD1, trans-Golgi network markers and proteins involved in vesicular trafficking. Activation of PKD1 by Bryostatin 1 decreases nuclear β -catenin expression and β -catenin/TCF transcription activity. Activation of PKD1 alters cellular aggregation and proliferation in prostate cancer cells associated with subcellular redistribution of E-cadherin and β -catenin. For the first time, we have identified Bryostatin 1 modulates β -catenin signaling through PKD1, which identifies a novel mechanism to improve efficacy of Bryostatin 1 in clinical setting.

During the 2009-10 funding cycle we have made significant progress on our project. We have published six papers and seven abstracts. In addition to publications, we have obtained grants from the state (Governor's 2010 initiative), NIH (NCI RO1) and pharmaceutical industries (Merck Pharmaceuticals, Investigator Initiated Grant). In this study cycle, we attempted to isolate stable C4-2 cell lines transfected with PKD1 mutant constructs in order to identify the domains involved in interaction and modulation of β -catenin activity. While we had difficult time generating and isolating stably transfected cell lines, we used transiently transfected C4-2 cell lines to investigate the effect of PKD mutants on the various aspects of cellular functions

including cell proliferation, colony formation and motility. The results from these experiments are presented below and provide promising results for further investigation. However, due to the low efficiency of transient transfection of C4-2 cells, we have decided to generate stably transfected C4-2 cell lines using retro-viral mediated transfection system to obtain reliable results. The retroviral system is a well established technique that yields much higher efficiency of generation of stable transfect compared to cationic-lipid mediated transfection. We, in collaboration with Dr. Chauhan, have also developed a xenograft mouse model system with the highly metastatic C4-2 cell lines. Our results are very encouraging and we have been able to generate highly vascularized tumors in nude mice. In addition, we have investigated the effects of PKD1 overexpression on gene transcription using PCR microarray techniques. We have also discovered a new method of PKD1 activation by a dietary compound curcumin, results were presented at the AACR 2010 meeting. Our work related to curcumin pre-treatment strategy of cancer cells induces chemo/radiosensitivity in cancer cells has been published. Based on clinical implications of this novel strategy, this paper was selected for press release.

Body:

Aim 1: Molecular Nature of PKD1 and β -catenin Interaction

To determine domain of PKD1 that are required for interaction with β -catenin:

We tried to generate stable clones of C4-2 cells with green fluorescent protein (GFP) fused PKD1 constructs in order to study the physiological significance of PKD1 in prostate cancer. We tried to isolate multiple colonies using standard techniques. However, repeated efforts at isolating colonies failed, since the colonies died very soon in isolation. We attempted transfection using multiple cationic reagents like Lipofectamine, Lipofectamine 2000, FuGENE HD, PolyFect and Effectene to raise stable transfection with little success.. Table 1 shows comparison between transfection efficiency of Lipofectamine 2000 and FuGENE HD. Among these various transfection reagents, we found FuGENE HD to produce maximal transfection efficiency Hence we used transient transfection of C4-2 cells with GFP fused PKD1 constructs with FuGENE HD to characterize effect on prostate cancer.

Generation of PKD1 mutant constructs and C4-2 cell lines expressing PKD-GFP construct:

The DNA constructs (2 μ g) of PKD1 mutants tagged with GFP and cloned in

DNA	FuGENE		Lipofectamine 2000	
	2 μ g	4 μ g	2 μ g	4 μ g
GFP	70.6	24.2	15.9	10.7
Δ AP	9.8	14.3	2.3	2.2
Δ C1a	12.3	10.3	3.2	1.4
Δ C1b	17.9	11.1	1.8	1.5
Δ CRD	11.4	1.8	0.0	2.4
Δ KD	28.3	3.8	0.0	2.2
Δ N	6.5	0.0	0.0	0.0

Table 1. Efficiency of transient transfection of C4-2 with FuGENE or Lipofectamine 2000 using 2 and 4 μ g DNA.

ability and motility characteristics.

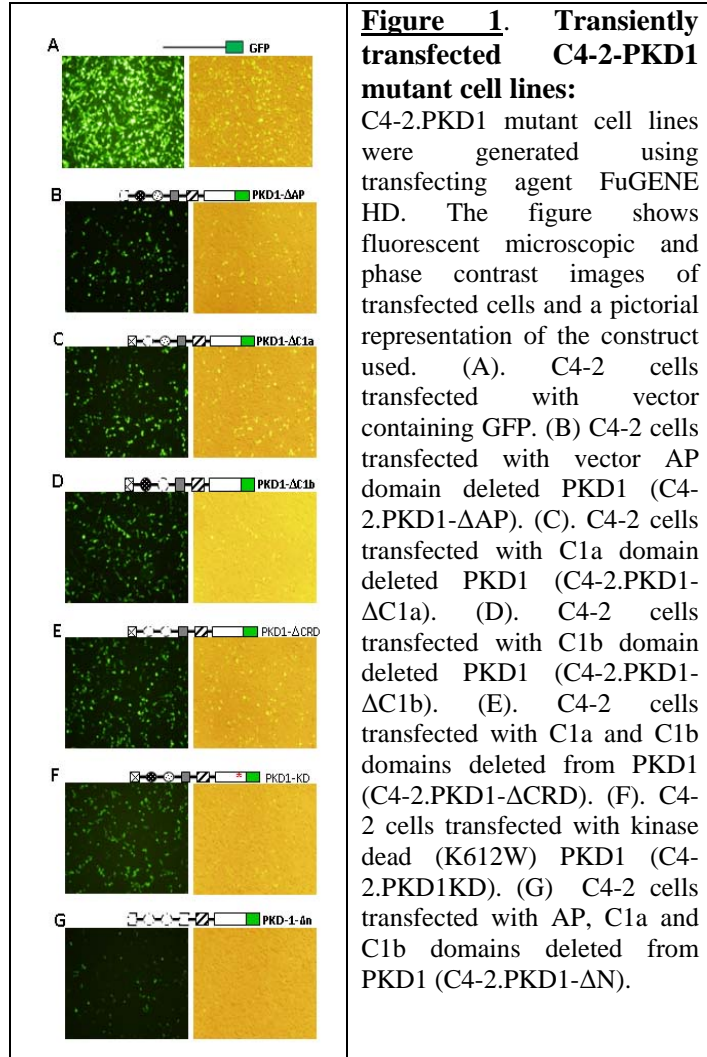


Figure 1. Transiently transfected C4-2-PKD1 mutant cell lines:

C4-2.PKD1 mutant cell lines were generated using transfecting agent FuGENE HD. The figure shows fluorescent microscopic and phase contrast images of transfected cells and a pictorial representation of the construct used. (A). C4-2 cells transfected with vector containing GFP. (B) C4-2 cells transfected with vector AP domain deleted PKD1 (C4-2.PKD1- Δ AP). (C). C4-2 cells transfected with C1a domain deleted PKD1 (C4-2.PKD1- Δ C1a). (D). C4-2 cells transfected with C1b domain deleted PKD1 (C4-2.PKD1- Δ C1b). (E). C4-2 cells transfected with C1a and C1b domains deleted from PKD1 (C4-2.PKD1- Δ CRD). (F). C4-2 cells transfected with kinase dead (K612W) PKD1 (C4-2.PKD1KD). (G) C4-2 cells transfected with AP, C1a and C1b domains deleted from PKD1 (C4-2.PKD1- Δ N).

pEGFP vector were obtained from our collaborator Dr. Angelika Hausser, University of Stuttgart, Germany. Transiently transfected C4-2 prostate cancer cell lines containing the mutant PKD constructs were generated by chemical transfection using FuGENE HD (Promega, USA). The cells were observed for GFP under a fluorescent microscope (Figure 1). After two days of incubation at 37°C/5%CO₂, the cells were trypsinized and used for further experiments. The transiently transfected C4-2 cell lines were checked for growth, colony formation

Effect of C4-2 cell lines expressing PKD1-GFP constructs on cell proliferation, colony formation and cell motility:

C4-2 cells transiently transfected with various PKD1-GFP mutant constructs were trypsinised, counted and plated for cell proliferation experiment. In brief, 20,000 cells were plated per well in a 6 well plate and incubated at 37°C/5%CO₂ for seven days (Figure 2). A single well was trypsinized each day and the total number of cells were counted. The doubling time was estimated using the formula $\text{Doubling time} = 0.693 (n)/\text{LN} (n_f/n_i)$, where n= number of hours, n_f= cell count at end point and n_i= cell count at initial time point. Despite the low transient transfection efficiency, the deletion of C1b domain from PKD1 results in a drastic increase in doubling time. The C1b domain of PKD1 is known to be involved in interaction with DAG and for plasma membrane recruitment of the protein following activation of the protein. The absence of this domain might indicate lack of recruitment and the following steps necessary for mediated cell signaling through PKD1 activation.

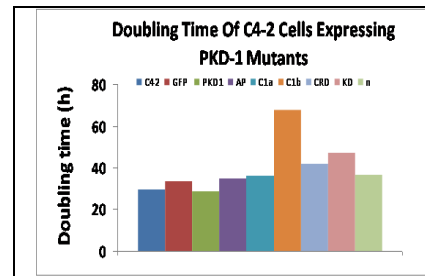


Figure 2. Effect of mutant PKD1 overexpression on C4-2 cell proliferation. Transiently transfected cells were plated at 20,000 cells per well in 6 well plates. The cells were counted for seven days by trypsinizing one well per day. The doubling time was calculated from the log phase of the cell growth.

Colony formation: The effect of C4-2 cells transiently transfected with various PKD1-GFP mutant constructs was assayed by plating 600 cells in a 60mm plate. The plates were incubated for 10 days at 37°C/5%CO₂. The colonies formed were fixed with methanol, stained with 0.05% crystal violet for 30 minutes and destained using water. The images of the plate were captured on Alpha imager and the software used for counting the colonies (Figure 3). Our results indicate an almost 25% decrease in colony formation of the C1b domain deleted PKD1, concurring with the proliferation data.

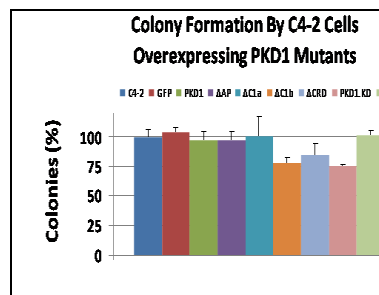


Figure 3. Effect of mutant PKD1 overexpression on colony formation ability of C4-2 cells. Transiently transfected cells were plated at 600 cells per plate in 60mm plates. After 10 days, the colonies were fixed, stained and counted. fixecounted for seven days by trypsinizing one well per day. The doubling time was calculated from the log phase of the cell growth.

Similar results were also seen with ΔCRD and PKD1. KD, the kinase dead mutant, indicating the importance of kinase activity and C1b domain for colony formation. All these experiments were performed in triplicates.

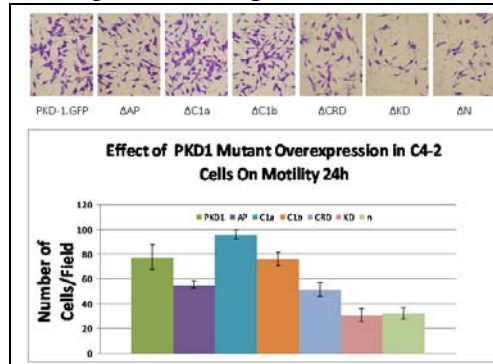


Figure 4. Effect of mutant PKD1 overexpression on cell motility. Boyden's chamber was used to probe the effect of mutant PKD1 expression on C4-2 cell's motility. The cells were plated in 1% FBS onto the chamber and a chemotactic gradient of 10% FBS was applied for 24h to facilitate cell motility. The cells were fixed, stained and images of ten radom area were captured and the number of cells were counted.

Cell Motility: The effect of PKD1-GFP mutant constructs on cell motility was assayed using Boyden's chamber. In short, 350,000 transiently transfected cells were loaded into the chamber in media containing 1% FBS. A chemotactic gradient of 10% FBS was applied to by incubating the chamber in a 6 well plate containing media+10% FBS. Following, incubation of the plates for

24h, the motile cells on the membrane were fixed in methanol for 5min, stained with crystal violet for 30min, the membrane dried and mounted onto pre-labeled slides. Ten independent images were taken and the motile cells that migrated across the membrane were counted. Our results indicate major difference in the migratory behavior of ΔN , ΔAP and PKD1.KD mutants, indicating the importance of these domains in cell motility (Figure 4). In the next cycle, we plan to generate stable transfects using retroviral system. Once the stable transfects are isolated, the interaction of PKD1-GFP mutant constructs with β -catenin will be analyzed by immunoprecipitation assays, using β -catenin and GFP specific antibodies as described previously. Additionally, the effect of the different constructs on β -catenin transcription will be analyzed.

Aim 2: To Demonstrate that Activation of PKD1 by Bryostatin 1 Influences the Cellular Phenotype in Prostate Cancer.

Time and dose dependent activation of PKD1 by Bryostatin 1

Treatment of the prostate cancer cells stably transfected with PKD1-GFP with increasing concentrations (10-30 nM) of Bryostatin 1 for 3 h demonstrated increased transphosphorylation of ser738 and ser742 and autophosphorylation of ser910 residues of PKD1 (Figure 5 A and B). The activation of PKD1 is phosphorylation-dependent, and serine738 and 742 residues in human PKD1 (corresponding to serine744 and 748 in mouse) have been identified as crucial phosphorylation sites. These serine residues are located in the activation loop of the PKD1 catalytic domain. The C-terminal serine916 residue has been identified as an

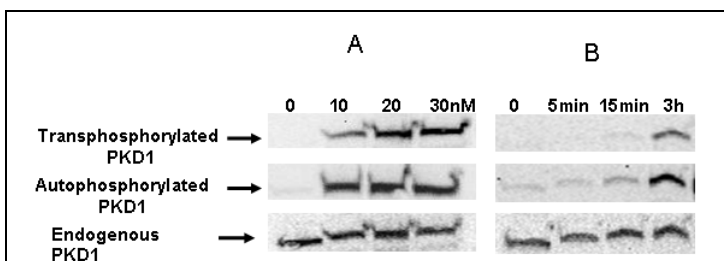


Figure 5: Time dependent phosphorylation of PKD1 in Bryostatin 1 treated cells, **A**, C4-2 cells stably transfected with GFP fused PKD1 (C4-2-PKD1-GFP) were treated with 0, 10, 20 and 30 nM Bryostatin 1. Cell extracts were immunoblotted with auto- and transphosphorylation site specific antibodies. Note optimum phosphorylation at 10 nM. **B**, C4-2 -PKD1-GFP cells were treated with 10 nM Bryostatin 1 for 0-3 h. Cell extracts were immunoblotted with auto- and transphosphorylation site specific antibodies. Note maximum phosphorylation at 3 h.

autophosphorylation site in PKD1 (1). Phosphorylation of these serine residues affects PKD1 activity and plays a role in modulation of PKD1 function *in vivo*. In order to exclude cell line specific effects we also confirmed that Bryostatin 1 activated and is associated with membrane translocation of PKD1 in androgen dependent LNCaP cells (data not shown).

autophosphorylation site in PKD1 (1). Phosphorylation of these serine residues affects PKD1 activity and plays a role in modulation of PKD1 function *in vivo*. In order to exclude cell line specific effects we also confirmed that Bryostatin 1 activated and is associated with membrane translocation of PKD1 in androgen dependent LNCaP cells (data not shown).

Effect of activation of PKD1 by Bryostatin 1 on E-cadherin and β -catenin subcellular localization

Subcellular localization of PKD1, E-cadherin and β -catenin in Bryostatin 1 activated C4-2-PKD1-GFP cells was analyzed by confocal microscopy. To examine PKD1 specific changes in subcellular localization of E-cadherin and β -catenin, we compared E-cadherin and β -catenin localization in Bryostatin 1 activated C4-2-GFP cells and C4-2-PKD1-GFP cells. In vector transfected C4-2 cells we did not detect any change in E-cadherin or β -catenin localization after Bryostatin 1 activation (Figure 6). Our immunofluorescence study clearly revealed perinuclear and membrane localization of PKD1-GFP upon activation by Bryostatin 1 (Figure 6). The most

striking observation was the colocalization of E-cadherin and β -catenin with PKD1-GFP in Bryostatin 1 activated C4-2-PKD1-GFP cells at perinuclear areas in addition to cell membranes (Figure 6, lane2, arrows). After 24 h of Bryostatin 1 treatment, strong membrane staining of E-cadherin/ β -catenin and some perinuclear staining was also noticed (Figure 6, lane3). While the C4-2-GFP cells do not over-express PKD1-GFP (Figure 6), they do not show perinuclear localization of E-cadherin/ β -catenin. This observation confirms that E-cadherin/ β -catenin subcellular distribution is specifically mediated by PKD1 activation and not by other kinases activated by Bryostatin 1.

Bryostatin treatment decreases β -catenin transcriptional activity

We investigated the effect of PKD1 activation on β -catenin mediated transcription activity and proliferation in prostate cancer cells. To investigate the effect of PKD1 on β -catenin mediated transcription activation of TCF, we transfected plasmids containing a wild type TCF-binding site (TOPFlash) or a mutated site as a negative control (FOPFlash) with pRL-TK (*Renilla* luciferase) in C4-2-PKD1-GFP cells activated with Bryostatin 1 or DMSO. The firefly and *Renilla* luciferase activities were measured with the Dual-Luciferase Reporter (DLR) Assay System. After normalizing the firefly luciferase activity to that of *Renilla* luciferase, the FOPFlash reporter plasmid luciferase values were subtracted from the normalized values obtained with the TOPFlash reporter plasmid. Bryostatin 1 activation in C4-2-PKD1-GFP cells led to a significant reduction (p value=0.019) in β -catenin reporter activity (Figure 7).

Effect of activation of PKD1 by Bryostatin 1 proliferation

The cell proliferation ability of Bryostatin 1 activated C4-2-PKD1-GFP cells was assayed by CellTiter-Glo. Bryostatin 1 activated C4-2-PKD1-GFP cells showed a 40% decrease in cell proliferation as compared to DMSO treated cells (Figure 7.2). A mixed ANOVA model will be used to compare the cell lines and doses. P-value < 0.05 was considered significant.

Effect of activation of PKD1 by Bryostatin1 on cellular aggregation

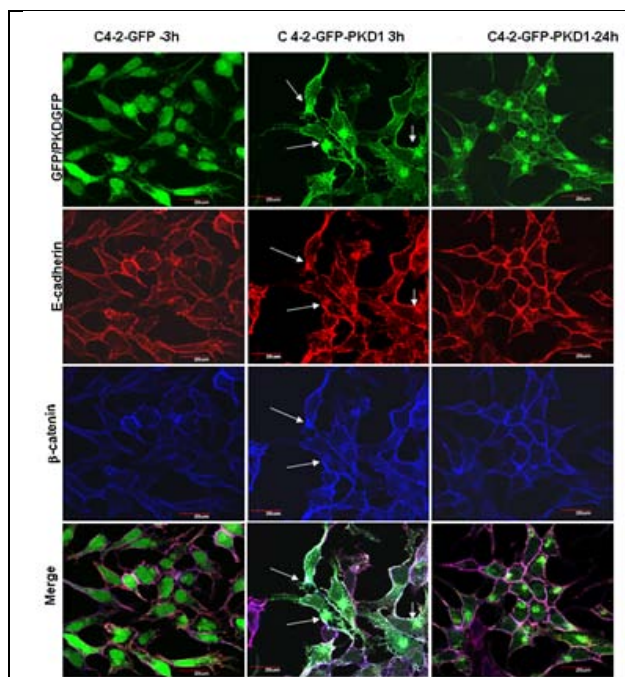


Figure 6: Activation of PKD1 by Bryostatin 1 on E-cadherin and β -catenin subcellular localization. Bryostatin 1 activated C4-2-GFP and C4-2-PKD1-GFP cells were stained for E-cadherin and β -catenin and analyzed by LSM. C4-2-GFP (3.1) and C4-2-PKD1-GFP (3.2 and 3.3) cells show differences in subcellular localization of E-cadherin (red) and β -catenin (blue). E-cadherin and β -catenin colocalizes with PKD1-GFP at perinuclear areas in addition to cell membranes (3.2 arrows) in Bryostatin 1 activated C4-2-PKD1-GFP cells (3.2 and 3.3) but not in C4-2-GFP cells.

PKD1 is also known to be involved with altered cellular aggregation, which is required for a cancer cell to successfully complete the metastatic cascade (2). Because we have demonstrated that PKD1 activation with Bryostatin 1 is involved in trafficking of β -catenin, we sought to determine the effect of Bryostatin 1 activation on cellular aggregation in C4-2 cells over-expressing PKD1. Aggregation assays were performed on C4-2 cells expressing PKD1-GFP as described previously. Our experiments demonstrated increased cellular aggregation in Bryostatin 1 treated C4-2-PKD1-GFP cells compared to vehicle only treated cells (Figure 7.3).

Effect of PKD1 inhibition on β -catenin subcellular localization

To further demonstrate the specific function of PKD1 in mediating the subcellular redistribution of β -catenin, PKD1 expression was inhibited 90% by using small interfering RNA (siRNA) in C4-2-PKD1-GFP cells activated with Bryostatin 1. After inhibition of PKD1 expression, cells transfected with non-targeted siRNA were activated with Bryostatin 1, stained for β -catenin and trans Golgi network (TGN) specific (p230) antibody and analyzed by confocal microscopy. Non-targeted siRNA transfected and Bryostatin 1 activated cells showed perinuclear localization of PKD1 and β -catenin. Merging of PKD1, β -catenin and p230 images from these cells shows colocalization of these three proteins at the perinuclear region and colocalization of PKD1 and β -catenin at the cell junction. Immunofluorescence images of PKD1 siRNA transfected C4-2-PKD1-GFP cells shows inhibition of PKD1-GFP (Figure 8.E), reduced staining of β -catenin at the membrane and lack of β -catenin localization at TGN (Figure 8 F). Merging of PKD1, β -catenin and p230 images taken at the same confocal level in PKD1 siRNA transfected C4-2-PKD1-GFP cells (Figure 8 H) do not show colocalization of the proteins at the perinuclear region. These results suggest that β -catenin subcellular localization is modulated predominantly by activated PKD1 and not by other kinases (PKC isoforms) activated by Bryostatin 1. Interestingly, down regulation of PKD1 by RNAi decreased β -catenin expression at the plasma membrane (Figure 8 F), which further suggests that PKD1 plays a major role in membrane transport of β -catenin. We have previously published that down regulation of PKD1 in fact increases total cellular β -catenin. This provides further corroborative evidence for role of PKD1 in membrane trafficking of β -catenin because

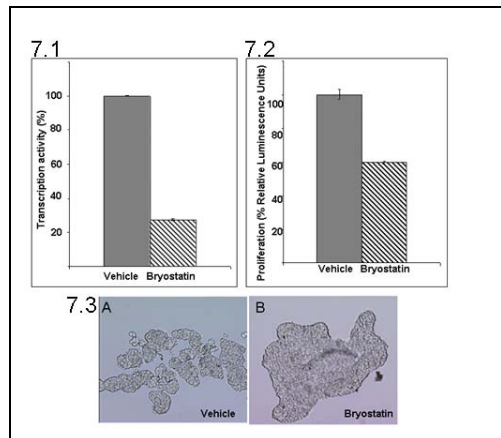


Figure 7: Bryostatin treatment decreases in β -catenin transcription activity, cell proliferation and increases cell-cell adhesion. **7.1)** Effect of Bryostatin treatment on β -catenin transcription activity. C4-2-PKD1-GFP cells were transfected with TOP or FOPFlash firefly luciferase reporter constructs and treated with 10 nM Bryostatin 1 or vehicle only. Data are expressed as fold induction normalized to the cotransfected Renilla luciferase-encoding pRL-TK plasmid. Treatment of C4-2-PKD1-GFP cells significantly decreased β -catenin mediated transcription activity as compared to vehicle only treated cells ($p = 0.019$). Error bars indicate standard error. **7.2)** Proliferation assay of Bryostatin 1 treated C4-2-PKD1-GFP cells. Proliferation assay after 48 h of 10 nM Bryostatin 1 treatment (see Materials and Methods) expressed as percent of control cells treated with vehicle only ($p=0.001$). Error bars indicate standard error. **7.3)** Bryostatin treatment increases cellular aggregation. Bryostatin 1 treated C4-2 -PKD1-GFP cells showed increased cellular aggregation (**B**) compared to vehicle only treated cells (**A**).

membrane β -catenin is decreased in spite of increased total levels of cellular β -catenin when PKD1 expression is reduced (3). However, the exact mechanism of regulation of β -catenin expression by PKD1 remains to be investigated.

Effect of PKD1 expression on apoptosis:

It has been shown that nuclear β -catenin forms a complex with TCF/LEF transcription factors and that this complex transactivates downstream targets such as *c-myc* and *cyclin D1*. These proteins have been implicated in cell cycle regulation. PKD1 overexpression in C4-2 cells decreases β -catenin/TCF transcription activity. Over expression of PKD1 causes increased

cellular aggregation and decreased motility in prostate cancer cells. In order to determine the effect of PKD1 on cell cycle distribution

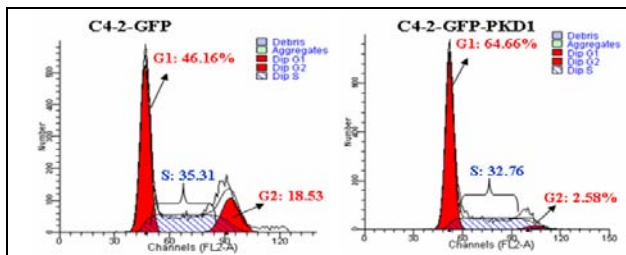


Figure 9. Cell cycle analysis: C4-2.GFP and C4-2.PKD1.GFP cells were stained with propidium iodide and cell cycle distribution was assessed by fluorescence activated cell sorting (FACS) analysis of DNA content.

Cell cycle distribution was assessed using BD FACSVantage SE pulse processing plus program for analysis of DNA content. C4-2-GFP vector and C4-2-GFP-PKD1 cells were stained with propidium iodide (PI). Each value represents percentage of cells in the noted cell cycle phase. Experiments were repeated three times and representative histograms are shown. The results show that PKD1 overexpression resulted increase of cells in G1 phase and concomitant decrease in cell in G2 phase, indicate cell cycle arrest in G1 phase (Figure 9).

Aim 3: To evaluate the expression of β -catenin and PKD1 proteins in progressive human prostate cancer:

Our preliminary IHC studies demonstrate that, in addition to downregulation of β -catenin in human prostate cancer compared to benign glands, there is a decreased expression of β -catenin in prostatic intraepithelial neoplasia in a small subset of our study patients and an increased nuclear

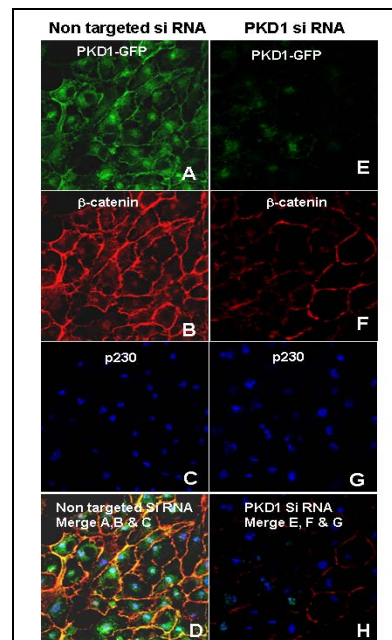


Figure 8: Inhibition of PKD1 on β -catenin subcellular localization. Bryostatin 1 treated C4-2-PKD1-GFP cells were transfected with a PKD1 silencing siRNA and stained for β -catenin and p230 antibodies. β -catenin shows strong membrane localization and perinuclear localization in control siRNA transfected cells, whereas PKD1 silenced cells showed punctuate membrane staining and does not show perinuclear staining.

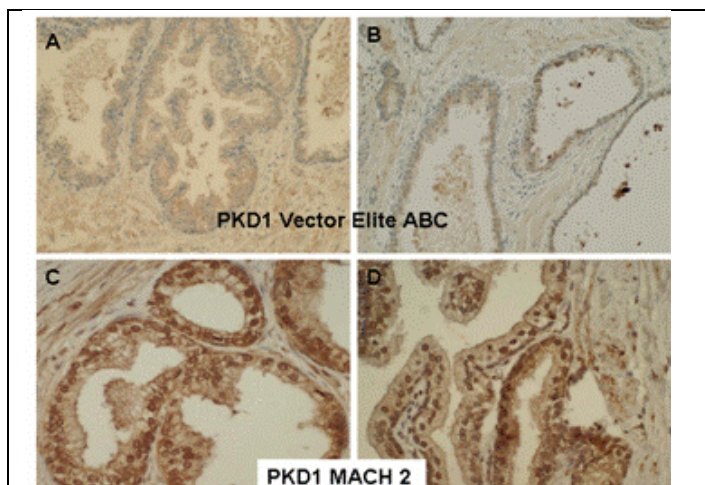


Figure 10. Comparative PKD1 expression by Vector Elite ABC kit (A-B) and MACH 2 (Biocare Medical) kit (C-D).

staining in high Gleason grade prostate cancer. This suggests an involvement of β -catenin and the Wnt signaling pathway in prostate cancer.

We have evaluated PKD1 and β -catenin protein expression in human prostate cancer tissues utilizing IHC (Vector Elite ABC kit). The cases and controls, matched one-to-one on the basis of patient age and year of biopsy, were included in this study. We have successfully collected 50 prostate cancer patient sample for analysis by immuno histochemistry (IHC). Initial experiments were done to standardize the staining technique with Vector Elite ABC kit, as proposed. However, the staining was not very effective (Figure 10). We have standardized staining procedure with the Mach2 kit to yield better results and plan using this kit for IHC staining of human prostate cancer tissues for PKD1 and β -catenin protein expression and correlated with serum PSA, to identify a potential role for these proteins as biomarkers.

Plan for next year:

Generation of stable C4-2 cells over expressing PKD1 mutant constructs: In the next cycle, we

plan to generate stable transfects using retroviral system as suggested in the diagram below (Figure 11). The retroviral system is a high efficiency method for generation of stably transfected cell lines that has been in use for many years. PKD1 mutant DNA previously cloned in pEGFP vector will be used to generate retroviral constructs in pRetroQ.AcGFP.N1 vector. The desired fragment will be isolated after double digestion with specific restriction enzyme and ligated into linearized retroviral vector. These viral vectors would be used to transfect special HEK cells (Phoenix) capable of producing gag-pol and envelope protein. Supernatant from these cells containing retroviral particles packed with the retroviral plasmid containing the gene of interest will be collected, filtered and used to infect C4-2 cells to generate homogenous stable transfects. Once the stable transfects are isolated, the interaction of PKD1-GFP mutant constructs with β -catenin will be analyzed by immunoprecipitation assays, using β -catenin and GFP specific antibodies as described previously. Additionally, the effect of the different constructs on β -catenin transcription activity will be analyzed.

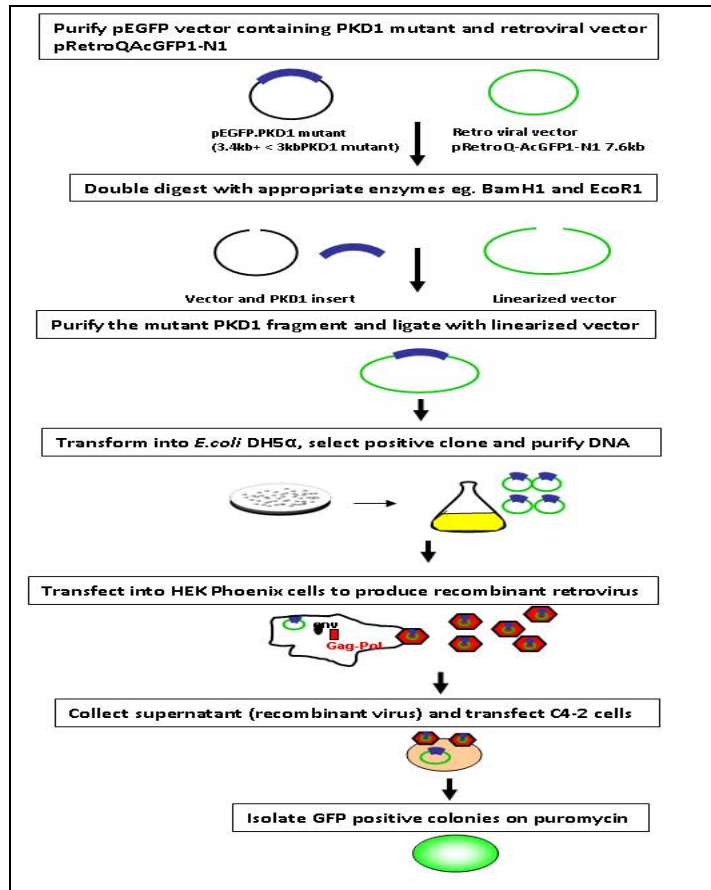


Figure 11: Schematic representation for the generation of stable transfects with retro virus. PKD1 mutant DNA previously cloned in pEGFP vector will be used to generate retroviral constructs in pRetroQ.AcGFP.N1 vector. These viral vectors would be used to transfect HEK cells (Phoenix) to generate retroviral particles packed with the retroviral plasmid containing the gene of interest. The particles will be used to infect C4-2 cells to generate homogenous stable transfects.

Generation of Effect of PKD1 mutant constructs β -catenin transcription: We will investigate the effect of PKD1 mutants on β -catenin mediated transcriptional activity and proliferation in prostate cancer cells. To investigate the effect of PKD1 mutants on β -catenin mediated transcriptional activation of TCF, we transfected plasmids containing a wild type TCF-binding site (TOPFlash) or a mutated site as a negative control (FOPFlash) with pRL-TK (*Renilla* luciferase) in C4-2-PKD1-GFP cells activated with Bryostatin 1 or DMSO. The firefly and *Renilla* luciferase activities were measured with the Dual-Luciferase Reporter (DLR) Assay System. After normalizing firefly luciferase activity to that of *Renilla* luciferase, the FOPFlash reporter plasmid luciferase values were subtracted from the normalized values obtained with the TOPFlash reporter plasmid. This study will determine site specific functions of PKD1 in β -catenin mediated cellular signaling.

Effect of activation of PKD1 by Bryostatin 1 on DNA damage induction and apoptotic cell death: Both parental C4-2 cells and C4-2 cells transfected with PKD1 will be seeded on coverslips, cultured for 24 hours, and treated with Bryostatin 1 at multiple time points (5, 10, 15 minutes, etc.) to study the rate of apoptotic cell death. Apoptosis will be assayed by TdT-mediated nick end labeling (TUNEL) by using an in situ cell death detection kit (Promega, Madison, WI). The rate of apoptosis of the treated cells will be compared to the controls.

Modulation of the tumorigenicity of prostate cancer cells by PKD1:

The ability of PKD1 to alter the growth potential of prostate cancer cells will be assayed by the classic transformation parameter of anchorage-dependent growth in soft agar. The assay will be conducted as previously described (4) with some modifications. Briefly, 2.5×10^2 cells will be suspended in 1ml RPMI containing a final concentration of 0.4% agar and 10% FBS. The cells will be plated on top of a solidified layer of 0.6% agar in six well plates. The numbers of colonies will be scored at day 15 and photographed using a phase microscope. In addition to in vitro studies we will perform in tumorigenicity assay using mouse xenograft model. Male athymic Swiss Webster nude mice, aged 6 to 8 weeks will be obtained from Jackson laboratories. We have already been able to optimize conditions for development of tumor with injection of C4-2 cells subcutaneously (Figure. 12). Prostate cancer cells with vector, PKD1 over-expressing and PKD1 silenced will be used for tumor development. At the end of the experiments all tumors will be dissected, measured, weighed and specimen saved at -80°C for correlative studies.

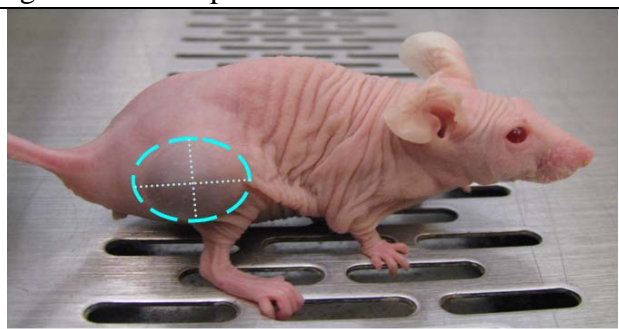


Figure 12: Animal model of C4-2 prostate cancer. Athymic mice were injected with 25×10^6 C4-2 cells subcutaneously. The blue ring shows the tumor that developed with C4-2 cells.

Effect of PKD1 expression influences motility and invasion of prostate cancer cells: The effect of PKD1 expression on motility will be studied by *in vitro* motility assays as described in our prior publication (2). We anticipate increased cell motility in the PKD1 knockdown as compared to controls.

Curcumin a new PKD modulator: During this current year, we investigated the effect of many natural compounds that can modulate prostate cancer cells growth and investigated the effects of these on β -catenin transcription activity. Our investigation with curcumin demonstrated that it can attenuates β -catenin transcription activity in prostate cancer cells and can also modulate the expression/activation of PKD1 (Figure 13). These results suggest a novel molecular mechanism of curcumin related suppression of prostate cancer cells growth through modulation of PKD1.

In addition, we investigated the effect of PKD1 overexpression in a cancer cell line model on gene expression within these cells. Our results show modulation of a number of different genes, five of the highest modulated RNAs are shown (Figure. 14). It is very likely that similar sets of genes are modulated by PKD1 in prostate cancer cells. We would explore this in prostate cancer *in vitro* and *in vivo* model.

Key Research Accomplishments: During 2008-10 funding period we made considerable progress on our grant proposal and published one paper in Molecular Cancer Therapeutics. Our research findings were considered for highlight and appeared on cover page (cover illustration, MCT September 2008, volume 7). Along with

publication few more papers were published from our group. In next funding cycle we are expected to make progress on remaining specific aims and to have couple more publications. In brief, in 2008-10 funding period we have investigated the effect of Bryostatin 1 on PKD1 expression, β -catenin transcription, cell proliferation, and cellular aggregation. In this study we examined the effect of Bryostatin 1 treatment on PKD1 activation, β -catenin translocation and transcription activity and malignant phenotype of prostate cancer cells. Initial activation of PKD1 with Bryostatin 1 leads to colocalization of the cytoplasmic pool of β -catenin with PKD1, trans-Golgi network markers and proteins involved in vesicular trafficking. Activation of PKD1 by Bryostatin 1 decreases nuclear β -catenin expression and β -catenin/TCF transcription activity. Activation of PKD1 alters cellular aggregation and proliferation in prostate cancer cells associated with subcellular redistribution of E-cadherin and β -catenin. For the first time, we have identified Bryostatin 1 modulates β -catenin signaling through PKD1, which identifies a novel mechanism to improve efficacy of Bryostatin 1 in clinical setting. We also explored the effect of transient overexpression of various PKD1 mutant constructs on proliferation, colony formation cell motility. Our experiments suggest important role for C1b domain for proliferation and

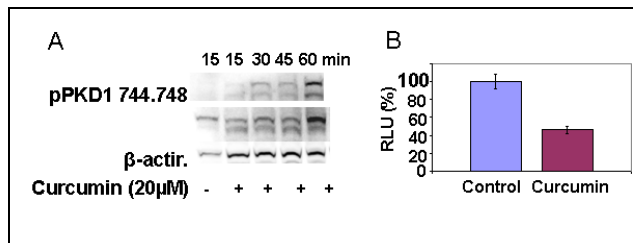


Figure 13: Curcumin modulates (A) PKD1 phosphorylation and (B) β -catenin transcription activity. Treatment of C4-2 cells or C4-2 cells over expressing PKD1.GFP with curcumin showed increase in PKD1 phosphorylation by 60 min. We also detected a ~50% reduction in β -catenin transcription activity (B).

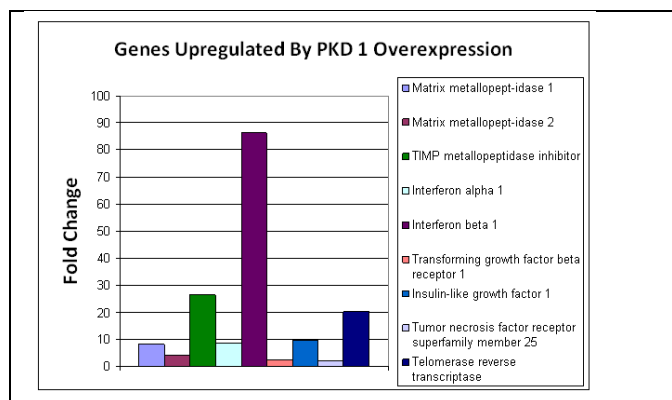


Figure 14. PCR-micro array data: PKD1 overexpression modulates expression of some key tumor associated genes. PCR microarray analysis was done using PKD1.GFP overexpressing cancer cells. In comparison to GFP vector control cells, we observe dramatic changes in some key genes as represented above.

colony formation and the N-terminal region for cell motility. We would like to explore this further using stably transfected cell lines. Also, in collaboration with Dr. Chauhan, we have been able to standardize condition for generation of C4-2 tumor xenograft in nude mice. We will use this model for further studies.

Reportable Outcomes:

- Published one paper in *Molecular Cancer Therapeutics*. Our research findings were considered for highlight and appeared on cover page (cover illustration, MCT September 2008, volume 7).
- In 2009-2010, we have published six papers and seven abstracts.
- For the first time, we have identified Bryostatin 1 modulates β -catenin signaling through PKD1.
- For the first time, we have shown that curcumin modulated PKD1 activation and subsequent β -catenin transcription activity.

Publication in year 2008-2010:

Yallapu MM., **Jaggi M**, and Chauhan SC. β -Cyclodextrin-Curcumin Self-assembly Enhances Curcumin Delivery in Prostate Cancer Cells. *Colloids and Surfaces B: Biointerfaces* (In Press)

Yallapu MM., **Jaggi M**, and Chauhan SC*. Poly(β -cyclodextrin)-Curcumin Self-assembly : A Novel Approach to Improve Curcumin Delivery and its Therapeutic Efficacy in Prostate Cancer Cells. *Macromolecular Bioscience* (In Press)

Yallapu MM., Maher DM., Sundram V., **Jaggi M**, and Chauhan SC. Curcumin induces chemo/radio-sensitization in ovarian cancer cells and curcumin nanoparticles inhibit ovarian cancer cell growth. *Journal of Ovarian Research* (In Press)

Chauhan SC., Kumar D. and **Jaggi M**. Mucins in ovarian cancer diagnosis and therapy. *Journal of Ovarian Research* 2009 Dec 24;2(1):21

Chauhan SC, **Jaggi M**, Bell MC, Verma M, Kumar D. Epidemiology of Human Papilloma Virus (HPV) in Cervical Mucosa. *Methods Mol Biol.* 2009;471:439-56.

Chauhan SC., Vannatta K., Ebeling MC., Vinayek N., Watanabe A., Pandey KK., Maher D., Bell MC., Koch MD., Aburatani H., Lio Y. and **Jaggi M**. Expression and *in vitro* functions of transmembrane mucin MUC13 in ovarian cancer. *Cancer Research* 2009;69(3) 765-774

Jaggi M., Du C., Zhang C. and Balaji KC. Protein kinase D1 (PKD1) mediated phosphorylation and subcellular localization of β -catenin. *Cancer Research* 2009;69(3) (1&2 equal contribution)

Jaggi M*, Chauhan SC., Du C. and Balaji KC. Bryostatin modulates β -catenin subcellular localization and transcription activity through protein kinase D1 activation. *Molecular Cancer Therapeutics* 2008;7(9):2703-12 (**Cover illustration**)

Paul M., **Jaggi M**., Viqar S., Chauhan SC., Hassan S., Biswas H., Balaji K.C. Protein kinase D1 (PKD1) influences androgen receptor (AR) function in prostate cancer cells. *Biochemical and Biophysical Research Communications* 2008 Sep 373:618-23.

Abstracts:

- Hughes JE., Chauhan SC., and **Jaggi M.** Protein kinase D1 attenuates tumorigenesis in SW 480 colon cancer cells by modulation β -catenin/T cell factor activity. 3rd *International Symposium on Translational Cancer Research* December 18-21, 2009, Bhubaneswar, Orissa, India.
- Sundram V., Chauhan SC. and **Jaggi M.** Curcumin suppresses prostate cancer cells through modulation of β -catenin and protein kinase D1. *101 AACR Annual Meeting 2010*, Washington DC.
- Prakash Preethi., Freiz MH., Bohlmeier T., Koch MRD., Chauhan SC., **Jaggi M.** Downregulation of Protein Kinase D1 in hepatocellular carcinoma (HCC): Potential as a diagnostic/prognostic molecular marker. *101 AACR Annual Meeting 2010*, Washington DC.
- Ebeling MC., **Jaggi M.** and Chauhan SC. Role of MUC13 mucin in pancreatic cancer diagnosis and pathogenesis. 3rd *International Symposium on Translational Cancer Research* December 18-21, 2009, Bhubaneswar, Orissa, India.
- Chauhan SC., Ebeling MC., Maher DM., Koch MRD., Friez MH. ⁴, Watanabe A., Aburatani Hiroyuki., Lio Y., Pandey KK and **Jaggi M.** MUC13 mucin augments pancreatic tumorigenesis. *101 AACR Annual Meeting 2010*, Washington DC
- Maher D., Yallapu MM., Sundram V., Bell MC., **Jaggi M.**, Chauhan SC. Curcumin induces chemo/radio-sensitization in ovarian cancer cells and curcumin nanoparticles inhibit ovarian cancer cell growth. *101 AACR Annual Meeting 2010*, Washington DC.
- Yallapu MM., **Jaggi M.**, Chauhan SC. Design of β -cyclodextrin-curcumin self-assembly: A new approach for enhanced curcumin delivery and therapeutic efficacy in prostate cancer cells. *101 AACR Annual Meeting 2010*, Washington DC.

Conclusions:

- Bryostatin 1 treatment modulates PKD1 expression, cell proliferation, and cellular aggregation and alters β -catenin translocation and transcription activity.
- Initial activation of PKD1 with Bryostatin 1 leads to colocalization of the cytoplasmic pool of β -catenin with PKD1, trans-Golgi network markers and proteins involved in vesicular trafficking.
- Activation of PKD1 by Bryostatin 1 decreases nuclear β -catenin expression and thereby suppresses β -catenin/TCF transcription activity.
- For the first time, we have identified Bryostatin 1 modulates β -catenin signaling through PKD1.
- We have identified curcumin as molecule that can be effectively used for controlling prostate cancer. We have shown for the first time that curcumin modulated PKD1 activation and subsequent β -catenin transcription activity.
- We have standardized method to generate xenograft C4-2 tumors in null mice. These can now be used for further studies.
- We have collected 50 prostate cancer samples and have standardized technique for effective IHC staining. We will use this procedure to probe the use of PKD1 and or β -catenin as cancer molecular markers.

Reference:

1. Vertommen, D., Rider, M., Ni, Y., Waelkens, E., Merlevede, W., Vandenhede, J. R., and Van Lint, J. Regulation of protein kinase D by multisite phosphorylation. Identification of phosphorylation sites by mass spectrometry and characterization by site-directed mutagenesis. *J Biol Chem*, 275: 19567-19576., 2000.
2. Jaggi, M., Rao, P. S., Smith, D. J., Wheelock, M. J., Johnson, K. R., Hemstreet, G. P., and Balaji, K. C. E-cadherin phosphorylation by protein kinase D1/protein kinase C{mu} is associated with altered cellular aggregation and motility in prostate cancer. *Cancer Res*, 65: 483-492, 2005.
3. Mak, P., Jaggi, M., Syed, V., Chauhan, S. C., Hassan, S., Biswas, H., and Balaji, K. C. Protein kinase D1 (PKD1) influences androgen receptor (AR) function in prostate cancer cells. *Biochem Biophys Res Commun*, 373: 618-623, 2008.
4. Amundadottir, L. T. and Leder, P. Signal transduction pathways activated and required for mammary carcinogenesis in response to specific oncogenes. *Oncogene*, 16: 737-746, 1998.

Appendices:

Copies of published/accepted articles.

[Print this Page](#)**AACR 101st ANNUAL MEETING 2010**

April 17-21, 2010 • Walter E. Washington Convention Center • Washington, DC

Presentation Abstract

Abstract Number: 1892

Presentation Title: Curcumin suppresses prostate cancer cells through modulation of β -catenin and protein kinase D1

Presentation Time: Monday, Apr 19, 2010, 9:00 AM -12:00 PM

Location: Exhibit Hall A-C, Poster Section 35

Poster Section: 35

Poster Board Number: 22

Author Block: Vasudha Sundram¹, Subhash C. Chauhan², Meena Jaggi². ¹Cancer Biology Research Center, Sanford Research/University of South Dakota, Sioux Falls, SD; ²Cancer Biology Research Center, Sanford Research/University of South Dakota, Departments of OB/GYN and Basic Biomedical Science Division, Sanford School of Medicine, Sioux Falls, SD

Abstract Body: **OBJECTIVE:** Prostate cancer is the most commonly diagnosed cancer in males in the US. One in every 6th male will be diagnosed with prostate cancer this year. Understanding the molecular basis of prostate cancer progression can serve as a tool for early stage diagnosis and development of novel treatment strategies for this disease. Inappropriate activation of β -catenin signaling is linked to a wide range of cancers, including prostate cancer, resulting in transcription of genes involved in cancer progression such as c-Myc, c-Jun and cyclin D1. However, strategies to regulate this specific signaling pathway are very limited or not well developed. Synthetic or natural products which regulate this signaling pathway can be developed as a novel therapeutic modality for prostate cancer treatment. Curcumin, the active ingredient of turmeric, has shown anti-cancer properties *via* modulation of a number of different molecular pathways. Herein, we have investigated a putative molecular mechanism involved in curcumin mediated suppression of prostate cancer cell growth and the effect of curcumin on prostate cancer cells growth and its effect on β -catenin transcription activity.

MATERIALS AND METHODS: Cellular characteristics of the C4-2 prostate cancer cells were measured using anchorage independent growth, anchorage dependent growth, motility, and proliferation assays. β -catenin/T cell factor (TCF) transcription activity was measured by luciferase reporter assays using reporter constructs Topflash or Fopflash and pRL-TK (*Renilla* luciferase). The Luciferase activities were assayed using the Dual Glo reagent (dual reporter assay, Promega, Madison, WI). Subcellular localization of Protein Kinase D1 (PKD1) and β -catenin was determined by confocal microscopy.

RESULTS: Our results demonstrate that curcumin effectively suppresses prostate cancer cell growth, proliferation and cellular motility. In the luciferase assays, curcumin treatment diminished β -catenin transcription activity in C4-2 prostate cancer cells. Moreover, curcumin treatment influences the translocation of β -catenin from the nucleus to the cell surface membrane. Interestingly, the suppression of β -catenin transcription activity was correlated with the modulation PKD1 expression/phosphorylation within 1-3 hrs post-curcumin treatment.

CONCLUSION: These results suggest that curcumin treatment attenuates β -catenin transcription activity in prostate cancer cells *via* modulating the expression/activation of PKD1. These results suggest a novel molecular mechanism of curcumin related suppression of prostate cancer cell growth.

American Association for Cancer Research
615 Chestnut St. 17th Floor
Philadelphia, PA 19106

[Print this Page](#)**AACR 101st ANNUAL MEETING 2010**

April 17-21, 2010 • Walter E. Washington Convention Center • Washington, DC

Presentation Abstract

Abstract
Number: 4621Presentation
Title: Downregulation of Protein Kinase D1 in hepatocellular carcinoma (HCC): Potential as a diagnostic/prognostic molecular marker.Presentation
Time: Tuesday, Apr 20, 2010, 2:00 PM - 5:00 PM

Location: Exhibit Hall A-C, Poster Section 30

Poster
Section: 30Poster Board
Number: 3

Author
Block: Preethi Prakash¹, Matt Freiz², Teresa Bohlmeier³, Micheal R.D Koch², Subhash C. Chauhan⁴, Meena Jaggi⁴. ¹Cancer Biology Research Center, Sanford Research/USD, Department of Internal Medicine, Sioux Falls, SD; ²Sanford School of Medicine/USD, Department of Pathology, Sioux Falls, SD; ³Cancer Biology Research Center, Sanford Research/USD, Sioux Falls, SD; ⁴Cancer Biology Research Center, Sanford Research/USD, Department of OB/GYN and Basic Biomedical Science Division, Sioux Falls, SD

Abstract
Body: **OBJECTIVE:** Protein Kinase D1 (PKD1) plays an important role in several cellular processes such as cell proliferation, oxidative stress signaling, adhesion and motility. PKD1 is of particular interest in diagnosis, prognosis and treatment of human diseases because of its enzymatic activity and susceptibility to successful therapeutic targeting. In our earlier study we have demonstrated suppression of PKD1 expression in advance stage prostate cancer. This led us to analyze PKD1 expression patterns in various other cancer tissue samples.

MATERIAL AND METHODS: Tissue microarrays containing various cancer samples with corresponding normal tissues were used to investigate the expression profile of PKD1 using immunohistochemistry (Biocare Medical, Concord, CA). Further studies on PKD1 expression profile in hepatocellular carcinoma (HCC) were carried out using tissue microarray (TMA) containing HCC samples (n=70) with normal tissues (n=4) and a HCC TMA with hepatitis B viral history (HBV) containing HCC samples (n=100) with normal tissues (n=4) (AccuMax Array). Immunostaining was graded by two independent pathologists. Intensity and extent of staining scores were multiplied to obtain the composite score (CS) of each sample.

RESULT: Differential expression pattern of PKD1 was observed in brain, skin, lung, kidney, thyroid and ovarian cancer samples. Along with stomach and colon cancer, HCC samples showed a marked downregulation of PKD1 expression compared to their respective normal tissues. PKD1 expression profile was further evaluated in a large cohort of HCC samples. Overall, HCC samples showed a significant ($p > 0.05$) downregulation (Mean CS=6.0) of PKD1 expression compared to normal liver samples (Mean CS=11.4). Among cancer samples, advanced stage samples showed a relatively lower PKD1 expression (Mean CS=5.4) compared to early stage (Mean CS=6.6) HCC samples. Similarly, advance stage HCC samples with HBV showed a lower PKD1 expression (Mean CS=6.9) compared to early stage samples (Mean CS=9.6) and non neoplastic samples (Mean CS=12).

CONCLUSION: The results of this study suggest suppression of PKD1 expression in HCC. In view of the limitations of the available diagnostic/prognostic studies for detection of HCC, the aberrant expression of PKD1 may serve as a novel biomarker for the diagnosis/prognosis of hepatocellular carcinoma.

American Association for Cancer Research
615 Chestnut St. 17th Floor
Philadelphia, PA 19106

[Print this Page](#)**AACR 101st ANNUAL MEETING 2010**

April 17-21, 2010 • Walter E. Washington Convention Center • Washington, DC

Presentation Abstract

Abstract
Number: 5381Presentation
Title: Curcumin induces chemo/radio-sensitization in ovarian cancer cells and curcumin nanoparticles inhibit ovarian cancer cell growthPresentation
Time: Wednesday, Apr 21, 2010, 8:00 AM -11:00 AM

Location: Exhibit Hall A-C, Poster Section 21

Poster
Section: 21Poster Board
Number: 13Author
Block: Diane Maher¹, Murali M. Yallapu¹, Vasudha Sundram¹, Maria C. Bell², Meena Jaggi², Subhash C. Chauhan². ¹Sanford Research/USD, Sioux Falls, SD; ²Sanford Research/USD and Department of Obstetrics and Gynecology, Sanford School of Medicine, University of South Dakota, Sioux Falls, SD

Abstract Body: **Background:** Chemo/radio-resistance is a major obstacle in treating advanced ovarian cancer. The efficacy of current treatments may be improved by increasing the sensitivity of cancer cells to chemo/radiation therapies. Curcumin is a naturally occurring compound with anti-cancer activity in multiple cancers; however, its chemo/radio-sensitizing potential is not well studied in ovarian cancer. Herein, we demonstrate the chemo/radio-sensitizing potential of curcumin in a cisplatin resistant ovarian cancer cell line model. Additionally, due to suboptimal pharmacokinetics and low uptake of curcumin in tumors *in vivo*, we developed a curcumin nanoparticle formulation to improve its therapeutic efficacy.

Methods: Cisplatin resistant A2780CP ovarian cancer cells were pre-treated with curcumin followed by exposure to cisplatin or radiation and the effect on cell growth was determined by MTS and colony formation assays. The effect of curcumin pre-treatment on the expression of apoptosis related proteins and β -catenin was determined by Western blotting or Flow Cytometry. A luciferase reporter assay was used to determine the effect of curcumin on β -catenin transcription activity. The poly(lactic acid-co-glycolic acid) (PLGA) nanoparticle formulation of curcumin (Nano-CUR) was developed by a modified nano-precipitation method and physico-chemical characterization was performed by transmission electron microscopy and dynamic light scattering methods.

Results: Curcumin pre-treatment considerably reduced the dose of cisplatin and radiation required to inhibit the growth of cisplatin resistant ovarian cancer cells. During the 6 hrs pre-treatment, curcumin down regulated the expression of Bcl-X_L and Mcl-1 pro-survival proteins. Curcumin pre-treatment followed by exposure to low doses of cisplatin increased apoptosis as indicated by annexin V staining and cleavage of caspase 9 and Poly (ADP-ribose) polymerase (PARP). Additionally, curcumin pre-treatment lowered β -catenin expression and transcriptional activity. Physico-chemical characterization of Nano-CUR indicated an average particle size of ~70 nm, steady release of curcumin over a period of 18 days and antibody conjugation characteristics. The Nano-CUR formulation also effectively inhibited the growth of ovarian cancer cells.

Conclusion: Curcumin pre-treatment enhances chemo/radio-sensitization in A2780CP ovarian cancer cells through multiple molecular mechanisms. Therefore, curcumin pre-treatment may effectively improve ovarian cancer therapeutics. A targeted PLGA nanoparticle formulation of curcumin is feasible and may improve the *in vivo* therapeutic efficacy of curcumin.

American Association for Cancer Research
615 Chestnut St. 17th Floor
Philadelphia, PA 19106

[Print this Page](#)**AACR 101st ANNUAL MEETING 2010**

April 17-21, 2010 • Walter E. Washington Convention Center • Washington, DC

Presentation Abstract

Abstract
Number: 2358Presentation
Title: MUC13 mucin augments pancreatic tumorigenesisPresentation
Time: Monday, Apr 19, 2010, 2:00 PM - 5:00 PM

Location: Exhibit Hall A-C, Poster Section 15

Poster
Section: 15Poster
Board
Number: 12

Author
Block: Subhash C. Chauhan¹, Mara C. Ebeling², Diane M. Maher², Michael D. Koch³, Matthew H. Friez⁴, Akira Watanabe⁵, Hiroyuki Aburatani⁵, Yuhlong Lio⁶, Krishan K. Pandey⁷, Meena Jaggi¹. ¹Cancer Biology Research Center, Sanford Research/USD and Departments of OB/GYN and Basic Biomedical Science Division, Sanford School of Medicine, Sioux Falls, SD; ²Cancer Biology Research Center, Sanford Research/USD, Sioux Falls, SD; ³Department of Laboratory Medicine and Pathology, Sanford School of Medicine, Sioux Falls, SD; ⁴Department of Pathology, Sanford School of Medicine, Sioux Falls, SD; ⁵The University of Tokyo, Tokyo, Japan; ⁶Department of Mathematical Science, The University of South Dakota, Vermillion, SD; ⁷Institute for Molecular Virology, Saint Louis University, Saint Louis, MO

Abstract
Body: Pancreatic cancer is one of the most lethal malignancies with extremely poor prognosis. The high death rate of pancreatic cancer is attributed to a lack of reliable methods of early diagnosis and underlying molecular mechanisms associated with aggressive pathogenesis. MUC13, a newly identified transmembrane mucin, is known to be aberrantly expressed in ovarian, gastric and colon cancer. However, the expression and functions of MUC13 in pancreatic cancer are unknown. Herein, we have investigated the expression and functions of MUC13 mucin, in pancreatic cancer to determine its potential for early cancer diagnosis and its role in pancreatic cancer pathogenesis. The expression profile of MUC13 in pancreatic cancer was investigated using a recently generated monoclonal antibody (MAb, clone PPZ0020) and pancreatic tissue microarrays. The expression of MUC13 was significantly ($p < 0.005$) higher in cancer samples compared to the normal/non-neoplastic pancreatic tissues. For the functional analyses, a full length MUC13 gene cloned in pcDNA3.1 was expressed in MUC13 null pancreatic cancer cell lines, MiaPaca and Panc1. The exogenous MUC13 expression induced morphological changes, including scattering of cells. These changes were abrogated through c-jun NH2-terminal kinase (JNK) chemical inhibitor (SP600125) or JNK2 siRNA. Additionally, a marked reduction in cell-cell adhesion and significant ($p < 0.05$) increases in cell motility, invasion, proliferation, clonogenicity and tumorigenesis in a xenograft mouse model system were observed upon exogenous MUC13 expression. These cellular characteristics were correlated with the up-regulation of HER2, p21-activated kinase1 (PAK1), extracellular signal-regulated kinase (ERK) and S100A4 (metastasin) and suppression of p53. Inhibition of MUC13 expression by MUC13 siRNA or shRNA resulted in suppression of tumorigenic characteristics in HPAFII pancreatic cancer cells. These results, for the first time, suggest that MUC13 expression augments pancreatic cancer progression and has potential as a diagnostic and/or therapeutic target.

American Association for Cancer Research
615 Chestnut St. 17th Floor
Philadelphia, PA 19106

[Print this Page](#)**AAOOR 101st ANNUAL MEETING 2010**

April 17-21, 2010 • Walter E. Washington Convention Center • Washington, DC

Presentation Abstract

Abstract Number: LB-425

Presentation Title: Design of β -cyclodextrin-curcumin self-assembly: A new approach for enhanced curcumin delivery and therapeutic efficacy in prostate cancer cells

Presentation Time: Wednesday, Apr 21, 2010, 8:00 AM -11:00 AM

Location: Exhibit Hall A-C, Poster Section 40

Author Block: *Murali M. Yallapu, Meena Jaggi, Subhash C. Chauhan.* Cancer Biology Research Center, Sanford Research/University of South Dakota, Sioux Falls, SD, Cancer Biology Research Center, Sanford Research/University of South Dakota and Department of OB/GYN and Basic Biomedical Science Division, Sanford School of Medicine, University of South Dakota, Sioux Falls, SD

Abstract Body: Curcumin (CUR), a hydrophobic polyphenolic compound derived from the rhizome of the herb *Curcuma longa*, has shown a wide range of biological applications including cancer prevention and treatment. However, low water solubility, poor pharmacokinetics and suboptimal tumor uptake, greatly hamper its anti-cancer efficacy. This study was designed to develop a novel β -cyclodextrin-curcumin (CD-CUR) self-assembly approach for sustained release and improved curcumin delivery in prostate cancer cells. Cyclodextrin-curcumin self-assemblies were prepared by solvent evaporation technique. The formation of self-assemblies was evaluated by Fourier Transform Infra-red (FTIR), Differential Scanning Calorimetry (DSC), Thermogravimetric Analysis (TGA), Scanning and Transmission Electron Microscopic (SEM/TEM) analyses. Intracellular uptake of these self-assemblies was evaluated by Flow cytometry and immunofluorescence microscopy analyses. Therapeutic efficacy of these self-assemblies was determined by cell proliferation and colony formation assays using C4-2, DU145, LNCaP and PC3 prostate cancer cells. The effect of CD-CUR formulation on apoptosis related proteins was determined by immunoblotting. Physico-chemical characterization analyses confirm the formation of CD-CUR self-assemblies, which demonstrated excellent stability and solubility in physiological solutions and showed enhanced intracellular uptake in cells. Additionally, CD-CUR formulation has exhibited an improved therapeutic efficacy and enhanced PARP cleavage in prostate cancer cells compared to free curcumin. In conclusion, CD-CUR self-assemblies enhance intracellular delivery of active curcumin in prostate cancer cells and improved its therapeutic efficacy. This study suggests that CD-CUR self-assembly may be a useful nanoscale formulation for improved curcumin delivery in prostate cancer cells. Tumor specific antibody targeted CD-CUR formulation can further improve the *in vivo* delivery of curcumin in prostate tumors.

American Association for Cancer Research
615 Chestnut St. 17th Floor
Philadelphia, PA 19106

β -Cyclodextrin-Curcumin Self-assembly Enhances Curcumin Delivery in Prostate Cancer Cells

Murali Mohan Yallapu¹, Meena Jaggi^{1,2} and Subhash C Chauhan^{1,2*}

¹Cancer Biology Research Center, Sanford Research/University of South Dakota, Sioux Falls, SD 57105, USA

²Department of OB/GYN and Basic Biomedical Science Division, Sanford School of Medicine, University of South Dakota, Sioux Falls, SD 57105, USA

Running Title: Cyclodextrin Mediated Curcumin Delivery to Cancer Cells

Key words: Curcumin, natural drug, drug delivery, cancer therapy, inclusion complex

*To whom correspondence should be addressed

Subhash C. Chauhan, PhD

Cancer Biology Research Center

Sanford Research/University of South Dakota

Department of OB/GYN and Basic Biomedical Science Division

Sanford School of Medicine, University of South Dakota

Sioux Falls, SD 57105

Phone: 605-328-0461, Fax: 605-328-0451

Email: chauhans@sanfordhealth.org (or) subhash.chauhan@usd.edu

Abstract

Curcumin, a hydrophobic polyphenolic compound derived from the rhizome of the herb *Curcuma longa*, possesses a wide range of biological applications which includes cancer therapy. However, its prominent application in cancer treatment is limited due to sub-optimal pharmacokinetics and poor bioavailability at the tumor site. In order to improve its hydrophilic and drug delivery characteristics, we have developed a β -cyclodextrin (CD) mediated curcumin drug delivery system *via* encapsulation technique. Curcumin encapsulation into the CD cavity was achieved by inclusion complex mechanism. Curcumin encapsulation efficiency was improved by increasing the ratio of curcumin to CD. The formations of CD-curcumin complexes were characterized by Fourier Transform Infra-red (FTIR), Differential Scanning Calorimetry (DSC), Thermo-gravimetric Analysis (TGA), Scanning Electron Microscope (SEM), and Transmission Electron Microscope (TEM) analyses. An optimized CD-curcumin complex (CD30) was evaluated for intracellular uptake and anti-cancer activity. Cell proliferation and clonogenic assays demonstrated that β -cyclodextrin-curcumin self-assembly enhanced curcumin delivery and improved therapeutic efficacy of curcumin in prostate cancer cells compared to free curcumin.

Key words: Curcumin, natural drug, inclusion complex, drug delivery, cellular uptake, cancer therapy

1. Introduction

The incidence of prostate cancer is much higher in males in Western countries (≥ 60.6 cases per 100,000) compared to Asian countries ($< 5-10$ cases per 100,000) [1, 2]. The current treatment for prostate cancer is a combination of surgery, radiation, and chemotherapy [3]. Clinically used therapeutic agents, such as mitoxantrone, estramustine, doxorubicin, etoposide, vinblastine, paclitaxel, carboplatin, vinorelbine, or combination drugs and anti-androgens, arrest the cancer growth and reduce symptoms, which ultimately improves quality of life [4-8]. All these chemotherapeutic agents, however, have shown enormous toxicity to normal organs that leads to severe side effects [4-6]. In addition, most of the chemotherapeutic agents may not kill all prostate cancer cells and their repeated administration develops drug resistance or androgen refractory stage which is most difficult to cure [9]. Therefore, an urgent need exists to develop new classes or better drug formulations to treat prostate cancer which have fewer side effects to normal organs.

Curcumin (CUR), bis(4-hydroxy-3-methoxyphenyl)-1,6-diene-3,5-dione, is a low molecular weight polyphenol yellow compound derived from the rhizome of the plant *Curcuma Longa* Linn. It has been widely used in traditional Ayurvedic and Chinese medicine since the second millennium BC. Curcumin has a wide range of pharmacological applications such as anti-inflammation, anti-human immunodeficiency virus, anti-microbial, anti-oxidant, anti-parasitic, anti-mutagenic and anti-cancer with low or no intrinsic toxicity [10-14]. Curcumin is a well studied natural compound due to its putative cancer prevention and anti-cancer activities which are mediated through influencing multiple signaling pathways [15-20]. The CUR inhibitory effects on protein kinase C [21-23], epidermal growth factor receptor tyrosine kinase [24, 25] and cytotoxicity activities have been demonstrated in various human cancer cell lines [26]. In

addition, CUR induces cell cycle arrest and/or apoptosis and blocks nuclear factor kappa B (NF- κ B) activity which is an important cellular target of cancer cells [27]. Clinical trials of CUR at a oral dose of up to 12 g per day for 3 months report no toxicity issues [13, 28, 29]. Despite all these extraordinary anti-cancer properties, curcumin suffers from low solubility in aqueous solution ($\approx 20 \mu\text{g/mL}$) and undergoes rapid degradation at physiological pH [30] which results in low systemic bioavailability, poor pharmacokinetics, and greatly hampers its *in vivo* efficacy [31].

To improve CUR application as anti-cancer agent, we need to improve its stability and solubility. In this regard, numerous formulations based on encapsulation in polymer nanoparticles or nanogels [32, 33], surfactants [34, 35], proteins [36], bilayers [37], phospholipids [38], and conjugates [39] have been generated. Alternatively, hybrid multi-component soluble carrier system bearing non-covalent bound drugs have been investigated [40, 41]. These systems not only improve drug solubility and stability but also provide drugs to the cancer cells in its active form. Among such carriers, cyclodextrins (α -, β -, γ -cyclodextrin) are widely used cyclic bucket shaped oligosaccharides linked by α -1,4-glycosidic bond to form macrocycle [42]. β -cyclodextrin has been selected for encapsulation of curcumin because it is a semi-natural product with extremely low toxicity and will enhance drug delivery through biological membranes [43]. In addition, some of the cyclodextrins are approved by FDA.

Therefore, in order to explore the cyclodextrin carrier properties for delivery of curcumin, we prepared a self-assembly of β -cyclodextrin and curcumin *via* inclusion complex mechanism [43] in which the cyclomaltoheptaose structure acts as a drug shuttle while hydroxyl groups of cyclodextrin impart good solubility to the system. The developed self-assemblies i.e., β -

cyclodextrin-curcumin (CD-CUR) inclusion complexes were confirmed by spectroscopy (FTIR, ¹H-NMR), thermal studies (DSC and TGA), X-ray diffraction and microscopic studies (SEM and TEM). An improved intracellular uptake of CD-CURs by cancer cells was observed. The anti-cancer efficacy of these formulations was evaluated by cell proliferation and clonogenic assays.

2. Materials and methods

2.1. Materials

β-cyclodextrin, curcumin (≥95% purity, (E,E)-1,7-bis(4-Hydroxy-3-methoxyphenyl)-1,6-heptadiene-3,5-dione), acetone (≥99.5, ACS reagent grade), dimethylsulfoxide (ACS reagent, UV spectrophotometry grade, ≥99.9%) were purchased from Sigma Chemical Co. (St Louis, MO, USA).

2.2. Preparation of inclusion complexes

β-cyclodextrin (CD) (40 mg) was dissolved in 8 mL deionized (DI) water in a 20 mL glass vial (Fisher Scientifics, Pittsburg, PA, USA) containing a magnetic bar. To this solution, different amounts of curcumin [2 mg (5%), 4 mg (10%), 8 mg (20%) and 12 mg (30%)] in 500 μL acetone were added under stirring at 400 rpm. Stirring was allowed without cap to evaporate the acetone. The solution was stirred overnight, centrifuged at 1000 rpm for 5 min, and a supernatant containing highly water soluble β-cyclodextrin-curcumin (CD-CUR) inclusion complexes was recovered by freeze drying (Labconco Freeze Dry System, Labconco, Kansas City, MO, USA; -48°C, 133 x 10⁻³ mBar). The CD-CUR inclusion complexes were stored at 4°C until further use. The resulted CD-CUR inclusion complexes were designated as CD5, CD10, CD20 and CD30 based on the % of CUR employed in the preparations.

2.3. Determination of curcumin (CUR) loading

Accurately weighted dry lyophilized CD-CUR inclusion complexes were dissolved in 1 mL dimethylsulfoxide (DMSO) to extract or dissolve CUR in DMSO for the loading/encapsulation estimations. The CD-CUR inclusion complex samples in DMSO were gently shaken on a shaker (Labnet S 2030-RC, RPM 150, Labnet International, Woodbridge, NJ) for 24 hrs at room temperature in the dark. The DMSO containing inclusion complex solutions were centrifuged at 14,000 rpm (Centrifuge 5415D, Eppendorf AG, Hamburg, Germany) and supernatant was collected. Supernatant (20 μ L) was diluted to 1 mL in DMSO and used for the estimations. The CUR concentrations were determined by a standard UV-Vis spectrophotometer method (Biomate 3, Thermo Electron Corporation, Hudson, NH, USA) at 450 nm, as described earlier [32]. A standard plot of CUR in DMSO (0-10 μ g/mL) was prepared under identical conditions. The CUR loading/encapsulation was calculated as follows: *CUR loading = (CUR recovered in CD-CUR complex/CD-CUR complex recovered)*.

2.4. Compatibility of CD-CUR inclusion complexes

To determine compatibility of CD-CUR inclusion complexes, an optical microscopy study was performed. For this study, CD10, CD20 and CD30 of CD-CUR inclusion complexes, CUR and β -cyclodextrin of equivalent concentration aqueous solutions (500 μ g/mL) were prepared. Two drops of these solutions were placed on a glass slide and allowed to dry under fume hood overnight. Care was taken to protect from light and not deposit any dust on glass slides. These cover slides containing samples were analyzed using optical microscopy (Olympus BX 41

microscope (Olympus, Center Valley, PA, USA). All the images were taken at 200X magnification.

2.5. *In vitro* stability of CD-CUR inclusion complexes

10 mg of curcumin containing CD-CUR inclusion complexes (CD5, CD10, CD20 and CD30) were dispersed in 5 mL of physiological buffer (1XPBS, 0.01 M PBS, pH 7.4). These suspensions were incubated at 37°C under gentle shaking on a shaker (Labnet S 2030-RC, RPM 150, Labnet International, Woodbridge, NJ). Curcumin retention was determined at different time intervals. The % curcumin retention was calculated using the following equation: $\% \text{ CUR retention} = [(CUR \text{ in inclusion complex} - \text{Released curcumin}) / (CUR \text{ inclusion complex})] \times 100$.

2.6. Characterization

Fourier Transform Infrared (FTIR) spectroscopy: FTIR spectra of CD, CUR and CD-CUR inclusion complexes were performed using a Smiths Detection IlluminatIR FT-IR microscope (Danbury, CT, USA) with diamond ATR objective. FTIR spectra of samples were acquired by placing fluffy powder on the tip of the ATR. Data was acquired between 4000 – 750 cm^{-1} at a scanning speed of 4 cm^{-1} and 32 scans. The average of 32 scans data was presented as FTIR spectra.

$^1\text{H-NMR}$ spectroscopy: All spectra were recorded in $\text{DMSO-}d_6$ using Bruker Avance DRX 500 MHz NMR spectrophotometer (Bruker BioSpin Corp., Billerica, MA, USA). The following parameters were used during the NMR experiments: number of scans, 64; relaxation delay, 1.0s; and pulse degree, 25°C. The chemical shifts are presented in terms of ppm with tetramethylsilane (TMS) as the internal reference.

Differential Scanning Calorimetry (DSC): DSC analysis of CD, CUR and CD-CUR inclusion complexes were performed using TA Instruments Q200 Differential Scanning Calorimeter (TA Instruments, New Castle, Delaware, USA) at The Applied Polymer Research Center, The University of Akron (Project # 139-10APRC). The cell constant calibration method was employed to study the DSC patterns of the samples from 25°C to 300°C at a heating ramp of 10°C, under a constant flow (100 mL/min) of nitrogen gas.

Thermo-gravimetric Analysis (TGA): The thermal history of CD, CUR and CD-CUR inclusion complexes were evaluated on a TA Instruments Q50 Thermogravimetric Analyzer (TA Instruments, New Castle, Delaware, USA) at The Applied Polymer Research Center, The University of Akron (Project # 139-10APRC) from 25°C to 700°C at a heating ramp of 10°C, under a constant flow (100 mL/min) of nitrogen gas. This study followed 20STD800 standard rubber analysis method.

X-ray Diffraction: X-ray diffraction measurements of CD, CUR and CD-CUR inclusion complexes were recorded using a D/Max – B Rigaku diffractometer (Rigaku Americas Corp, Woodlands, TX) using Cu radiation at $\lambda = 0.1546$ nm, running at 40 kV and 40 mA. For this study, samples were mounted on double sided silicone tape and measurements were performed from 20° to 80° at a scan speed of 2° per minute.

Scanning Electron Microscopy (SEM): The surface morphology of CD, CUR and CD-CUR inclusion complexes was studied using a Quanta 450 Scanning Electron Microscope (S.No.

D9234, FEI™, Hillsboro, Oregon) at an accelerating voltage of 5 kV. All the dry samples were spread on double sided carbon tape, mounted on SEM stage before scanning.

Transmission Electron Microscopy (TEM): Transmission Electron Microscopy was employed to view the exact morphology of samples suspended in water. To prepare TEM samples, 2–3 drops of aqueous solutions of CD-CUR inclusion complexes on a 200 mesh formvar-coated copper TEM grid (grid size: 97 μm) (Ted Pella, Inc., Redding, CA, USA) followed by removing excess solution using a piece of fine filter paper and the samples were allowed to dry in air overnight prior to image particles. The morphology of samples was observed under JEOL-1210 transmission electron microscope (JEOL, Tokyo, Japan) operating at 60 kV.

2.7. Cell culture

Prostate cancer cells lines C4-2, DU-145, PC-3 cells were generously provided by Dr. Meena Jaggi. These cells were maintained as monolayer cultures (C4-2 and PC-3) in RPMI-1640 medium or in MEM medium (DU-145) (Hycone Laboratories, Inc., Logan, UT) and supplemented with 10% fetal bovine serum (Atlanta Biologicals, Lawrenceville, GA) and 1% penicillin-streptomycin (Gibco BRL, Grand Island, NY) at 37°C in a humidified atmosphere (5% CO₂).

2.8. CUR and CD-CUR inclusion complexes cellular uptake

For a comparative visualization of CUR and CD-CUR inclusion complexes uptake in cancer cells, 5×10^5 cells were seeded in 6-well plates in 2 mL medium. After cells were attached to the plate, media was replaced with 20 μg free curcumin or equivalent curcumin containing CD-CUR

inclusion complexes. After 6 hrs, cells were examined under an Olympus BX 51 fluorescence microscope (Olympus, Center Valley, PA).

To investigate which CD-CUR inclusion complex has superior CUR uptake, prostate cancer cells (5×10^5) were seeded in 6-well plates (2 mL medium), and allowed overnight to attach. Cells were then treated with 10 μg or 20 μg CUR in each well or equivalent CD-CUR inclusion complexes. After 2 days cells were washed twice with 1X PBS, trypsinized, centrifuged and collected in 2 mL media. The cell suspension (50 μl) was injected into Accuri C6 flow cytometer (Accuri Cytometers, Inc., Ann Arbor, MI, USA) to determine the fluorescence levels in FL1 channel (488 excitation, Blue laser, 530 ± 15 nm, FITC/GFP).

2.9. *In vitro* cytotoxicity (MTS assay)

To examine the anti-tumor activity of the CD-CUR inclusion complex (CD-30), cell proliferation assays were performed using C4-2, DU-145 and PC-3 prostate cancer cell lines. Prostate cancer cells (5000 cells/well in 100 μL media) were seeded in 96-well plates and allowed to attach overnight. The next day the media was replaced with different concentrations (5-40 μM) of CUR or CD30. PBS or DMSO equivalent amounts containing media were used as the control. After day 2 replaced with fresh media and the anti-proliferative effect of the CUR and CD30 was determined using a standard 3-(4,5-dimethylthiazol-2-yl)-2,5-diphenyltetrazolium bromide (MTS) based colorimetric assay (CellTiter 96 AQueous, Promega, Madison, WI). The reagent (25 μL /well) was added to each well and plates were incubated for 3 hrs at 37°C. The color intensity was measured at 492 nm using a microplate reader (BioMate 3 UV-Vis spectrophotometer, Thermo Electron Corporation, Hudson, NH). The anti-proliferative effect of CUR and CD30 treatments was calculated as a percentage of cell growth with respect to the DMSO and PBS controls. Just

before adding MTS reagents, representative phase contrast microscope images of cells were taken using an Olympus BX 41 microscope (Olympus, Center Valley, PA, USA).

2.10. Colony formation assay

Prostate cancer cells (1000) were seeded in 2 mL media in 6-well plates and allowed 2-3 days to attach and initiate the colony formations. Then cells were treated with different concentrations (2-10 μ M) of CUR or CD30 over a period of 10 days. The plates were then washed twice with PBS, fixed in chilled methanol, stained with hematoxylin (Fisher Scientific, Fair Lawn, NJ, USA), washed with water and air dried. The number of colonies was counted by a MultiImageTM Cabinet (Alpha Innotech Corporation, San Leandro, CA, USA) using AlphaEase Fc software. The percent of colonies were calculated using the number of colonies formed in treatment divided by number of colonies formed in DMSO or PBS controls.

2.11. Statistical analysis

All results were processed using Microsoft Excel 2007 software and expressed as mean \pm standard error of the mean (S.E.M.). Statistical analyses were performed using an unpaired, two tailed student t-test. A value of $p < 0.05$ was considered as significant. All the graphs were plotted using Origin 6.1 software.

3. Results and discussion

The main focus of the present study was to develop a β -cyclodextrin-curcumin (CD-CUR) self-assembly to enhance the efficacy of curcumin for prostate cancer treatment. It has been reported previously that supramolecular chemistry of β -cyclodextrin offers water soluble inclusion complexes with different drug molecules including anti-cancer chemotherapeutic agents [44-49].

Until now, only a few studies have dealt with increasing the stability and solubility characteristics of CUR to improve bioavailability through CD-CUR inclusion complexes [50-53]. Additionally, no report has focused on the anti-cancer properties of this formulation in prostate cancer cells. In this study, we have explored a supramolecular chemistry approach to stabilize/solubilize curcumin *via* solvent evaporation encapsulation technique (Figure 1).

This technique allows us to load or encapsulate different amounts of curcumin into β -cyclodextrin cavities. The loading capacity of CUR in CD cavities increased from CD5 to CD30 (Figure 2). The self-assembly process normally results in higher entrapment compared to drug encapsulation into nanoparticles. In the case of nanoparticles, only 5-10% of loading is possible with respect to weight of nanoparticles [32, 33, 53]. This lower drug loading capacity is only suitable for first line chemotherapeutic agents (doxorubicin, paclitaxol, cisplatin, dexamethasone, etc.) because even nanomolar concentrations of drugs will act efficiently to kill cancer cells. On the other hand, second line natural therapeutic agents (including curcumin) relatively higher doses to kill cancer cells; therefore, large amount of nanoparticles carrier is required where the nanoparticles also give some toxicity to the cells. Thus, the current self-assembly process appears to be suitable for second line therapeutic agents. According to our study up to 25% of CUR can be encapsulated into the β -CD inclusion complexes.

The CD-CUR self-assemblies have shown improvement in the aqueous solubility of curcumin. The pure CUR solubility in PBS solution is $\sim 20 \mu\text{g/mL}$. It has been determined that the solubility of CD-CUR inclusion complexes are 1.48, 1.62, 1.76 and 1.84 mg of curcumin equivalent CD5, CD10, CD20 and CD30, respectively. This behavior can be seen in Figure 1C. A previous study on β -curcumin-CD complex in water reports up to 0.6 mg/mL of CUR. The compatibility study also revealed that CD and CUR compounds were dispersed in CD-CUR

complexes while CUR in aqueous dispersions exhibited clumps (Figure 3A). In addition, these CD-CUR inclusion complexes have shown high *in vitro* stability at physiological conditions (Figure 3B) whereas CUR did not showed much stability [30,34,51]. The order of stability was noticed as CD30 > CD20 \geq CD10 > CD5. Only 10% of drug is precipitated in the case of CD30 while CUR precipitates almost 100%.

3.1. Physical characterization of CD-CUR inclusion complexes

3.1.1. Spectral studies

FTIR spectroscopy was used to ascertain the formation of CD-CUR inclusion complex. The solid samples were recorded for FTIR. The FTIR spectra of CD, CUR and CD-CUR inclusion complex are represented in Figure 4A. The FTIR spectrum of curcumin exhibited an absorption band at 3496 cm^{-1} attributed to the phenolic O-H stretching vibration. Additionally, sharp absorption bands at 1605 cm^{-1} (stretching vibrations of benzene ring of CUR), 1502 cm^{-1} (C=O and C=C vibrations of CUR), 1435 cm^{-1} (olefinic C-H bending vibration), 1285 cm^{-1} (aromatic C-O stretching vibrations), and 1025 cm^{-1} (C-O-C stretching vibrations of CUR) were noticed. CD has showed characteristic peaks at 3325 cm^{-1} and 1025 cm^{-1} due to the O-H stretching vibrations and C-O-C stretching vibrations. In the case of CD-CUR inclusion complex spectrum the sharp peaks belonging to CUR have disappeared and only CD characteristic peaks are visible. CD-CUR inclusion complex have shown all the peaks belonging to CD and also some of the curcumin peaks between 1 and 2 ppm (Figure 4B) [54]. However, still specific peaks of CUR between 5 and 7 ppm are not visible, which is a typical pattern of inclusion complex. This data indicate the successful formation of inclusion complexes.

3.1.2. Microscopy studies

The overall bulk surface morphology of CD, CUR and CD-CUR inclusion complexes (for powder) was studied by SEM (Figure 5). CD shows flake-like structures throughout the sample while CUR exhibited crystal-like structures. However, CD-CUR inclusion complexes demonstrated apparent change in the flakes structures due to curcumin encapsulation in their cavities. Further, these flake structures become smaller with increase of CUR content to CD. This alteration of crystal and powder structures suggests the formation of inclusion complexes. The TEM analysis of CD, CUR and CD-CUR complex samples in solution provides the exact assembly or inclusion complexation process (Figure 6). The CD5 formulation shows less than 100 nm irregular assemblies with a few larger clusters. This cluster formation was increased with increase of CUR in CD inclusion complexation (CD10 to CD 30) (Figure 6A). At higher concentration of CUR in CD, complexation results in formation of nanoparticles \approx 500 nm. From the TEM study it is clear that the nano- or self-assembly or inclusion complexation process between cyclodextrin and curcumin occurred *via* van der Waals interaction, hydrogen bonding and hydrophobic interactions. Possible mechanisms are proposed for CD-CUR nano-assembly or inclusion complex formation in Figure 6B (a, b) (need some more information about fig 6B a, b). During this process, release of high energy water molecules from the cavity of CD and enters curcumin molecule. The feasibility of entire process was reported for various binary complexes of curcumin with hydrophobic molecule of CD [52].

3.1.3. Physical state of complexes

X-ray diffraction (XRD) and thermal methods (DSC and TGA) are useful tools in identifying the physical state of drugs that exist in various polymers, complexes and nanoparticles. In particular,

complexation of a drug and cyclodextrin or polymer results in the absence/shifting of endothermic peaks, indicating a change in the crystal lattice, melting, boiling, or sublimation points. Therefore, these measurements can provide both qualitative and quantitative information of drug present in the inclusion complexes.

X-ray diffraction patterns of CD, CUR and CD-CUR inclusion complexes are presented in Figure 7A. Curcumin has displayed the characteristic crystalline peaks between 20 and 30 (21.26, 23.35, 24.68 and 26.54°). Few crystalline peaks were also noticed for CD. However, CD-CUR inclusion complex did not contain any such crystalline peaks, suggesting the formation of inclusion complex with CD and conversion into amorphous form. This is in accordance with previous reports of CD inclusion complexes [33, 52]. The DSC thermograms of CD, CUR and CD-CUR inclusion complexes are shown in Figure 7B. CD and CUR have shown individual endothermic peaks at 99.5°C and 172°C, respectively, due to their melting points. Whereas in the case of CD-CUR inclusion complex, prominent peaks belonging to CUR at 172°C completely disappeared and also lowered the CD melting peak to 86.5°C compared to 99.5°C. This can be attributed to the drug molecules being completely included into the cavity of CD by replacing water molecules. Further, this behavior is an indication of stronger interactions between CD and CUR in solid state. In addition, an improved thermal stability was obtained for CD-CUR inclusion complex compared to CD (Figure 7C). This was due to CUR inclusion complexation with CD.

Our studies (section 3.1.1. to 3.1.4) clearly demonstrate the formation of CD-CUR inclusion complexes by various self-assemblies depending on the composition. It was also observed in a previous study that complex formation of curcumin and cyclodextrin is highly favored by Gibbs' free energy law [52] which states that CD solutions offer a favorable environment over water for

curcumin. The lyophilic cavity of CD protects the lipophilic guest molecule (in this case curcumin) from aqueous environment, while the polar outer surface of the CD molecules provides the stabilization effect. It has been confirmed that the polarity of the CD cavity is equivalent to 40% solution of ethanol in water [55]. This particular characteristic prompted the use of CD in various pharmaceutical preparations. Here our main aim is to employ these self-assemblies of CD-CUR inclusion complexes as anti-cancer agents.

3.2. Cellular uptake

For passive targeting of cancerous tissues, drug loaded cyclodextrins should be able to retain the drug for a prolonged time in circulation [56-58]. Curcumin itself has an inherent green fluorescence property which we have utilized in the cellular uptake studies (Figure 8A). The microscope images of control cells without curcumin and cells incubated with cyclodextrin did not show any fluorescence. Whereas, the images of cells treated with CD-CUR inclusion complexes exhibited relatively more green fluorescence compared to free curcumin treated cells. This data suggest that CD-CUR inclusion complexes enhanced curcumin uptake in the cancer cells. In order to determine an exact internalization capability of various CD-CUR inclusion complexes, FACS analysis was performed and compared with free curcumin uptake.

Cellular uptake or retention of CUR and all CD-CUR inclusion complexes was investigated by FACS to determine which particular complex has a better endocytosis in prostate cancer cells. For this study, DU145 cells were incubated with 10 μ g CUR/CD-CUR formulations for 1 and 2 days. The relative fluorescence values demonstrate a significant increase of intracellular drug uptake of CD-CUR inclusion complexes by cancer cells compared to CUR (Figure 8B (a)). This

phenomenon was progressively increased from CD5 to CD30 inclusion complex. Since CD30 formulations have higher amounts of CUR per CD molecule they have exhibited highest uptake. However, we did not observe uptake difference between day 1 and day 2, indicating a rapid uptake process. On the other hand, this data also suggest that even after 2 days the endocytosed drug is in active form. The uptake is dependent upon concentration of the CUR/CD-CUR inclusion complex employed (Figure 8B (b)). Further, it can be speculated that CD30 may exhibit enhanced cytotoxicity compared to CUR or CD-CUR inclusion complexes (CD5, CD10 and CD20) due to prolonged retention of CUR in the cells. Therefore, CD-30 formulation was used for *in vitro* cytotoxicity assays (MTS assay and clonogenic assay) in different prostate cancer cell lines.

3.3. Effect of CUR and CD30 in cell viability and colony formation of cancer cells

In order to evaluate anti-tumor efficacy of the CUR and CD30 (CD-CUR inclusion complex), cell proliferation assay was performed in four different prostate cancer cell lines ([DU145 (non-metastatic), C4-2 and PC3 (metastatic cell lines)]. These cells were incubated with equivalent doses of 2.5-40 μ M CUR or CD30 for 2 days and then examined by MTS assay for cell proliferation. Control cells were treated with equivalent amounts of DMSO or PBS. Both CUR and CD30 have shown a dose dependent anti-proliferative effect in all tested cancer cells (Figure 9).

The comparative anti-cancer effects of CD30 and CUR is also evident in phase contrast microscopy analysis (Figure 10A). From these images it can be concluded that CUR treatment resulted in a moderate decrease in cell number while CD30 not only reduced cell number but also imparted morphological change related to apoptosis. In general, therapeutic efficacy of any

chemotherapeutic drug can be achieved by an efficient delivery into the cytoplasm. This results only when the drug release in its active form is taken up by cancer cells. We expect that due to self-assembly of CD and CUR, CUR is accumulated, retained, and released in a sustained manner in the cancer cells which causes pronounced effects over free CUR. In this case, CD30 must exhibit its superior effects on cellular and molecular pathways. Therefore, we have investigated the expression of PARP (**Poly (ADP-ribose) polymerase** which is a [protein](#) involved in a number of [cellular](#) processes involving mainly [DNA repair](#) and [programmed cell death](#)) in prostate cancer cells treated with 10 and 20 μM CUR or equivalent amounts of CD30. The effects of these treatments can be seen in our molecular pathways studies (Figure 10B). We found that CD30 treatment considerably full length PARP (apoptosis associated proteins, 116 kDa) into cleaved PARP (86 kDa), as a result allow cells to undergo cell death. In addition, these self-assemblies may also overcome membrane associated efflux transporter protein and drug resistance [59].

In addition, to evaluate long-term anti-cancer efficacy of CUR and CD30, colony forming assays (clonogenic assays) were performed in C4-2, DU145 and PC3 prostate cancer cell lines. These cells were either treated with equivalent doses (2-10 μM), CD or CUR or CD30 or DMSO and density of colonies was measured (Figure 8A). Similar to cell proliferation studies, CD30 treatment showed a better therapeutic efficacy compared to free curcumin in colony formation assays in all three cell lines (Figure 11). These data suggest an enhanced efficacy of CD30 formulation compared to free curcumin. Future studies, however, are warranted to investigate the efficacy of this formulation in pre-clinical and clinical models.

4. Conclusions

In this study, we have demonstrated feasibility of β -cyclodextrin and curcumin self-assembly *via* inclusion complexation by using a solvent evaporation technique. Our study showed that curcumin was efficiently encapsulated in β -cyclodextrin cavities and formed different types of self-assemblies. The inclusion complex formation was confirmed by spectral, thermal, X-ray diffraction and electron microscopy studies. CD-CUR inclusion complex (CD30) showed an improved uptake by DU145 cancer cells compared to free CUR. Additionally, this formulation demonstrated greater potent therapeutic efficacy in prostate cancer cells versus free CUR. Our studies suggest that CD30 formulation can be an effective drug formulation for prostate cancer therapy.

Acknowledgements

The authors thank Cathy Christopherson (Sanford Research/USD) for editorial assistance. We acknowledge Robert Japs (Sanford Health), Sara Basiaga (Department of Chemistry, UN-Lincoln), Shah Valloppilly (Nebraska Center for Materials and Nanoscience, UN-Lincoln) and Crittenden J. Ohlemacher (Applied Polymer Research Center, University of Akron) their help in characterization of our samples. We also thank Dr. Diane Maher, Dr. Vasudha Sundram and Mara Ebeling (Sanford Research/USD) for their suggestions throughout the current study. This work was supported in part by a Sanford Research/USD grant and Department of Defense Grants awarded to SCC (PC073887) and MJ (PC073643).

References

[1] M. Garcia, A. Jemal, E. M. Ward, M. M. Center, Y. Hao, R. L. Siegel and M. J. Thun, Global Cancer Facts & Figures 2007. , (2007) 1-46.

- [2] A. Jemal, R. Siegel, E. Ward, Y. Hao, J. Xu and M. J. Thun, Cancer statistics, 2009, *CA Cancer J Clin*, 59 (2009) 225-249.
- [3] M. Kohli and D. J. Tindall, New developments in the medical management of prostate cancer, *Mayo Clin Proc*, 85 (2010) 77-86.
- [4] R. Autorino, G. Di Lorenzo, R. Damiano, S. De Placido and M. D'Armiento, Role of chemotherapy in hormone-refractory prostate cancer. Old issues, recent advances and new perspectives, *Urol Int*, 70 (2003) 1-14.
- [5] W. R. Berry, The evolving role of chemotherapy in androgen-independent (hormone-refractory) prostate cancer, *Urology*, 65 (2005) 2-7.
- [6] E. D. Crawford, Summary: the role of the urologist in chemotherapy of hormone refractory prostate cancer, *Urology*, 54 (1999) 51-52.
- [7] W. K. Oh, M. H. Tay and J. Huang, Is there a role for platinum chemotherapy in the treatment of patients with hormone-refractory prostate cancer?, *Cancer*, 109 (2007) 477-486.
- [8] D. P. Petrylak, The current role of chemotherapy in metastatic hormone-refractory prostate cancer, *Urology*, 65 (2005) 3-7; discussion 7-8.
- [9] S. Urakami, H. Shiina, M. Sumura, S. Honda, K. Wake, T. Hiraoka, S. Inoue, N. Ishikawa and M. Igawa, Long-term control or possible cure? Treatment of stage D2 prostate cancer under chemotherapy using cisplatin and estramustine phosphate followed by maximal androgen blockade, *Int Urol Nephrol*, 40 (2008) 365-368.
- [10] G. Bar-Sela, R. Epelbaum and M. Schaffer, Curcumin as an Anti-Cancer Agent: Review of the Gap between Basic and Clinical Applications, *Curr Med Chem*, (2009).
- [11] J. S. Jurenka, Anti-inflammatory properties of curcumin, a major constituent of *Curcuma longa*: a review of preclinical and clinical research, *Altern Med Rev*, 14 (2009) 141-153.

- [12] R. K. Maheshwari, A. K. Singh, J. Gaddipati and R. C. Srimal, Multiple biological activities of curcumin: a short review, *Life Sci*, 78 (2006) 2081-2087.
- [13] A. S. Strimpakos and R. A. Sharma, Curcumin: preventive and therapeutic properties in laboratory studies and clinical trials, *Antioxid Redox Signal*, 10 (2008) 511-545.
- [14] R. A. Sharma, W. P. Steward and A. J. Gescher, Pharmacokinetics and pharmacodynamics of curcumin, *Adv Exp Med Biol*, 595 (2007) 453-470.
- [15] B. K. Jaggi, S. C. Chauhan and M. Jaggi, Review of Curcumin Effects on Signaling Pathways in Cancer, *Proceedings of the South Dakota Academy of Science*, 86 (2007) 283-293.
- [16] S. Karmakar, N. L. Banik, S. J. Patel and S. K. Ray, Curcumin activated both receptor-mediated and mitochondria-mediated proteolytic pathways for apoptosis in human glioblastoma T98G cells, *Neurosci Lett*, 407 (2006) 53-58.
- [17] S. Shishodia, H. M. Amin, R. Lai and B. B. Aggarwal, Curcumin (diferuloylmethane) inhibits constitutive NF-kappaB activation, induces G1/S arrest, suppresses proliferation, and induces apoptosis in mantle cell lymphoma, *Biochem Pharmacol*, 70 (2005) 700-713.
- [18] G. Sa and T. Das, Anti cancer effects of curcumin: cycle of life and death, *Cell Div*, 3 (2008) 14.
- [19] P. Anand, C. Sundaram, S. Jhurani, A. B. Kunnumakkara and B. B. Aggarwal, Curcumin and cancer: an "old-age" disease with an "age-old" solution, *Cancer Lett*, 267 (2008) 133-164.
- [20] T. Dorai and B. B. Aggarwal, Role of chemopreventive agents in cancer therapy, *Cancer Lett*, 215 (2004) 129-140.
- [21] M. Hasmeda and G. M. Polya, Inhibition of cyclic AMP-dependent protein kinase by curcumin, *Phytochemistry*, 42 (1996) 599-605.

- [22] J. K. Lin, Suppression of protein kinase C and nuclear oncogene expression as possible action mechanisms of cancer chemoprevention by Curcumin, *Arch Pharm Res*, 27 (2004) 683-692.
- [23] J. Epstein, G. Docena, T. T. Macdonald and I. R. Sanderson, Curcumin suppresses p38 mitogen-activated protein kinase activation, reduces IL-1beta and matrix metalloproteinase-3 and enhances IL-10 in the mucosa of children and adults with inflammatory bowel disease, *Br J Nutr*, (2009) 1-9.
- [24] T. Dorai, N. Gehani and A. Katz, Therapeutic potential of curcumin in human prostate cancer. II. Curcumin inhibits tyrosine kinase activity of epidermal growth factor receptor and depletes the protein, *Mol Urol*, 4 (2000) 1-6.
- [25] R. L. Hong, W. H. Spohn and M. C. Hung, Curcumin inhibits tyrosine kinase activity of p185neu and also depletes p185neu, *Clin Cancer Res*, 5 (1999) 1884-1891.
- [26] B. B. Aggarwal, A. Kumar and A. C. Bharti, Anticancer potential of curcumin: preclinical and clinical studies, *Anticancer Res*, 23 (2003) 363-398.
- [27] A. C. Bharti, N. Donato, S. Singh and B. B. Aggarwal, Curcumin (diferuloylmethane) down-regulates the constitutive activation of nuclear factor-kappa B and IkappaBalpha kinase in human multiple myeloma cells, leading to suppression of proliferation and induction of apoptosis, *Blood*, 101 (2003) 1053-1062.
- [28] H. Hatcher, R. Planalp, J. Cho, F. M. Torti and S. V. Torti, Curcumin: from ancient medicine to current clinical trials, *Cell Mol Life Sci*, 65 (2008) 1631-1652.
- [29] R. G. Tunstall, R. A. Sharma, S. Perkins, S. Sale, R. Singh, P. B. Farmer, W. P. Steward and A. J. Gescher, Cyclooxygenase-2 expression and oxidative DNA adducts in murine intestinal

adenomas: modification by dietary curcumin and implications for clinical trials, *Eur J Cancer*, 42 (2006) 415-421.

[30] Y. J. Wang, M. H. Pan, A. L. Cheng, L. I. Lin, Y. S. Ho, C. Y. Hsieh and J. K. Lin, Stability of curcumin in buffer solutions and characterization of its degradation products, *J Pharm Biomed Anal*, 15 (1997) 1867-1876.

[31] P. Anand, A. B. Kunnumakkara, R. A. Newman and B. B. Aggarwal, Bioavailability of curcumin: problems and promises, *Mol Pharm*, 4 (2007) 807-818.

[32] S. Bisht, G. Feldmann, S. Soni, R. Ravi, C. Karikar, A. Maitra and A. Maitra, Polymeric nanoparticle-encapsulated curcumin ("nanocurcumin"): a novel strategy for human cancer therapy, *J Nanobiotechnology*, 5 (2007) 3.

[33] J. Shaikh, D. D. Ankola, V. Beniwal, D. Singh and M. N. Kumar, Nanoparticle encapsulation improves oral bioavailability of curcumin by at least 9-fold when compared to curcumin administered with piperine as absorption enhancer, *Eur J Pharm Sci*, 37 (2009) 223-230.

[34] H. H. Tonnesen, Solubility, chemical and photochemical stability of curcumin in surfactant solutions. *Studies of curcumin and curcuminoids, XXVIII, Pharmazie*, 57 (2002) 820-824.

[35] Z. Wang, M. H. Leung, T. W. Kee and D. S. English, The Role of Charge in the Surfactant-Assisted Stabilization of the Natural Product Curcumin, *Langmuir*, (2009).

[36] M. H. Leung and T. W. Kee, Effective stabilization of curcumin by association to plasma proteins: human serum albumin and fibrinogen, *Langmuir*, 25 (2009) 5773-5777.

[37] H. I. Ingolfsson, R. E. Koeppe, 2nd and O. S. Andersen, Curcumin is a modulator of bilayer material properties, *Biochemistry*, 46 (2007) 10384-10391.

- [38] K. Maiti, K. Mukherjee, A. Gantait, B. P. Saha and P. K. Mukherjee, Curcumin-phospholipid complex: Preparation, therapeutic evaluation and pharmacokinetic study in rats, *Int J Pharm*, 330 (2007) 155-163.
- [39] A. Safavy, K. P. Raisch, S. Mantena, L. L. Sanford, S. W. Sham, N. R. Krishna and J. A. Bonner, Design and development of water-soluble curcumin conjugates as potential anticancer agents, *J Med Chem*, 50 (2007) 6284-6288.
- [40] K. T. Al-Jamal, C. Ramaswamy and A. T. Florence, Supramolecular structures from dendrons and dendrimers, *Adv Drug Deliv Rev*, 57 (2005) 2238-2270.
- [41] O. M. Koo, I. Rubinstein and H. Onyuksel, Role of nanotechnology in targeted drug delivery and imaging: a concise review, *Nanomedicine*, 1 (2005) 193-212.
- [42] J. Szejtli, Introduction and General Overview of Cyclodextrin Chemistry, *Chem Rev*, 98 (1998) 1743-1754.
- [43] G. Horvath, T. Premkumar, A. Boztas, E. Lee, S. Jon and K. E. Geckeler, Supramolecular nanoencapsulation as a tool: solubilization of the anticancer drug trans-dichloro(dipyridine)platinum(II) by complexation with beta-cyclodextrin, *Mol Pharm*, 5 (2008) 358-363.
- [44] T. Cserhati, E. Forgacs and J. Hollo, Interaction of taxol and other anticancer drugs with alpha-cyclodextrin, *J Pharm Biomed Anal*, 13 (1995) 533-541.
- [45] P. Y. Grosse, F. Bressolle, P. Rouanet, J. M. Joulia and F. Pinguet, Methyl-beta-cyclodextrin and doxorubicin pharmacokinetics and tissue concentrations following bolus injection of these drugs alone or together in the rabbit, *Int J Pharm*, 180 (1999) 215-223.

- [46] M. Jumaa, B. Carlson, L. Chimilio, S. Silchenko and V. J. Stella, Kinetics and mechanism of degradation of epothilone-D: an experimental anticancer agent, *J Pharm Sci*, 93 (2004) 2953-2961.
- [47] N. J. Medlicott, K. A. Foster, K. L. Audus, S. Gupta and V. J. Stella, Comparison of the effects of potential parenteral vehicles for poorly water soluble anticancer drugs (organic cosolvents and cyclodextrin solutions) on cultured endothelial cells (HUV-EC), *J Pharm Sci*, 87 (1998) 1138-1143.
- [48] F. Quaglia, L. Ostacolo, A. Mazzaglia, V. Villari, D. Zaccaria and M. T. Sciortino, The intracellular effects of non-ionic amphiphilic cyclodextrin nanoparticles in the delivery of anticancer drugs, *Biomaterials*, 30 (2009) 374-382.
- [49] J. J. Torres-Labandeira, P. Davignon and J. Pitha, Oversaturated solutions of drug in hydroxypropylcyclodextrins: parenteral preparation of pancratistatin, *J Pharm Sci*, 80 (1991) 384-386.
- [50] E. M. Bruzell, E. Morisbak and H. H. Tonnesen, Studies on curcumin and curcuminoids. XXIX. Photoinduced cytotoxicity of curcumin in selected aqueous preparations, *Photochem Photobiol Sci*, 4 (2005) 523-530.
- [51] H. H. Tonnesen, M. Masson and T. Loftsson, Studies of curcumin and curcuminoids. XXVII. Cyclodextrin complexation: solubility, chemical and photochemical stability, *Int J Pharm*, 244 (2002) 127-135.
- [52] V. R. Yadav, S. Suresh, K. Devi and S. Yadav, Effect of cyclodextrin complexation of curcumin on its solubility and antiangiogenic and anti-inflammatory activity in rat colitis model, *AAPS PharmSciTech*, 10 (2009) 752-762.

- [53] C. Daniela, G. Marina, T. Michele, E. C. Maria, C. G. Emanuela and C. Giancarlo, Influence of α - and γ -cyclodextrin lipophilic derivatives on curcumin-loaded SLN, *J Incl Phenom Macrocycl Chem*, 65 (2009) 391-402.
- [54] M. B. A. Gloria, L. Peret-Almeida, R. J. Alves, L. Dufosse and A. P. F. Cherubino, Separation and determination of the physico-chemical characteristics of curcumin, demethoxycurcumin and bisdemethoxycurcumin, *Food Res Inter*, 38 (2005) 1039-1044.
- [55] K. H. Fromming and J. Szejtli, *Cyclodextrins in pharmacy*, Kluwer Academic, Dordrecht, 1994.
- [56] B. McCormack and G. Gregoriadis, Entrapment of cyclodextrin-drug complexes into liposomes: potential advantages in drug delivery, *J Drug Target*, 2 (1994) 449-454.
- [57] P. Caliceti, S. Salmaso, A. Semenzato, T. Carofiglio, R. Fornasier, M. Fermeiglia, M. Ferrone and S. Pricl, Synthesis and physicochemical characterization of folate-cyclodextrin bioconjugate for active drug delivery, *Bioconjug Chem*, 14 (2003) 899-908.
- [58] E. Bilensoy and A. A. Hincal, Recent advances and future directions in amphiphilic cyclodextrin nanoparticles, *Expert Opin Drug Deliv*, 6 (2009) 1161-1173.
- [59] H. R. Mellor and R. Callaghan, Resistance to Chemotherapy in Cancer: A Complex and Integrated Cellular Response., *Pharmacology*, 81 (2008) 275-300.

Figure 1. (A) Schematic illustration of curcumin supramolecular encapsulation (inclusion complexation) into β -cyclodextrin using solvent evaporation technique. (B) Solid powder samples of β -cyclodextrin, curcumin and CD-CUR inclusion complex (CD30). (C) Aqueous solubility of β -cyclodextrin, curcumin and CD-CUR inclusion complex (CD30) (5 mg/mL).

Figure 2. Curcumin loading into β -cyclodextrin cavities. CD5, CD10, CD20 and CD30 inclusion complexes represents β -cyclodextrin with different amounts of curcumin used for self-assembly formation. Drug loading was determined using UV-visual spectrophotometer at 450 nm.

Figure 3. (A) Optical microscopic images of β -cyclodextrin, curcumin and β -cyclodextrin-curcumin inclusion complexes films obtained from aqueous solutions. Original magnifications 200x. (B) Stability curves of β -cyclodextrin-curcumin inclusion complexes with time.

Figure 4. (A) FTIR spectra of curcumin, β -cyclodextrin and β -cyclodextrin-curcumin inclusion complex (CD30). Spectra were recorded for solid powders on ATR-FTIR place. (B) $^1\text{H-NMR}$ spectra of β -cyclodextrin, curcumin and β -cyclodextrin-curcumin inclusion complex (CD30). Spectra were recorded for samples in *d*-DMSO solutions.

Figure 4. (A) FTIR spectra of curcumin, β -cyclodextrin and β -cyclodextrin-curcumin inclusion complex (CD30). Spectra were recorded for solid powders on ATR-FTIR place. (B) $^1\text{H-NMR}$

spectra of β -cyclodextrin, curcumin and β -cyclodextrin-curcumin inclusion complex (CD30). Spectra were recorded for samples in *d*-DMSO solutions.

Figure 5. Scanning Electron Microscope images of β -cyclodextrin (CD), curcumin (CUR), and β -cyclodextrin-curcumin inclusion complexes (CD5, CD10, CD20 and CD30). Scale bar on SEM image represents 400 μ m.

Figure 6. (A) Transmission Electron Microscopic (TEM) images of CD-CUR inclusion complexes (a) CD5, (b) CD10, (c) CD20 and (d) CD30. (e-f) Higher magnification TEM images of CD 30. (B) (a) Putative structures of cyclodextrin-curcumin inclusion complexes and (b) self-assembly process of β -cyclodextrin and curcumin.

Figure 7. (A) X-ray diffraction patterns of β -cyclodextrin, curcumin and β -cyclodextrin-curcumin inclusion complex (CD30). (B) Differential Scanning Calorimeter endothermic curves of β -cyclodextrin, curcumin and β -cyclodextrin-curcumin inclusion complex (CD30). (C) Thermo-gravimetric curves of β -cyclodextrin, curcumin and β -cyclodextrin-curcumin inclusion complex (CD30).

Figure 8. Cellular uptake of curcumin or cyclodextrin-curcumin (CD-CUR) inclusion complex in prostate cancer cells. (A) Fluorescence images of C4-2, DU145 and PC3 prostate cancer cells treated with CD, CUR, or CD-CUR inclusion complex (CD30). Cells were treated with 20 μ g of CUR or equivalent CD-CUR inclusion complex for 6 hrs. After changing media, images were taken on Olympus BX 51 fluorescence microscope. Original magnification 200X. (B) Flow Cytometric analysis for cellular uptake of curcumin and CD-CUR inclusion complexes in DU145 cells (a) Cells treated with 10 μ g and (b) Cells treated with 20 μ g. Mean fluorescence of cells treated with curcumin or and CD-CUR was measured by Accuri Flow Cytometer. Data represents average of 3 repeats. * $p < 0.05$ represents significant different from the curcumin uptake.

Figure 9. β -cyclodextrin-curcumin (CD30) treatment suppresses cell proliferation in prostate cancer cells. Prostate cancer cells (C4-2, DU145 and PC3) were treated with curcumin or CD30 for 48 hours. Cell proliferation was determined by MTS assay and normalized to cells treated with equivalent amounts of respective controls (DMSO for curcumin and cyclodextrin for CD30). Data represent mean \pm SE of 8 repeats of each treatment group.

Figure 10. (A) Phase contrast microscopy images of 20 μ M CUR or CD30 treated prostate cancer cells. Note: CD30 has shown an improved therapeutic effect on prostate cancer cells. Original Magnifications 200X. (B) Immunoblot analysis for PARP cleavage in curcumin or CD30 treated prostate cancer cells. β -actin was used as an internal loading control. Note: CD30 has shown enhanced PARP cleavage compared to curcumin.

Figure 11. CD30 inhibits the clonogenic potential of prostate cancer cells. C4-2 or DU145 or PC3 cells (1000) were seeded in 6 well culture dishes and after 24 hrs treated with the indicated amounts of curcumin or CD30. Cells were allowed to grow for 8-10 days, colonies were fixed and stained. (A) Representative images of colony forming assays. (B) Colony densities were measured by densitometer using AlphaEase Fc software and expressed as a percent of the DMSO or β -cyclodextrin control. Data represent mean of 3 repeats for each treatment (Mean \pm SE; * $p < 0.05$, compared to the same curcumin dose).

Figure 1
[Click here to download high resolution image](#)

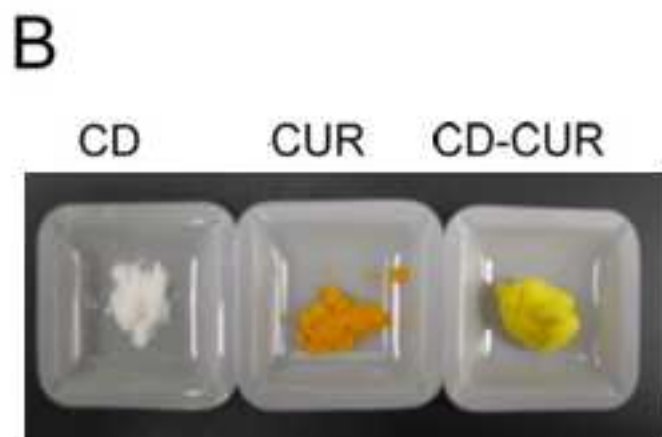


Figure 2
[Click here to download high resolution image](#)

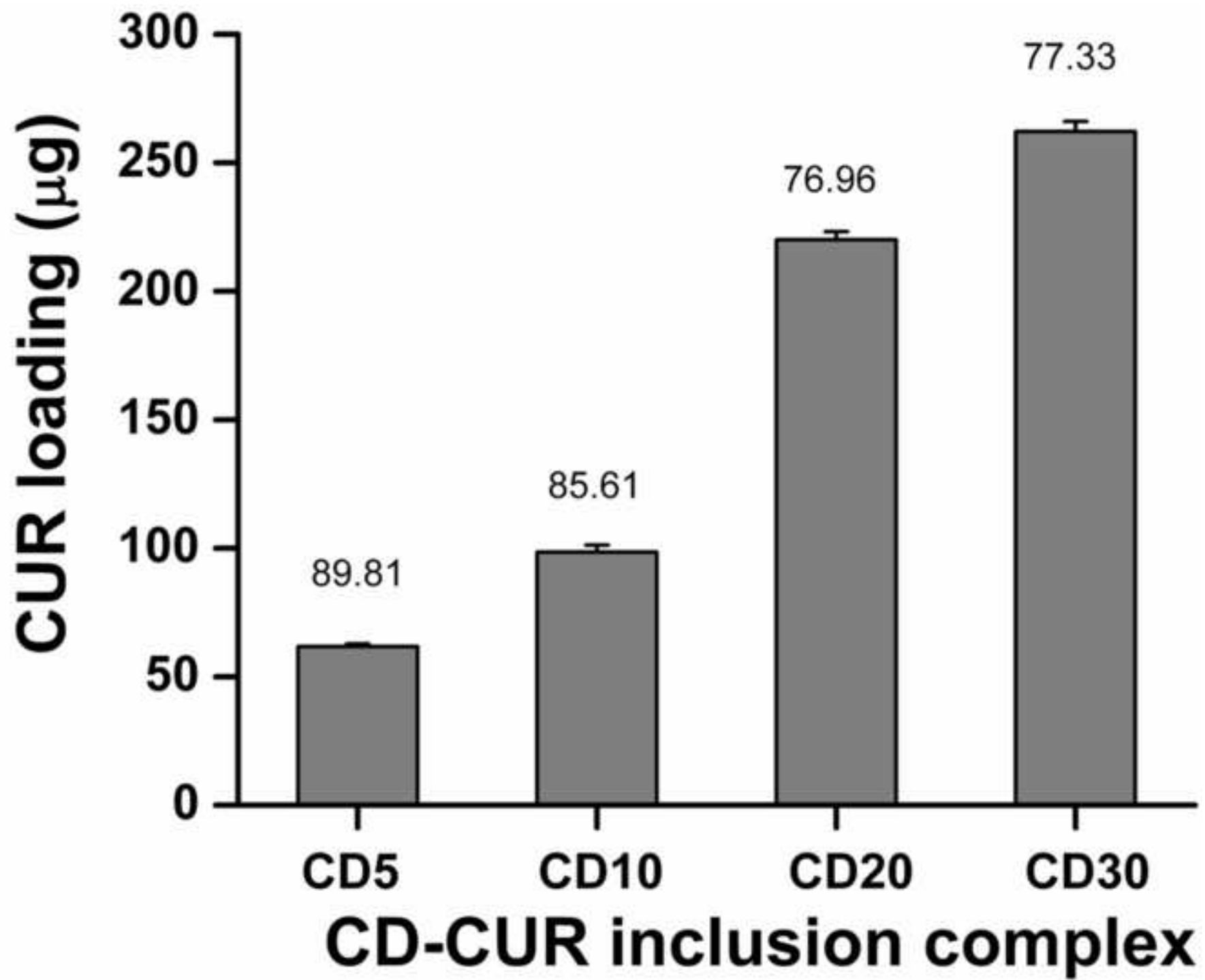


Figure 3
[Click here to download high resolution image](#)

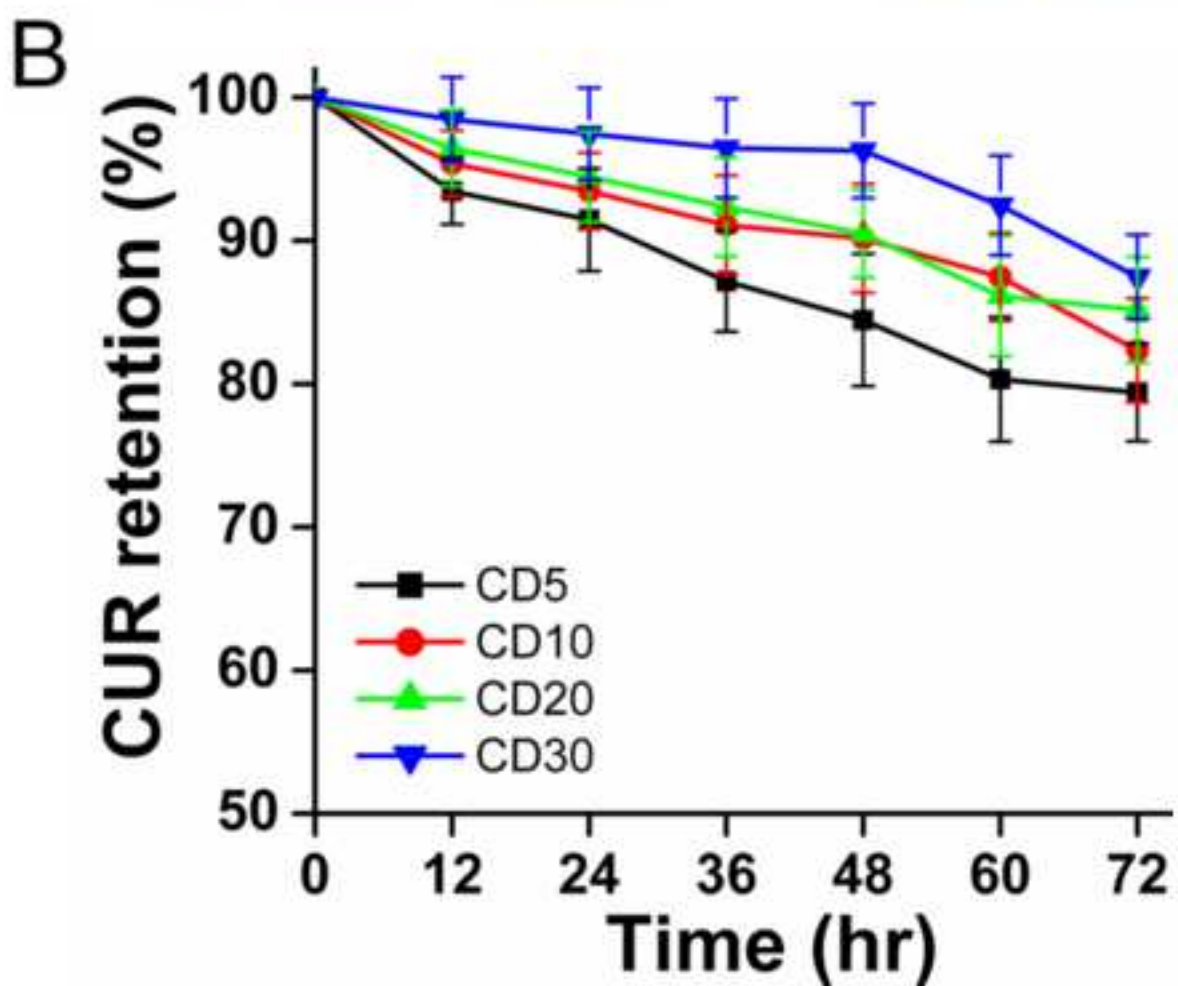
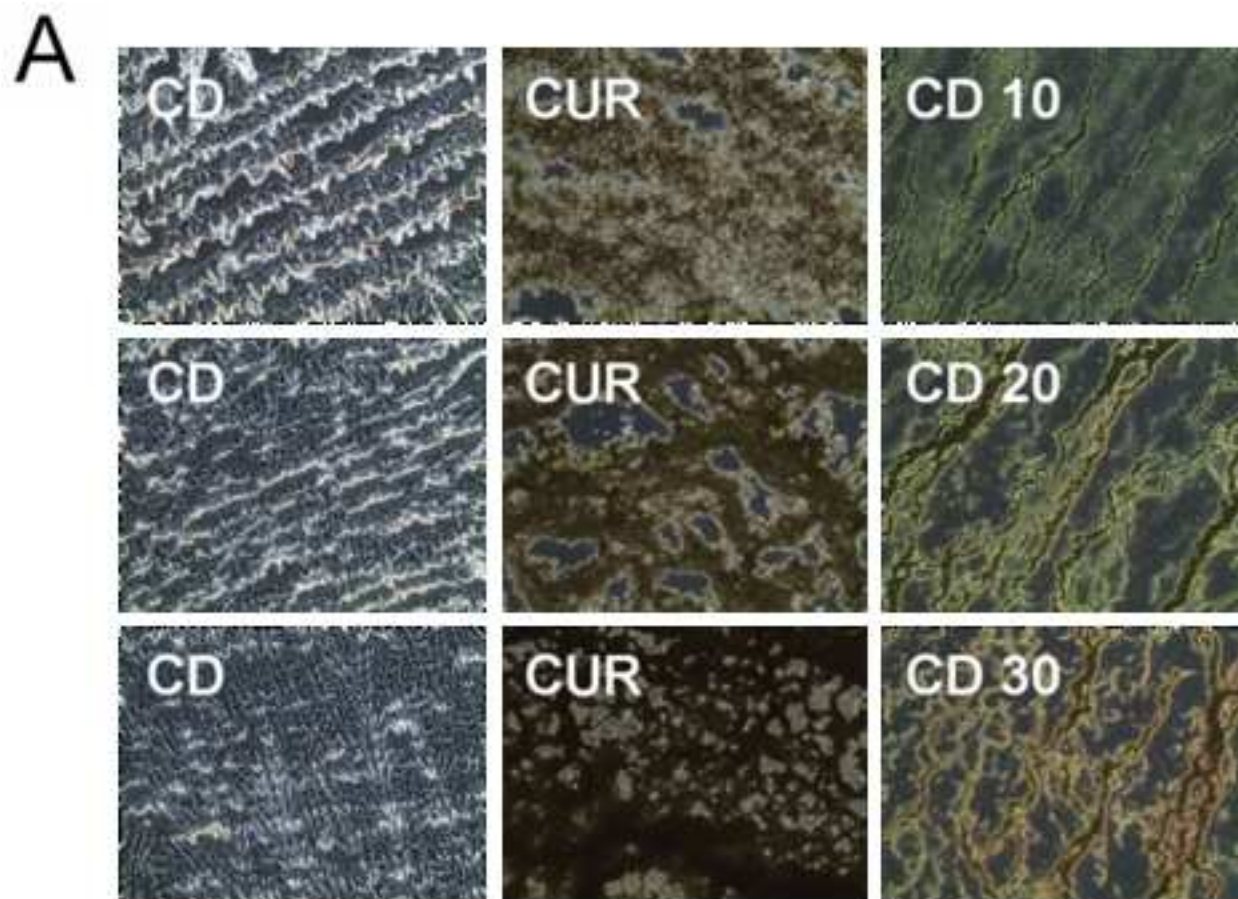


Figure 4
[Click here to download high resolution image](#)

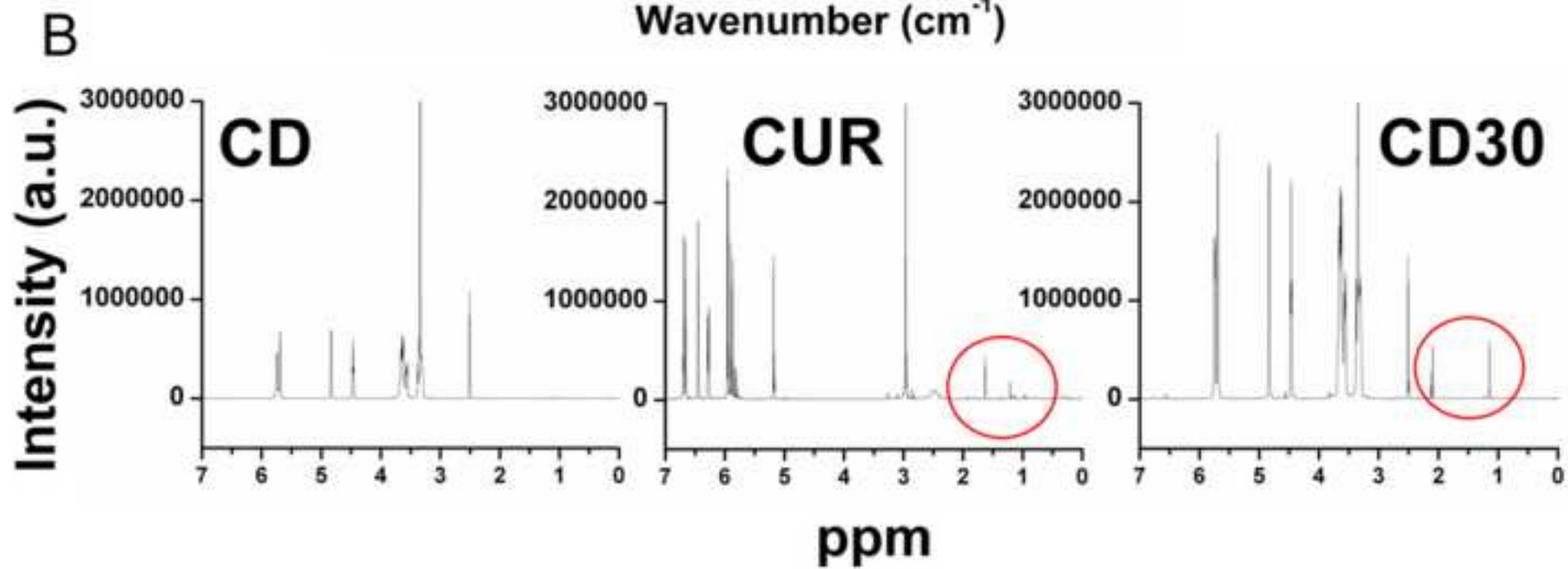
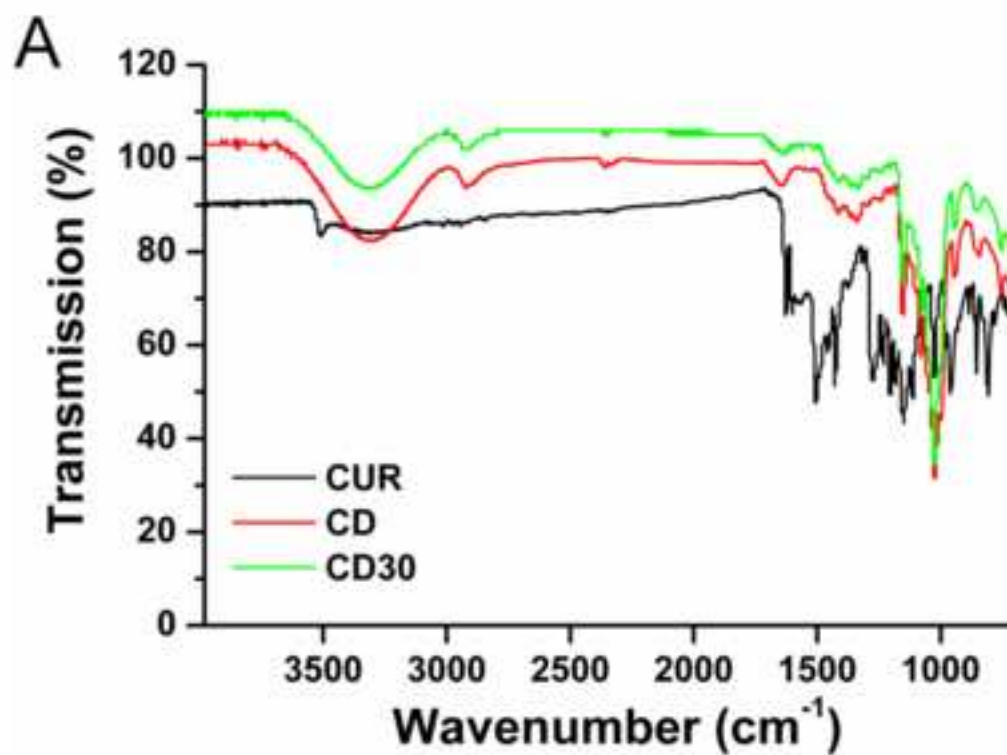


Figure 5
[Click here to download high resolution image](#)

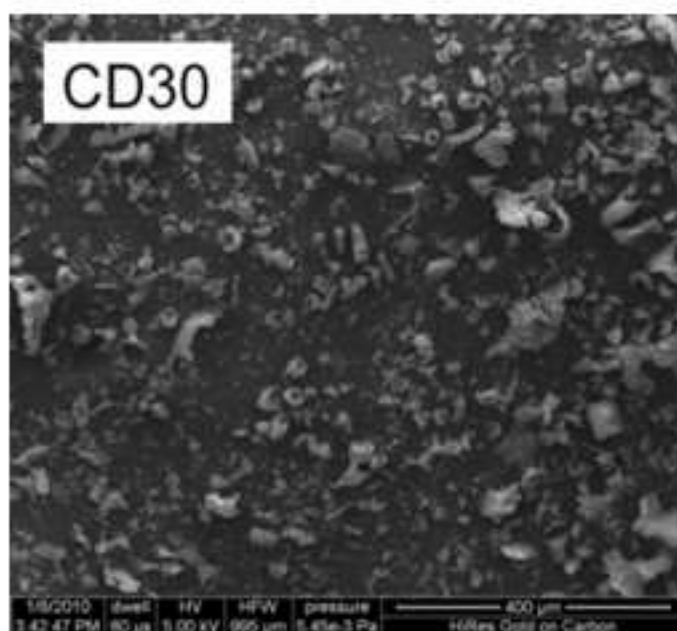
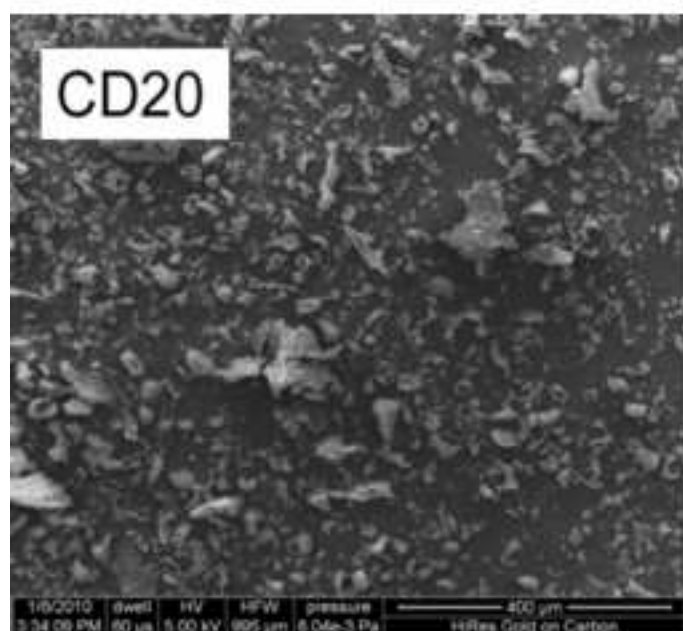
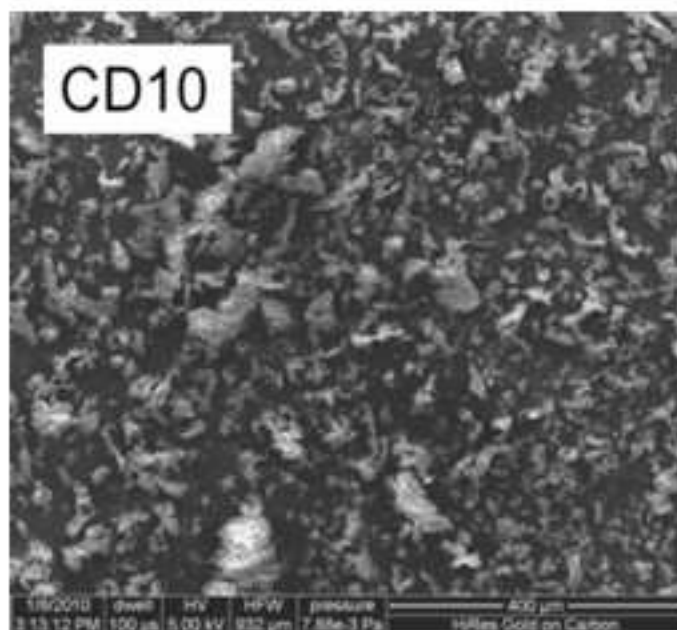
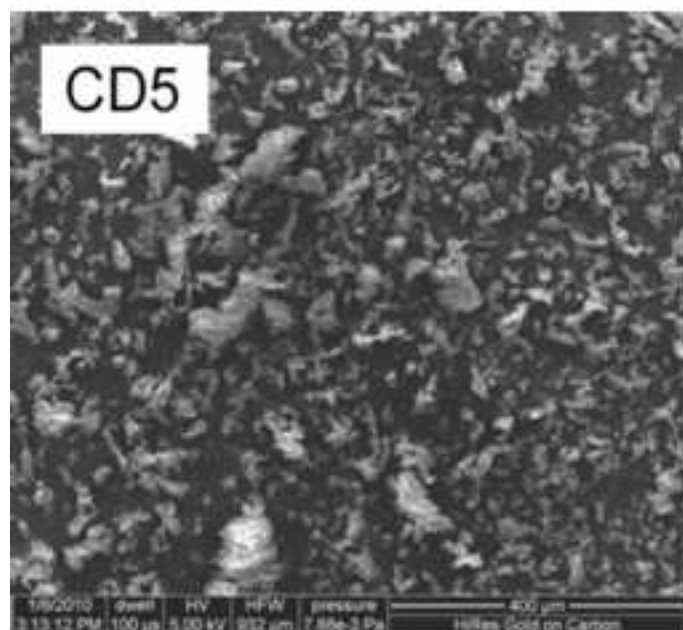
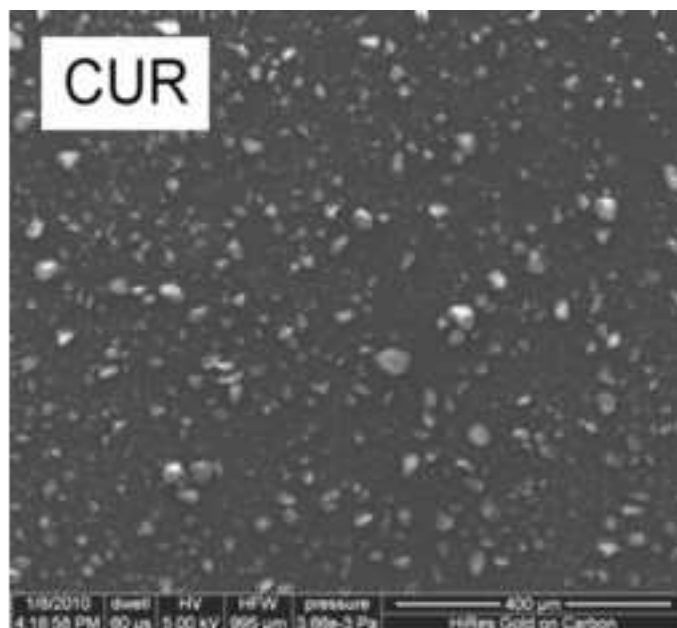
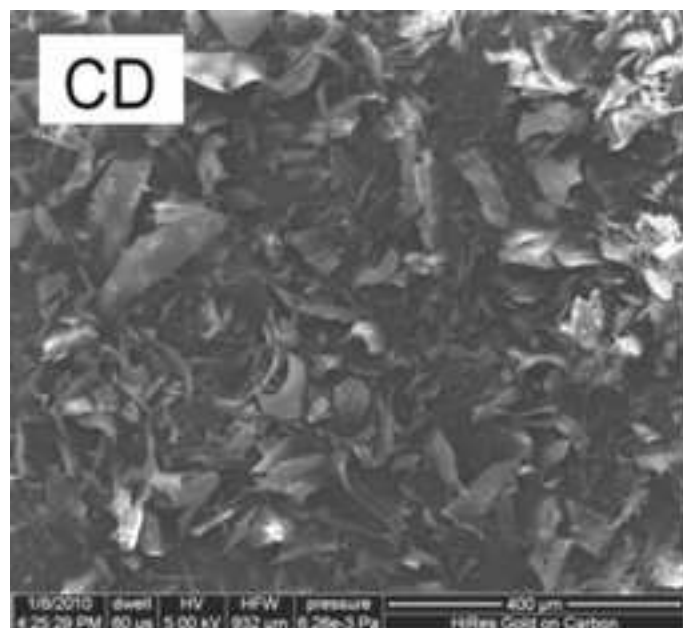


Figure 6
[Click here to download high resolution image](#)

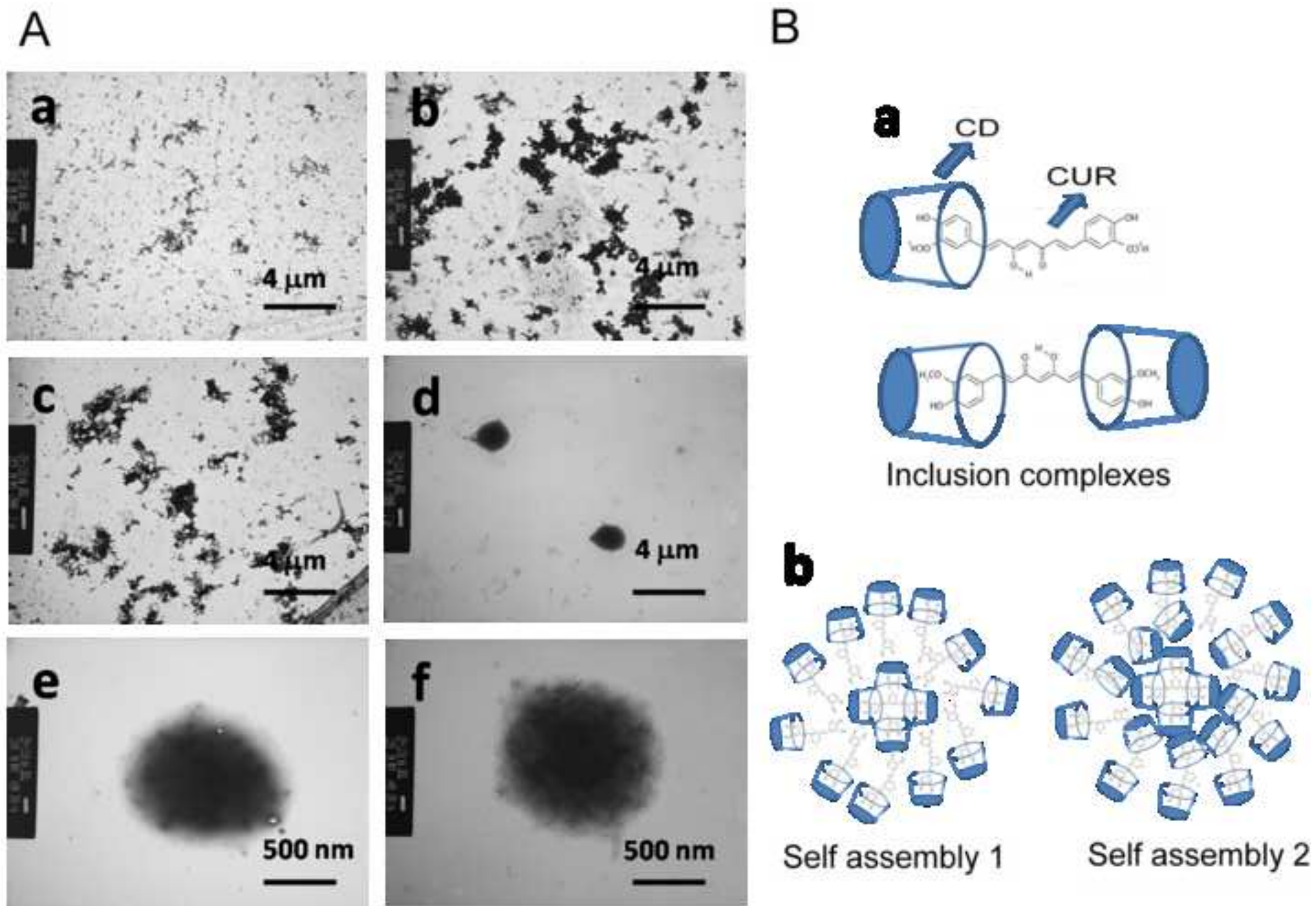


Figure 7
[Click here to download high resolution image](#)

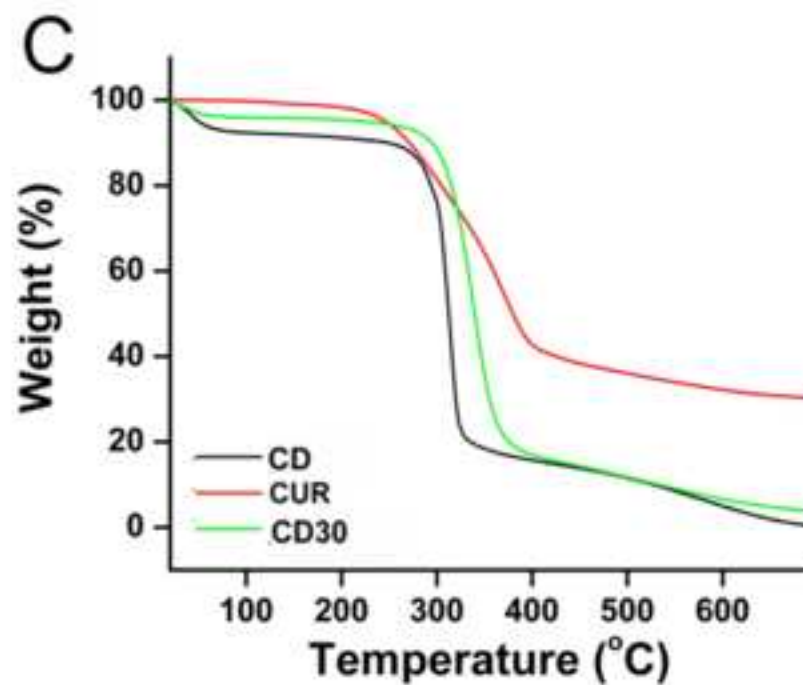
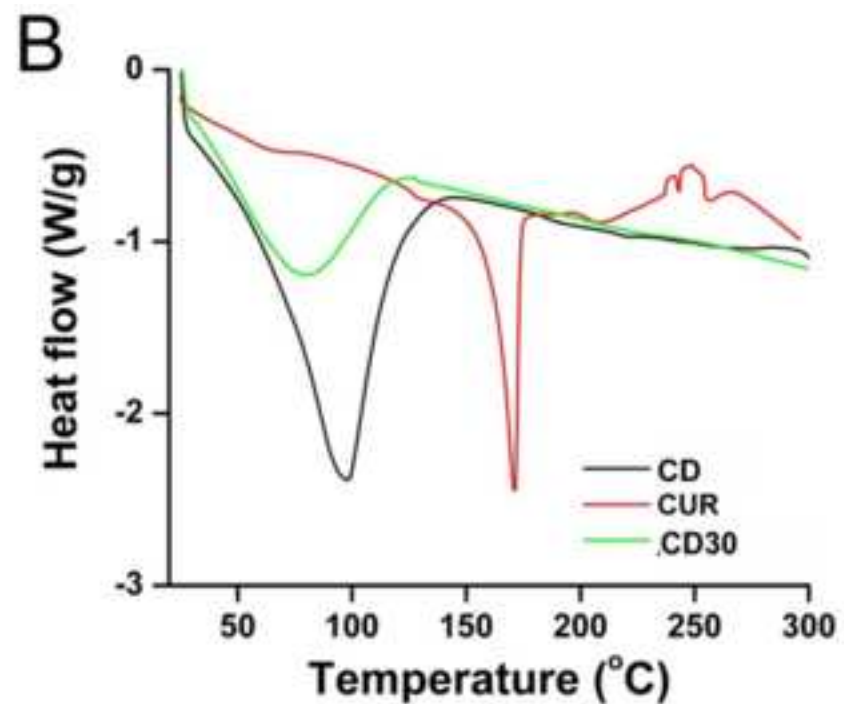
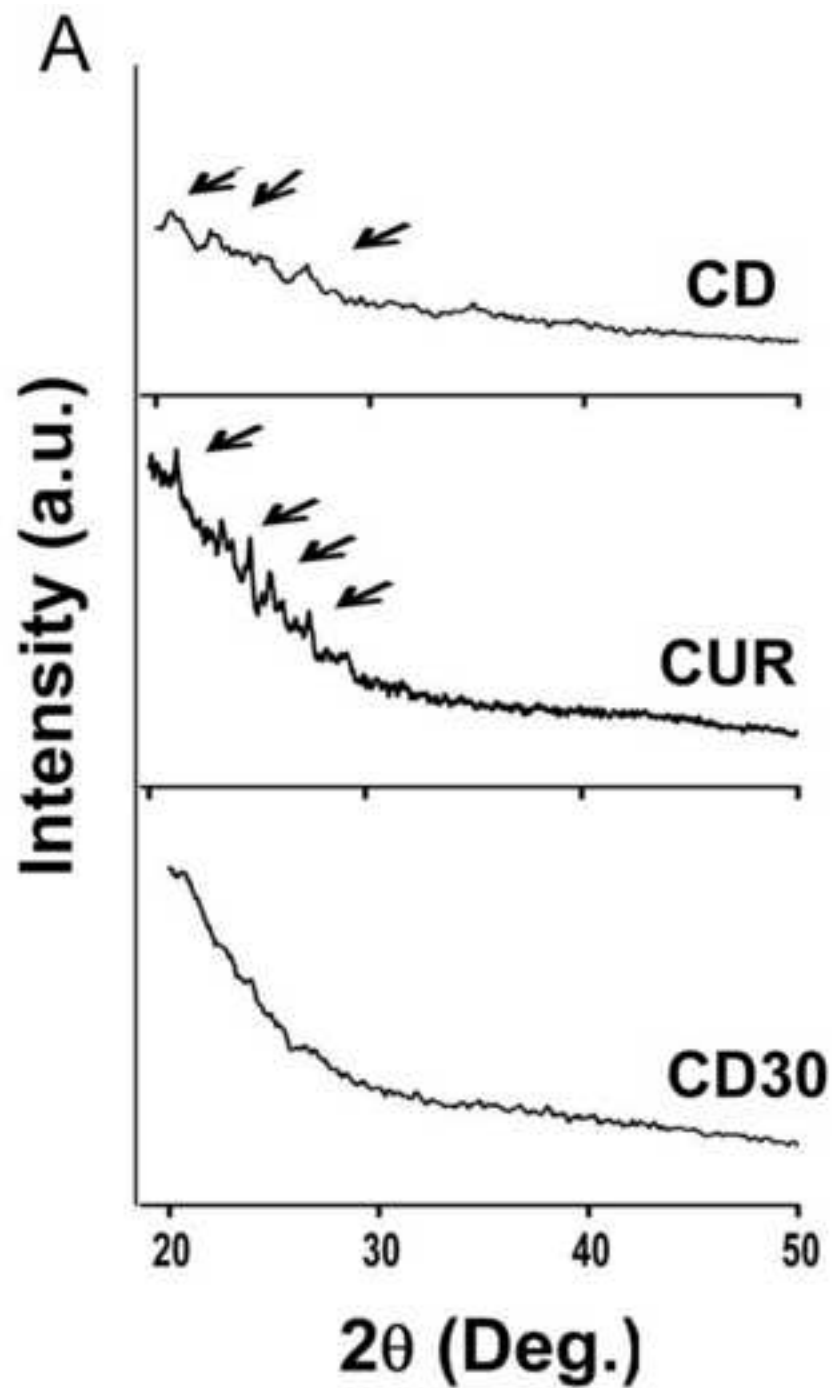


Figure 8
[Click here to download high resolution image](#)

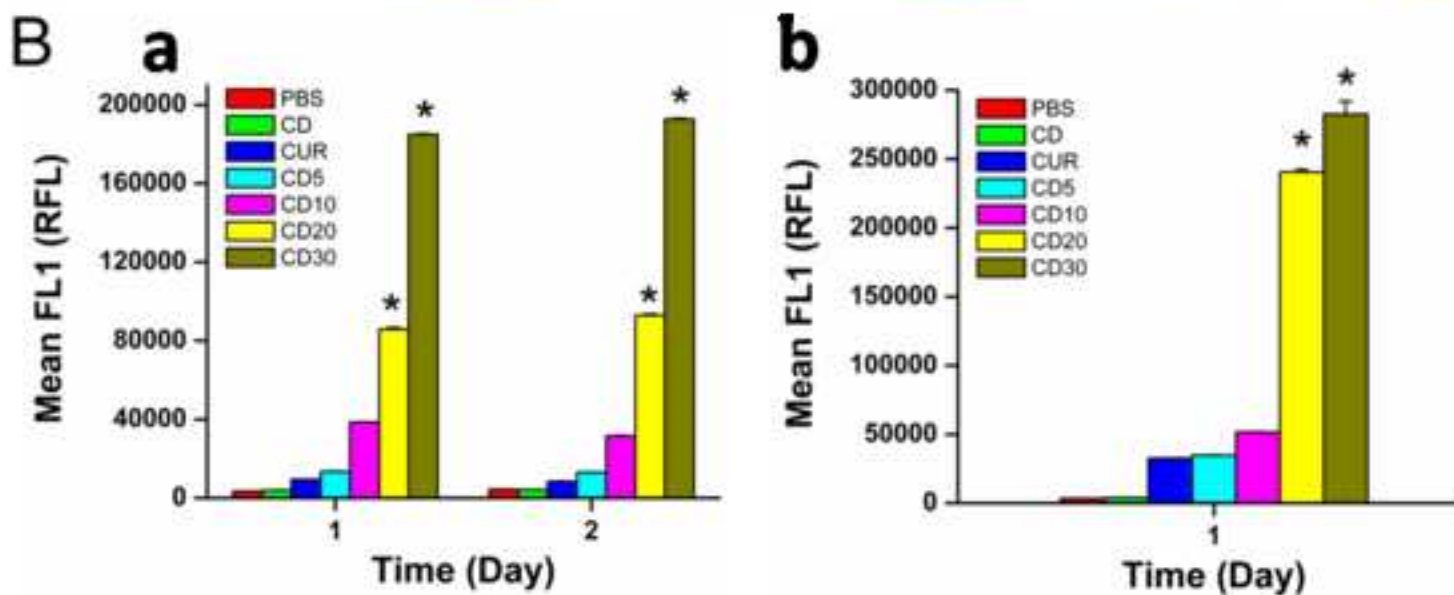
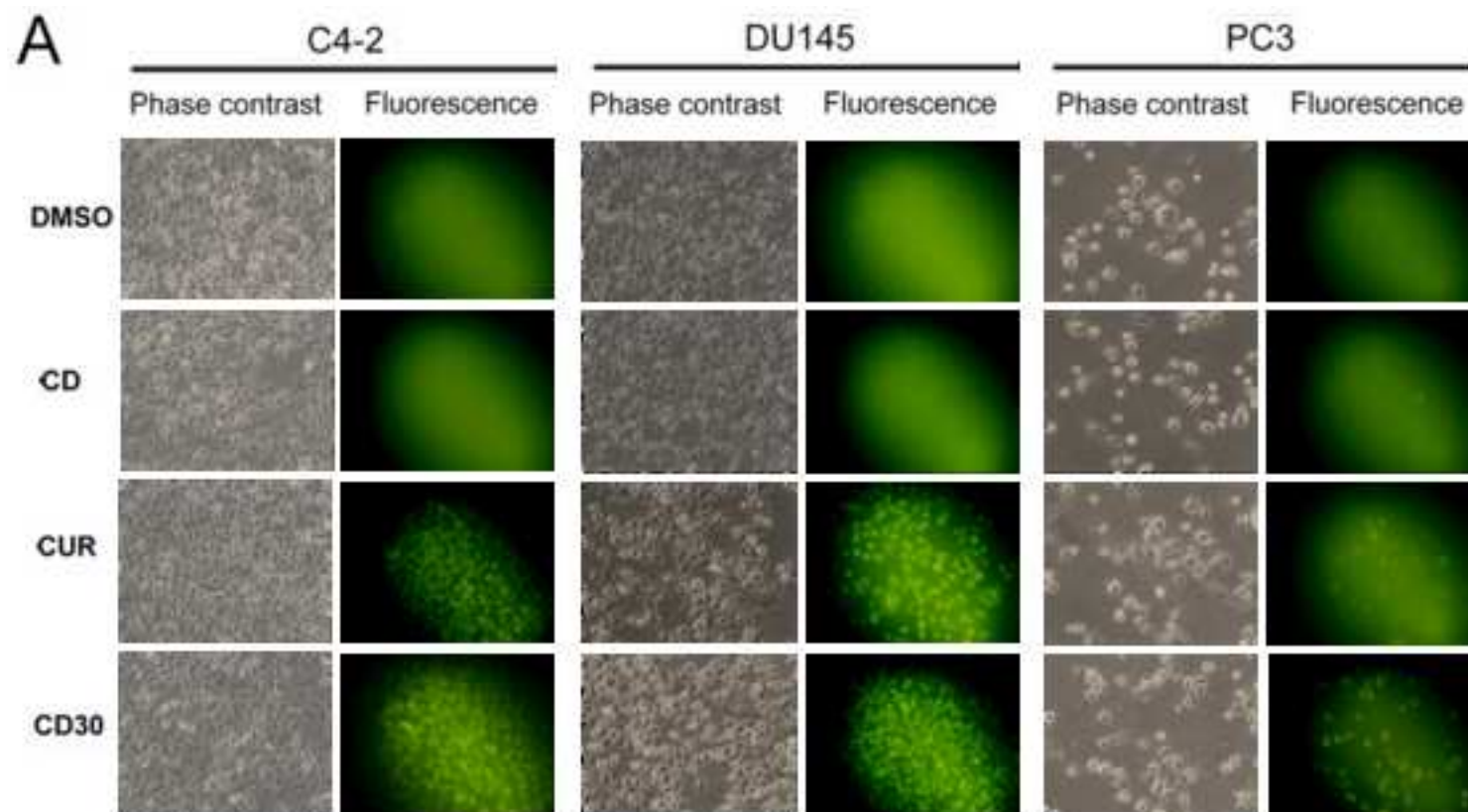


Figure 9
[Click here to download high resolution image](#)

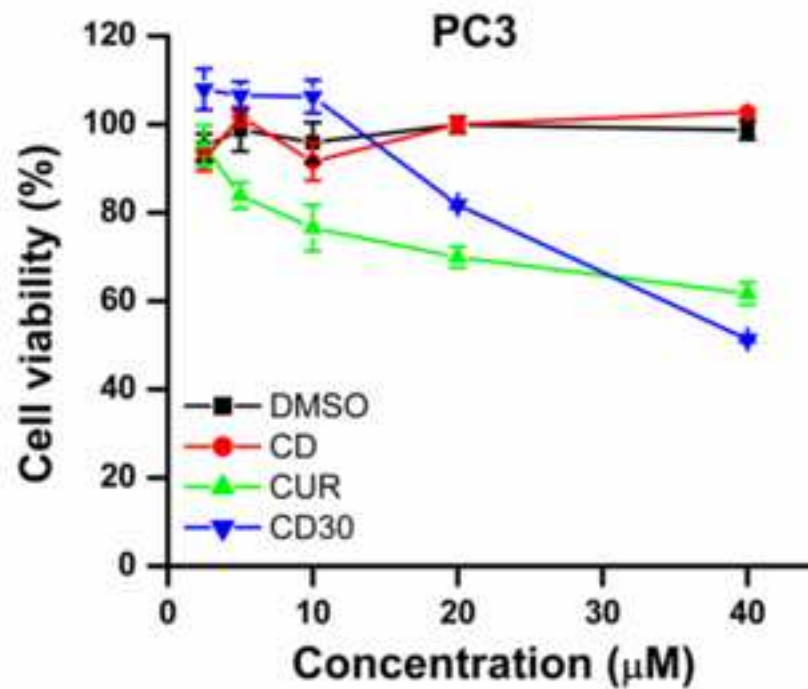
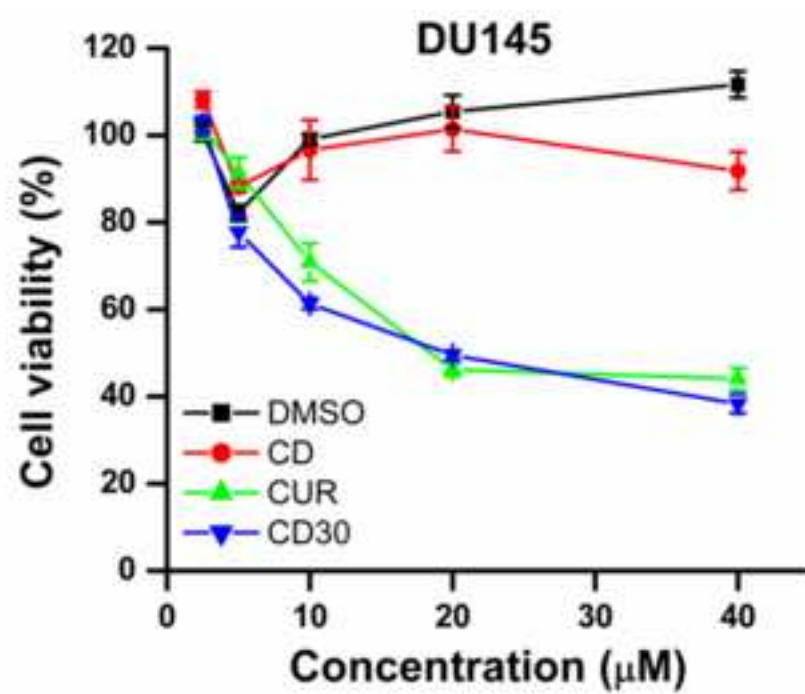
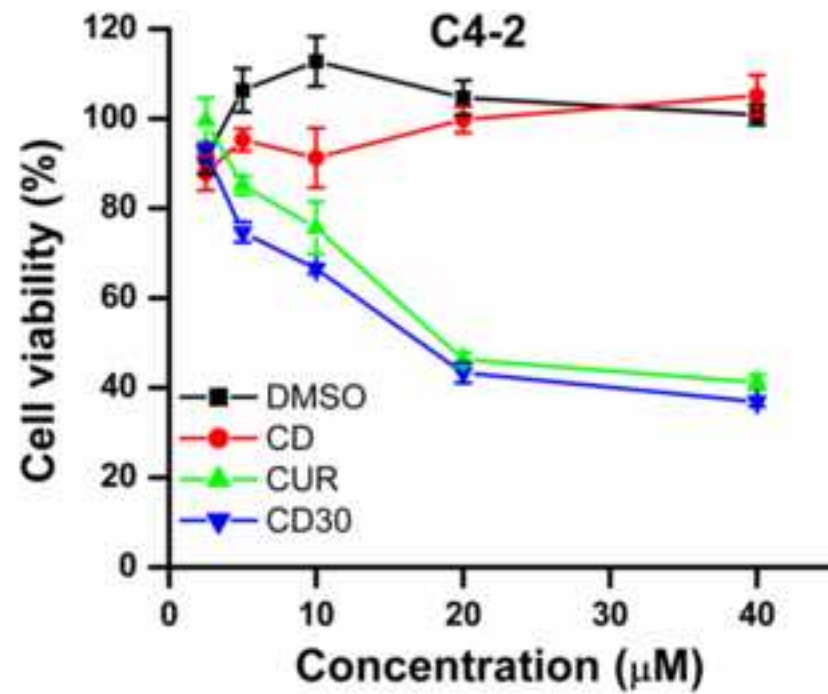


Figure 10
[Click here to download high resolution image](#)

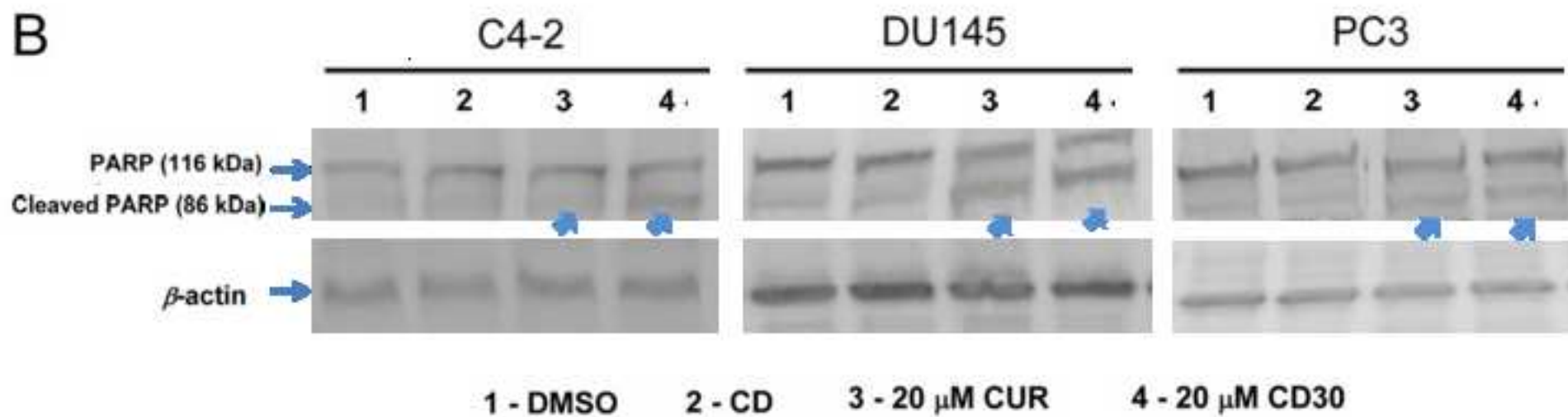
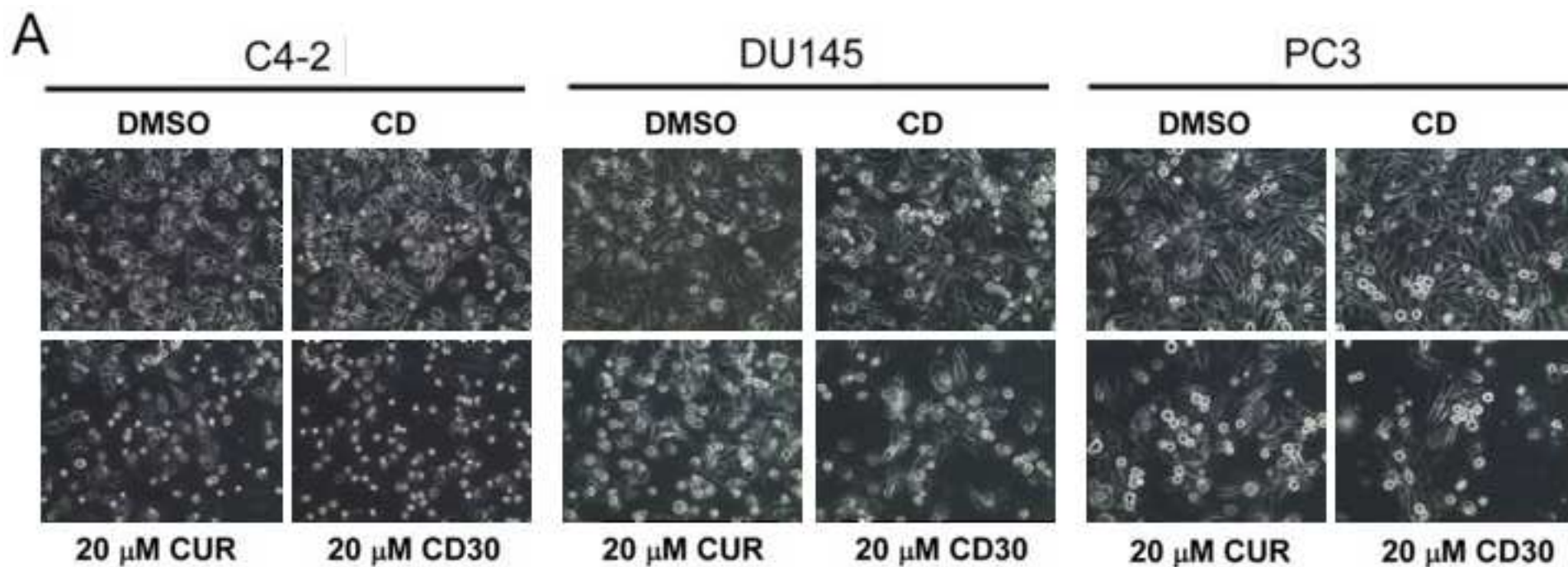
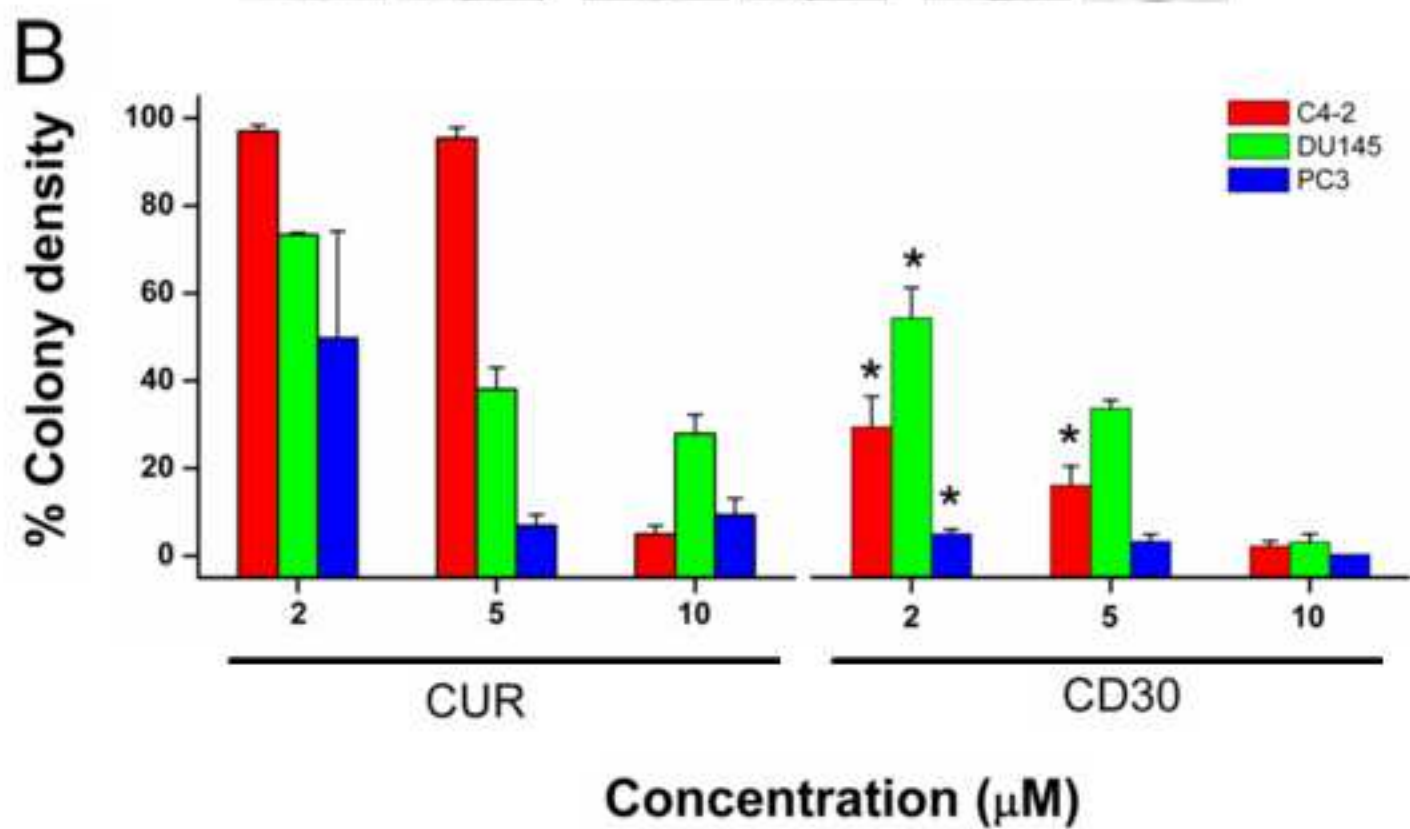
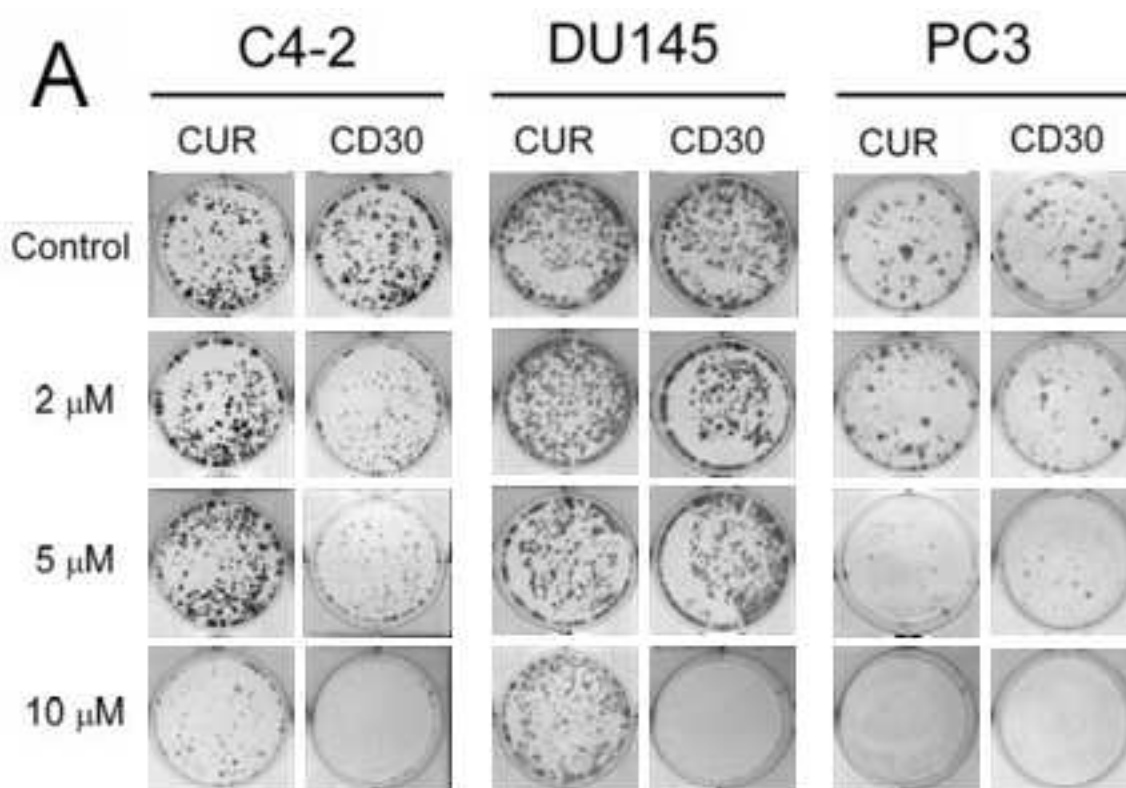


Figure 11

[Click here to download high resolution image](#)



Curcumin induces chemo/radio-sensitization in ovarian cancer cells and curcumin nanoparticles inhibit ovarian cancer cell growth

Murali M Yallapu^{1#}, Diane M Maher^{1#}, Vasudha Sundram¹, Maria C Bell², Meena Jaggi^{1, 2},
and Subhash C Chauhan^{1, 2*}

¹Cancer Biology Research Center, Sanford Research/University of South Dakota, Sioux Falls, SD 57105, USA

²Department of Obstetrics and Gynecology, Sanford School of Medicine, University of South Dakota, Sioux Falls, SD 57105, USA

Email addresses:

MMY: yallapum@sanfordhealth.org

DMM: maherd@sanfordhealth.org

VS: sundramv@sanfordhealth.org

MCB: bellm@sanfordhealth.org

MJ: jaggim@sanfordhealth.org

SCC: Chauhans@sanfordhealth.org

#Equal Contribution

*To whom correspondence should be addressed

Subhash C. Chauhan, **Cancer Biology Research Center, Sanford Research/University of South Dakota**. Department of Obstetrics and Gynecology, **Sanford School of Medicine** The University of South Dakota, Phone: 605-357-1389, Fax: 605-357-1409, **Email:** chauhans@sanfordhealth.org, subhash.chauhan@usd.edu

Abstract

Background: Chemo/radio-resistance is a major obstacle in treating advanced ovarian cancer. The efficacy of current treatments may be improved by increasing the sensitivity of cancer cells to chemo/radiation therapies. Curcumin is a naturally occurring compound with anti-cancer activity in multiple cancers; however, its chemo/radio-sensitizing potential is not well studied in ovarian cancer. Herein, we demonstrate the effectiveness of a curcumin pre-treatment strategy for chemo/radio-sensitizing cisplatin resistant ovarian cancer cells. To improve the efficacy and specificity of curcumin induced chemo/radio sensitization, we developed a curcumin nanoparticle formulation conjugated with a monoclonal antibody specific for cancer cells.

Methods: Cisplatin resistant A2780CP ovarian cancer cells were pre-treated with curcumin followed by exposure to cisplatin or radiation and the effect on cell growth was determined by MTS and colony formation assays. The effect of curcumin pre-treatment on the expression of apoptosis related proteins and β -catenin was determined by Western blotting or Flow Cytometry. A luciferase reporter assay was used to determine the effect of curcumin on β -catenin transcription activity. The poly(lactic acid-*co*-glycolic acid) (PLGA) nanoparticle formulation of curcumin (Nano-CUR) was developed by a modified nano-precipitation method and physico-chemical characterization was performed by transmission electron microscopy and dynamic light scattering methods.

Results: Curcumin pre-treatment considerably reduced the dose of cisplatin and radiation required to inhibit the growth of cisplatin resistant ovarian cancer cells. During the 6 hr pre-treatment, curcumin down regulated the expression of Bcl-X_L and Mcl-1 pro-survival proteins.

Curcumin pre-treatment followed by exposure to low doses of cisplatin increased apoptosis as indicated by annexin V staining and cleavage of caspase 9 and PARP. Additionally, curcumin pre-treatment lowered β -catenin expression and transcriptional activity. Nano-CUR was successfully generated and physico-chemical characterization of Nano-CUR indicated an average particle size of ~ 70 nm, steady and prolonged release of curcumin, antibody conjugation capability and effective inhibition of ovarian cancer cell growth.

Conclusion: Curcumin pre-treatment enhances chemo/radio-sensitization in A2780CP ovarian cancer cells through multiple molecular mechanisms. Therefore, curcumin pre-treatment may effectively improve ovarian cancer therapeutics. A targeted PLGA nanoparticle formulation of curcumin is feasible and may improve the *in vivo* therapeutic efficacy of curcumin.

Background

Ovarian cancer is the most lethal gynecological cancer and the fifth most common cause of cancer mortality in women in the United States: in 2009 it is estimated that 21,550 women will be diagnosed with ovarian cancer and 14,600 women will die due to this disease [1]. A high percent of women with ovarian cancer are diagnosed at an advanced stage (67%) and have a 5 year survival rate of only 46% [1]. The usual treatment modality involves surgical cytoreduction followed by treatment with a combination of platinum (cisplatin or carboplatin) and taxane based therapies. This is effective in 60-80% of patients; however, the majority of women with advanced disease will have cancer recurrence [2, 3]. Unfortunately, almost all relapsing ovarian cancers eventually develop platinum resistance and patients with resistant tumors have a median survival time of 6 months, with only 27% living longer than 12 months [4]. In addition to improving diagnosis of ovarian cancer, there is an urgent need to develop effective therapeutic modalities for advanced stage drug resistant ovarian cancer.

Although the mechanism of resistance to cisplatin has been widely studied *in vitro*, the actual reasons underlying cisplatin resistance *in vivo* is still not well understood. Cisplatin functions primarily by forming DNA adducts that inhibit cell replication and induce apoptosis if the DNA damage is not repaired by the cell. Recently, it has been suggested that while initial sensitivity to cisplatin is *via* nonfunctional DNA repair genes (i.e. BRCA1/2), cisplatin resistance may be acquired through a gain of function in BRCA1/2 [5]. Independent of the mechanism of resistance, inhibition of cell death *via* apoptosis is an important event leading to cisplatin resistance. Another important aspect limiting the use of cisplatin is the negative side effects which accumulate in severity with multiple cisplatin treatments and include gastrointestinal

distress, kidney and nerve damage, hearing loss, and bone marrow suppression [2, 3, 6].

Additionally, treatment of ovarian cancer with radiation is limited due to gastrointestinal toxicity [6]. While significant progress has been made in developing targeted radioimmunotherapy (RIT), current drawbacks to this therapy include toxicity and resistance to radiation [7, 8].

One strategy to improve the effectiveness and limit the toxicity of cisplatin and/or radiation therapy is to induce chemo/radio-sensitization in cancer cells. A number of natural dietary phytochemicals, such as curcumin, quercetin, xanthorrhizol, ginger, green tea, genistein, etc., are candidates for inducing chemo/radio-sensitization of cancer cells [9-11]. Among these agents, curcumin (diferuloyl methane), a polyphenol derived from the rhizomes of tumeric, *Curcuma longa*, has received considerable attention due to its beneficial chemopreventive and chemotherapeutic activity *via* influencing multiple signaling pathways, including those involved in survival, growth, metastasis and angiogenesis in various cancers [12-15]. Importantly, curcumin has demonstrated no toxicity to healthy organs at doses as high as 8 grams/day [16]. However, the low bioavailability and poor pharmacokinetics of curcumin limits its effectiveness *in vivo* [17]; therefore, we have developed a PLGA nanoparticle formulation of curcumin (Nano-CUR) to provide increased bioavailability as well as antibody conjugation abilities for targeted delivery of curcumin into tumors.

Given the need for therapies to treat cisplatin resistant ovarian cancer, we investigated the effect of curcumin pre-treatment on a cisplatin resistant ovarian cancer cell line model. We demonstrate, for the first time, that curcumin pre-treatment sensitizes A2780CP cells (which are cisplatin resistant) to cisplatin and radiation treatment. Curcumin pre-treatment dramatically

inhibits proliferation and clonogenic potential of cisplatin resistant cells in the presence of low levels of cisplatin or radiation. We also identified molecular pathways involved in curcumin mediated sensitization to cisplatin/radiation induced apoptosis. This study advances the understanding regarding the molecular mechanisms involved in curcumin mediated chemo/radio-sensitization in ovarian cancer cells.

Materials and Methods

Cell culture and drugs

A2780 and A2780CP (resistant to cisplatin) paired cells [18] were generously provided by Dr. Stephen Howell, University of California, San Diego. These cells were maintained as monolayer cultures in RPMI-1640 medium (HyClone Laboratories, Inc. Logan, UT) supplemented with 10% fetal bovine serum (Atlanta Biologicals, Lawrenceville, GA) and 1% penicillin-streptomycin (Gibco BRL, Grand Island, NY) at 37°C in a humidified atmosphere (5% CO₂). Curcumin (≥95% purity, (E,E)-1,7-bis(4-Hydroxy-3-methoxyphenyl)-1,6-heptadiene-3,5-dione, Sigma, St. Louis, MO) was stored at -20°C as 10 mM stock solution in DMSO and protected from light. Cisplatin (cis-Diammineplatinum(II) dichloride, Sigma) was stored at 4°C as 10 mM stock solution in 0.9% saline.

Cell growth and viability

Cells were seeded at 5,000 per well in 96-well plates, allowed to attach overnight and different concentrations (2.5-40 μM) of curcumin or cisplatin diluted in medium were added. DMSO and PBS containing medium served as the respective controls. In another set, cells were treated for 6 hrs with 10 or 20 μM curcumin in medium and followed by cisplatin treatment (2.5-40 μM).

DMSO-PBS medium was used as a control. The anti-proliferative effect of these drugs was determined at 2 days with a MTS based colorimetric assay (CellTiter 96 AQueous One Solution Cell Proliferation Assay, Promega, Madison, WI). The reagent (20 μ L/well) was added to each well and plates were incubated for 2 hrs at 37°C. The color intensity was measured at 492 nm using a microplate reader (BioMate 3 UV-Vis spectrophotometer, Thermo Electron Corporation, Waltham, MA). The anti-proliferative effect of each treatment was calculated as a percentage of cell growth with respect to the appropriate controls after subtracting intensity values for curcumin, DMSO, PBS and DMSO-PBS in medium without cells. Phase contrast microscope cell images were taken on an Olympus BX 41 microscope (Olympus, Center Valley, PA).

Colony formation assay

For this assay, cells were seeded at 500 cells per 100 mm culture dish and allowed to attach overnight. The cells were treated with curcumin or cisplatin or with a pre-treatment of curcumin followed by cisplatin treatment and maintained under standard cell culture conditions at 37°C and 5% CO₂ in a humid environment. After 8 days, the dishes were washed twice in PBS, fixed with methanol, stained with hematoxylin (Fisher Scientific, Pittsburgh, PA), washed with water and air dried. The number of colonies was determined by imaging with a MultimageTM Cabinet (Alpha Innotech Corporation, San Leandro, CA) and using AlphaEase Fc software. The percent of colonies was calculated using the number of colonies formed in treatment divided by number of colonies formed in DMSO or PBS or DMSO-PBS control.

Radiation

Cells were seeded at 200 per well in 6 well plates and allowed to attach overnight. These cells were treated with different concentrations of curcumin for 6 hrs and exposed to 1-5 Gy dose of radiation. A 1060 kV industrial RS-2000 Biological X-ray irradiator (Radiation Source, Alpharetta, GA) was used to irradiate the cultures at room temperature. The machine was operated at 25 mA. The dose rate with a 2 mm Al and 1 mm Be filter was ~ 1.72 Gy/min at a focus surface distance of 15 cm. Cells treated with different concentrations of curcumin or radiation alone was used as controls. These cells were maintained under standard cell culture conditions at 37°C and 5% CO₂ in a humid environment. After 8 days, the colonies were counted as described earlier.

Immunoblot assay

Following treatment, cells were processed for protein extraction and Western blotting using standard procedures as described earlier [19]. Briefly, 800,000 cells per 100 mm cell culture dish were plated, allowed to attach overnight and treated with curcumin or cisplatin or pretreated with curcumin followed by cisplatin. After 48 hrs cells were washed twice with PBS, lysed in SDS buffer (Santa Cruz Biotechnology, Santa Cruz, CA) and kept at 4°C for 30 min. Cell lysates were passed through one freeze-thaw cycle and sonicated on ice for 30 sec (Sonic Dismembrator Model 100, Fisher Scientific) and the protein concentration was normalized using SYPRO Orange (Invitrogen, Carlsbad, CA). The cell lysates were heated at 95°C for 5 min, cooled down to 4°C, centrifuged at 14,000 rpm for 3 min and the supernatants were collected. SDS-PAGE (4-20%) gel electrophoresis was performed and the resolved proteins were transferred onto PVDF membrane. After rinsing in PBS, membranes were blocked in 5% nonfat dry milk in TBS-T (Tris

buffered saline containing 0.05% Tween-20) for 1 hr and incubated with Bcl-X_L, Mcl-1, Caspase 3, 7 and 9, Poly (ADP-ribose) polymerase (PARP), β -catenin, c-Myc and β -actin specific primary antibodies (Cell Signaling, Danvers, MA) overnight at 4°C. The membranes were washed (4x10 min) in TBS-T at room temperature and then probed with 1:2000 diluted horseradish peroxidase-conjugated goat anti-mouse or goat anti-rabbit secondary antibody (Promega) for 1 hr at room temperature and washed (5x10 min) with TBS-T. The signal was detected with the Lumi-Light detection kit (Roche, Nutley, NJ) and a BioRad Gel Doc (BioRad, Hercules, CA).

Annexin V staining

Cells were plated, allowed to attach overnight and treated with cisplatin or curcumin alone or pre-treated with curcumin for 6 hrs and followed by cisplatin treatment for an additional 42 hrs. Both adherent and floating cells were collected, washed with PBS, suspended in Annexin V binding buffer, stained with Annexin V-PE (BD Biosciences, San Diego, CA) and analyzed by flow cytometry using an Acuri C6 flow cytometer (Accuri Cytometers, Inc., Ann Arbor, MI).

TOPFlash reporter assay

The β -catenin-TCF transcription activity was measured using a luminescence reporter assay as described earlier [20]. In short, 200,000 cells were plated per well in a 12 well plate for 16 hrs prior to transient transfection with reporter construct TOPFlash or FOPFlash (Gift from Dr. R. Moon, Washington University) and cotransfected with Renilla luciferase (pRL-TK, Promega). After 3 hrs of transfection, the wells were treated with either 20 μ M curcumin, 5 μ M cisplatin or a 6 hr pre-treatment with 20 μ M curcumin followed by treatment with 5 μ M cisplatin. After a 24

hr incubation, the cells were harvested in luciferase lysis buffer and the luciferase activity was assayed using Dual-Glo luciferase assay system with a GLOMAX™ 96 microplate luminometer (Promega).

Curcumin-PLGA Nanoparticles (Nano-CUR)

PLGA nanoparticles (PLGA NPs) containing curcumin were prepared from curcumin and PLGA (50:50 lactide-glycolide ratio; inherent viscosity 1.32 dL/g in at 30°C) (Birmingham Polymers, Pelham, AL) using modified nano-precipitation technique [21]. In brief, 90 mg of PLGA was dissolved in 10 mL of acetone over a period of 3 hrs and 1 mg of curcumin was added to get a uniform PLGA-curcumin solution. This solution was drop wise added to 20 mL of aqueous solution containing 2% (wt./v.) poly(vinyl alcohol) (PVA) (M.W. 30,000-70,000) and 10 mg of poly-L-lysine (M.W. 30,000-70,000) (PLL), over a period of 10 min on a magnetic stir plate operated at 800 rpm. Within a few minutes precipitation can be observed in the aqueous layer. This suspension was stirred at room temperature for ~24 hrs to completely evaporate the acetone. Untrapped curcumin was removed by centrifugation at 5,000 rpm on an Eppendorf Centrifuge 5810 R (Eppendorf AG, Hamburg, Germany) for 10 min. PLGA NPs with entrapped curcumin were recovered by ultracentrifugation at 30,000 rpm using Rotor 30.50 on an Avanti J-30I Centrifuge (Beckman Coulter, Fullerton, CA) and were subsequently lyophilized using a freeze dry system (-48 °C, 133x10⁻³mBar Freeze zone[®], Labconco, Kansas City, MO) and stored at 4°C until further use. Curcumin loading and release was estimated at 450 nm using Biomate 3 UV-vis spectrophotometer (Thermo Electron) as described earlier [22].

Internalization of PLGA NPs

Cellular uptake of PLGA NPs was determined with nanoparticles prepared as described above but with 500 µg of fluorescein-5'-isothiocyanate (FITC) used in place of curcumin. The FITC loading in PLGA NPs was determined using UV-vis spectrophotometer [23] at 490 nm after extracting FITC for 1 day in acetone. FITC standards (1-10 µg/ml) were used for estimation of FITC in PLGA NPs. To determine the PLGA NPs uptake in A2780CP cells, 50,000 cells were plated in 4 well chamber slides and after 24 hrs the media was replaced with PLGA NPs (20 µg of FITC) diluted in media. After 6 hrs incubation with FITC-PLGA NPs, cells were washed twice in PBS, fixed with ice cold methanol for 10 min, washed with PBS and stained with DAPI (1:1000 dilution) (Invitrogen) to label the nucleus of the cells. Fluorescence microscope images were taken on an Olympus BX 51 microscope (Olympus, Center Valley, PA) equipped with an X-cite series (ExFo, Quebec Canada) excitation source and an Olympus DP71 camera.

Anti-TAG-72 MAb conjugation to PLGA NPs

The feasibility of antibody conjugation was determined with PLGA NPs. The conjugation reaction was performed with anti-TAG-72 MAb (CC49) and PLGA NPs utilizing conjugation chemistry employing a reactive di-functional cross-linker, NANOCS NHS-PEG-NHS (MW 5,000) (NANOCS, New York, NY) at a ratio 1:20 (antibody to NPs), as shown in Figure Six F. Unconjugated anti-TAG-72 MAb was removed by ultra centrifugation. The antibody conjugation was confirmed by immunoblotting. The samples (5 µg of anti-TAG-72 MAb conjugated PLGA NPs, PLGA NPs or 2 µg free anti-TAG-72 MAb) were heated at 95°C for 5 min, cooled down to 4 °C and centrifuged at 14,000 rpm for 3 min and supernatants were collected. Following gel

electrophoresis and protein transfer, membranes were probed with a horseradish peroxidase-conjugated goat anti-mouse antibody and the signal was detected as described above.

Statistical Methods

Analysis of variance (ANOVA) was followed by the student t-test with Bonferroni correction for multiple comparisons (to be considered significant, the p value must be less than 0.017 (0.05/3=0.017)). Normality of distribution, equal variance, ANOVA, and t-tests were performed using the statistical software package, JMP 8.0 (SAS, Carry, NC).

Results

Curcumin pre-treatment induces chemo/radio-sensitization in ovarian cancer cells

To determine if curcumin could sensitize cisplatin-resistant ovarian cancer cells (A2780CP) to cisplatin treatment, we designed a curcumin pre-treatment strategy and compared individual treatments (curcumin or cisplatin) to a combination of treatments (curcumin and cisplatin) (Figure 1A). When used individually, curcumin and cisplatin have limited dose dependent anti-proliferative effects on A2780CP cells (Figure 1B, CUR + CIS). However, pre-treatment with 20 μ M curcumin for 6 hrs followed by treatment with 2.5-40 μ M cisplatin for an additional 42 hrs resulted in drastic cell growth inhibition compared to each agent alone (Figure 1B, CUR + CIS). The cisplatin sensitive ovarian cancer cell line, A2780 (the parental cell line of A2780CP), also showed increased sensitivity to cisplatin following pre-treatment with curcumin (data not shown). Additionally, a 6 hr pre-treatment with curcumin was more effective than treating the cells with curcumin and cisplatin simultaneously (data not shown). Of note, the MTS assay that is used to determine cell proliferation does not directly distinguish between induction of cell

death or prevention of cell division; however, the result is clear that curcumin pretreatment dramatically increases the effects of cisplatin on ovarian cancer cells. Microscopic examination of treated cells revealed that 2.5 μM cisplatin did not change cell number or morphology and that 20 μM curcumin had a moderate decrease in cell number (Figure 1C). However, when pre-treated with 20 μM curcumin, 2.5 μM cisplatin drastically reduced the cell survival (Figure 1C).

To determine the long-term effect of chemo-sensitization with curcumin pre-treatment, we performed colony forming assays with cells either treated individually with curcumin or cisplatin, or with a 6 hr pre-treatment of curcumin followed by cisplatin treatment (Figure 2). Pre-treatment of cells with curcumin (2 and 4 μM) followed by cisplatin (1-3 μM) resulted in a greater inhibition of colony formation than each agent alone (Figure 2). Due to the prolonged incubation after drug treatment(s), it is not surprising that lower doses of cisplatin/curcumin had significant effects compared to the 48 hr proliferation assay. Further, we have determined the effect of curcumin pre-treatment on ovarian cancer cell's sensitivity to radiation. Pre-treatment of cells with curcumin (2-8 μM) followed by radiation exposure (2-8 Gy) resulted in greater inhibition of colony formation than curcumin or radiation alone (Figure 3). From these data, it is apparent that curcumin can induce chemo/radio-sensitization in ovarian cancer cells and may considerably lower the minimum effective dose of cisplatin or radiation treatment.

Curcumin pre-treatment modulates the expression of pro-survival/pro-apoptosis proteins

To examine the possible molecular mechanisms by which curcumin induces chemo/radio-sensitization effects in A2780CP cells, we examined the expression pattern of pro-survival Bcl-2 family members expressed by A2780CP cells (data shown for Bcl-X_L and Mcl-1). Following a 6

hr pre-treatment with 20 μ M curcumin, the expression of Bcl-X_L and Mcl-1 was decreased (Figure 4A), which would suggest increased sensitivity to apoptosis. Hence, we sought to determine if cell death was occurring through an apoptotic pathway. Following curcumin pre-treatment, both adherent and floating cells were collected, stained with Annexin V-PE and analyzed by flow cytometry. Curcumin pre-treatment followed by cisplatin treatment resulted in a substantial increase in Annexin V positive cells (Figure 4B), indicating induction of cell death *via* an apoptotic pathway. We confirmed this observation by probing for the expression of PARP and caspases 3, 7 and 9, as proteolytic cleavage and subsequent activation of these molecules activate apoptotic pathways. A2780CP cells pre-treated with curcumin and then treated with cisplatin showed higher levels of cleaved caspase 9, in contrast to cells treated with curcumin or cisplatin alone (Figure 4C). Additionally, the expression level of full-length caspase 3 and 7 was decreased, suggesting cleavage and activation of the caspase pathway; however, cleaved products of caspase 3 or 7 were not detectable (data not shown). Furthermore, we also assessed treated cells for cleavage of PARP, a classic marker for apoptotic cells. Pre-treatment with curcumin followed by cisplatin exposure resulted in increased PARP cleavage in a dose dependent manner, while cisplatin alone was unable to induce PARP cleavage even at the highest dose (Figure 4C and D). We detected an increase in full length PARP after 20 μ M cisplatin treatment (Figure 4C), which could be an indication of the cancer cell's attempt to survive cisplatin induced DNA damage by increasing DNA repair proteins, such as PARP. However, in curcumin pre-treated cells, cisplatin exposure resulted in a significant ($p < 0.05$) increase in PARP cleavage, indicating the induction of apoptosis.

Curcumin suppresses β -catenin activity

Inappropriate activation of β -catenin is linked with the development of a wide variety of cancers, including melanoma, colorectal and prostate cancer [24, 25]. Additionally, deregulation of the Wnt/ β -catenin pathway has also been shown in ovarian cancer [26, 27]. As a modulator of the Wnt signaling pathway, β -catenin functions as a transcription factor that is translocated into the nucleus where it binds with the TCF transcription factor and up-regulates the expression of cell survival genes such as c-Myc and c-Jun, which as a result, enhances cell proliferation in cancer cells. It has also been shown that β -catenin activity can also inhibit apoptosis in cancer cells [28-31]. Therefore, we sought to investigate the effects of curcumin treatment on nuclear β -catenin function in cisplatin resistant ovarian cancer cells using TOPFlash reporter assay. The cells were treated with either curcumin, cisplatin or a 6 hr pre-treatment with curcumin followed by treatment with cisplatin. After 24 hrs of incubation, cell lysates were collected and analyzed for β -catenin transcription activity. While treatment of the cells with cisplatin caused no change in the β -catenin activity, curcumin treatment repressed the β -catenin mediated transcription activity by 60% (Figure 5A).). The combination of curcumin and cisplatin also reduced β -catenin activity to similar levels as when treated with curcumin (there is not a significant difference between curcumin only and combination treatment with curcumin and cisplatin). To further investigate curcumin mediated repression of β -catenin activity, we analyzed the overall expression of β -catenin levels and the expression of a downstream target of nuclear β -catenin signaling (c-Myc) by Western blotting. Curcumin treatment leads to ~50% reduction in β -catenin and c-Myc protein levels (Figure 5B). This data suggest that curcumin treatment attenuates nuclear β -catenin signaling, which is known to play a significant role in cancer cell proliferation.

PLGA nanoparticle formulation of curcumin (Nano-CUR) effectively inhibits ovarian cancer cells growth

While we have shown that curcumin has effective chemo/radio sensitization effects in ovarian cancer cells, low water solubility and poor pharmacokinetics greatly hamper curcumin's *in vivo* therapeutic efficacy. Therefore, we decided to synthesize a PLGA nanoparticle (NP) formulation of curcumin, which is expected to improve bioavailability *in vivo* [32, 33]. Following synthesis, Nano-CUR was physically characterized by both dynamic light scattering (DLS) and transmission electron microscopy (TEM). The average size of Nano-CUR was observed to be ~72 nm by DLS (Figure 6A) and 70 ± 3.9 nm by TEM (Figure 6B). Additionally, curcumin is released from PLGA NPs in a controlled fashion, which may be useful for sustained and long term delivery of curcumin for ovarian cancer treatment (Figure 6C). Following particle characterization, we examined the *in vitro* therapeutic efficacy of Nano-CUR and found that Nano-CUR treatment effectively inhibited proliferation of ovarian cancer cells (Figure 6D). Additionally, PLGA NPs are efficiently internalized by A2780CP cells (Figure 6E). Further, to verify that these nanoparticles are capable of antibody conjugation for targeted delivery specifically to ovarian cancer cells, we conjugated nanoparticles with anti-TAG-72 monoclonal antibody (MAb) (Figure 6F). TAG-72, a tumor-associated glycoprotein, is over-expressed in various tumors, including ovarian cancer [34]. Western blot analysis of conjugated PLGA NPs revealed that anti-TAG-72 MAb was effectively conjugated to PLGA NPs (Figure 6G). These data suggest that, in the future, targeted delivery of curcumin specifically to tumors will be possible. This strategy will improve the therapeutic efficacy of curcumin and will be useful for specific chemo/radio-sensitization of cancer cells.

Discussion

Most ovarian cancers initially respond well to current treatment modalities, but the majority of patients will experience recurrence. Unfortunately, almost all recurrent ovarian cancers eventually develop resistance to platinum based treatment. Tumors with intrinsic or acquired resistance may have various altered characteristics, including: (a) altered membrane transport properties, (b) altered expression of target enzymes, (c) promotion of DNA repair, (d) degradation of drug molecules, and (e) generalized resistance to apoptosis [35-37]. A promising strategy for improving current ovarian cancer therapy is to employ a chemo/radio-sensitizer along with chemo/radiation therapies.

Curcumin is an excellent candidate as a chemo/radio sensitizer and has been shown to have *in vitro* chemo-sensitization effects for cervical cancer and radio-sensitizing effects for prostate cancer [38, 39]. However, curcumin's utility for ovarian cancer treatment has not been fully explored [40-42]. Chirnomas et al. reported that a functional Fanconi anemia (FA)/BRCA pathway limits sensitivity to cisplatin and that curcumin can inhibit this pathway, leading to increased sensitivity to cisplatin treatment in ovarian cancer cells [41]. Our study shows that a 6 hr pre-treatment with curcumin effectively sensitized cisplatin resistant ovarian cancer cells to the cytotoxic effects of cisplatin, at doses at least 10 times lower compared to cisplatin treatment alone. Using clonogenic assays, we assessed the long term effects of curcumin pre-treatment along with cisplatin treatment or radiation exposure. We found that curcumin pre-treatment followed by cisplatin or radiation exposure dramatically reduced colony formation compared to either treatment alone. Curcumin pre-treatment clearly lowers the dose of cisplatin and radiation treatment needed to suppress the growth of ovarian cancer cells.

Apoptosis is normally a carefully balanced system of checks and balances. In cancer cells, often the balance has been tilted to be more resistant to the initiation of apoptosis. Over-expression of pro-survival Bcl2 family members is common in many types of cancer and has been correlated with decreased sensitivity to chemotherapy and radiation [43]. We found that curcumin pre-treatment reduced the expression of two pro-survival proteins, Bcl-X_L and Mcl-1, potentially allowing curcumin treated cells to undergo apoptosis upon cisplatin treatment. Indeed, pre-treatment with curcumin followed by cisplatin increased the percent of Annexin V positive cells and increased the amount of cleaved caspase 9 and PARP, as compared to cisplatin or curcumin alone, indicating that curcumin pre-treatment followed by cisplatin enhanced apoptosis.

Curcumin treatment reduced the transcriptional activity and expression level of β -catenin. The β -catenin pathway is known to be disrupted in a variety of cancers, including ovarian cancer. Activation of the β -catenin signaling pathway leads to nuclear localization of β -catenin which interacts with the TCF transcription factor and modulates the expression of a wide range of proto-oncogenes. The functions of these responsive genes are thought to increase proliferation and recent studies have also suggested that β -catenin signaling may also inhibit apoptosis [28-31]. Taken together, these results suggest that curcumin pre-treatment increases the effectiveness of cisplatin treatment in cisplatin resistant cells by increasing the sensitivity of cells to apoptotic pathways and modulating nuclear β -catenin signaling.

Curcumin is in early phase clinical trials for various types of cancers [44]. Curcumin is remarkably well tolerated and has no toxicity issues [45, 46], but it has limited bioavailability and

poor pharmacokinetics [47, 48]. To improve curcumin's *in vivo* effectiveness we have developed a PLGA nanoformulation of curcumin. Nanoparticles can deliver anti-cancer drugs to the site of disease with an antibody targeting approach; however, major drawbacks include interaction with serum proteins (causing opsonization), clearance by the reticuloendothelial system, and non specific accumulation in organs [49]. To counter these difficulties and to extend the circulation time of nanoparticles in the blood, nanoparticles may be modified with inert hydrophilic polymers, such as poly(ethylene glycol) and poly(vinyl alcohol). In addition, formulating a small particle size (less than 100 nm) with high antibody conjugation efficiency will further enhance the ability to target tumors efficiently [50]. In our current study, we have developed PLGA nanoparticles which are made using FDA approved polymer (PLGA) and coated with poly(vinyl alcohol). The formulated Nano-CUR effectively inhibits proliferation in cisplatin resistant ovarian cancer cell lines. The size of these PLGA NPs were formulated to ~70 nm which is an important parameter for enhancing the circulation life time and ensuring diffusion of particles into tumor sites. Recent literature suggests that antibody conjugated nanoparticles could efficiently deliver chemotherapeutic drugs to the tumor site [51-53]. Accordingly, we have shown efficient conjugation of anti-TAG-72 MAb to PLGA NPs with our conjugation chemistry for targeting applications. Targeted delivery of curcumin will improve the therapeutic efficacy of curcumin and will be useful for specific chemo/radio-sensitization of cancer cells. Overall, the results of this study suggest that curcumin pre-treatment induces chemo/radio-sensitization in ovarian cancer cells *via* modulating pro-survival cellular signaling and nanoparticle mediated curcumin delivery may further improve the therapeutic efficacy of curcumin.

Conclusion

We report that curcumin acts as a chemo/radio-sensitizer by modulating the expression of pro-survival proteins and increasing apoptosis in response to a low dose of cisplatin. Nanoparticle mediated curcumin delivery will further improve the sensitization and therapeutic capabilities of curcumin. This study demonstrates a novel curcumin pre-treatment strategy that could be implemented in pre-clinical animal models and in future clinical trials for the effective treatment of chemo/radio-resistant ovarian cancers.

Competing interests

The author(s) declare that they have no competing interests.

Authors' Contributions

MMY designed and performed MTS assays, colony formation assays, Western blotting, and synthesis of PLGA NP formulations. DM participated in the design of the study, provided technical support and performed flow cytometry analysis. DM and MMY drafted the manuscript together. VS performed and analyzed the β -catenin assays and participated in manuscript preparation. SCC and MJ participated in the inception of the idea, experimental design, and revision of the manuscript. All authors read and approved the manuscript.

Acknowledgements

Authors thankfully acknowledge Cathy Christopherson for editorial assistance and James Pottala for statistical consultation. This work was supported in part by a Sanford Research/USD grant and Department of Defense Grants awarded to SCC (PC073887) and MJ (PC073643).

References

1. Jemal A, Siegel R, Ward E, Hao Y, Xu J, Thun MJ: **Cancer statistics, 2009.** *CA Cancer J Clin* 2009, **59**:225-249.
2. Armstrong DK: **Relapsed ovarian cancer: challenges and management strategies for a chronic disease.** *Oncologist* 2002, **7 Suppl 5**:20-28.
3. Markman M: **Pharmaceutical management of ovarian cancer : current status.** *Drugs* 2008, **68**:771-789.
4. Markman M, Webster K, Zanotti K, Peterson G, Kulp B, Belinson J: **Survival following the documentation of platinum and taxane resistance in ovarian cancer: a single institution experience involving multiple phase 2 clinical trials.** *Gynecol Oncol* 2004, **93**:699-701.
5. Borst P, Rottenberg S, Jonkers J: **How do real tumors become resistant to cisplatin?** *Cell Cycle* 2008, **7**:1353-1359.
6. Herzog TJ, Pothuri B: **Ovarian cancer: a focus on management of recurrent disease.** *Nat Clin Pract Oncol* 2006, **3**:604-611.
7. Alvarez RD, Huh WK, Khazaeli MB, Meredith RF, Partridge EE, Kilgore LC, Grizzle WE, Shen S, Austin JM, Barnes MN, et al: **A Phase I study of combined modality (90)Yttrium-CC49 intraperitoneal radioimmunotherapy for ovarian cancer.** *Clin Cancer Res* 2002, **8**:2806-2811.
8. Meredith RF, Buchsbaum DJ, Alvarez RD, LoBuglio AF: **Brief overview of preclinical and clinical studies in the development of intraperitoneal radioimmunotherapy for ovarian cancer.** *Clin Cancer Res* 2007, **13**:5643s-5645s.
9. Meenakshi Kumar SI, and Neeta Singh: **Curcumin and Quercetin Combined with Cisplatin to Induce Apoptosis in Human Laryngeal Carcinoma Hep-2 Cells through the Mitochondrial Pathway.** *Journal of Cancer Molecules* 2007, **3**:121-128.
10. Cheah YH, Nordin FJ, Sarip R, Tee TT, Azimahtol HL, Sirat HM, Rashid BA, Abdullah NR, Ismail Z: **Combined xanthorrhizol-curcumin exhibits synergistic growth inhibitory activity via apoptosis induction in human breast cancer cells MDA-MB-231.** *Cancer Cell Int* 2009, **9**:1.
11. Siddiqui IA, Malik A, Adhami VM, Asim M, Hafeez BB, Sarfaraz S, Mukhtar H: **Green tea polyphenol EGCG sensitizes human prostate carcinoma LNCaP cells to TRAIL-mediated apoptosis and synergistically inhibits biomarkers associated with angiogenesis and metastasis.** *Oncogene* 2008, **27**:2055-2063.
12. Bal Krishnan Jaggi SCC, and Meena Jaggi: **Review of Curcumin Effects on Signaling Pathways in Cancer.** *Proceedings of the South Dakota Academy of Science* 2007, **86**:283-293.
13. Karmakar S, Banik NL, Patel SJ, Ray SK: **Curcumin activated both receptor-mediated and mitochondria-mediated proteolytic pathways for apoptosis in human glioblastoma T98G cells.** *Neurosci Lett* 2006, **407**:53-58.
14. Shishodia S, Amin HM, Lai R, Aggarwal BB: **Curcumin (diferuloylmethane) inhibits constitutive NF-kappaB activation, induces G1/S arrest, suppresses proliferation, and induces apoptosis in mantle cell lymphoma.** *Biochem Pharmacol* 2005, **70**:700-713.
15. Shishodia S, Chaturvedi MM, Aggarwal BB: **Role of curcumin in cancer therapy.** *Curr Probl Cancer* 2007, **31**:243-305.

16. Cheng AL, Hsu CH, Lin JK, Hsu MM, Ho YF, Shen TS, Ko JY, Lin JT, Lin BR, Ming-Shiang W, et al: **Phase I clinical trial of curcumin, a chemopreventive agent, in patients with high-risk or pre-malignant lesions.** *Anticancer Res* 2001, **21**:2895-2900.
17. Garcea G, Jones DJ, Singh R, Dennison AR, Farmer PB, Sharma RA, Steward WP, Gescher AJ, Berry DP: **Detection of curcumin and its metabolites in hepatic tissue and portal blood of patients following oral administration.** *Br J Cancer* 2004, **90**:1011-1015.
18. Hamaguchi K, Godwin AK, Yakushiji M, O'Dwyer PJ, Ozols RF, Hamilton TC: **Cross-resistance to diverse drugs is associated with primary cisplatin resistance in ovarian cancer cell lines.** *Cancer Res* 1993, **53**:5225-5232.
19. Chauhan SC, Vannatta K, Ebeling MC, Vinayek N, Watanabe A, Pandey KK, Bell MC, Koch MD, Aburatani H, Lio Y, Jaggi M: **Expression and functions of transmembrane mucin MUC13 in ovarian cancer.** *Cancer Res* 2009, **69**:765-774.
20. Jaggi M, Chauhan SC, Du C, Balaji KC: **Bryostatins 1 modulates beta-catenin subcellular localization and transcription activity through protein kinase D1 activation.** *Mol Cancer Ther* 2008, **7**:2703-2712.
21. Govender T, Stolnik S, Garnett MC, Illum L, Davis SS: **PLGA nanoparticles prepared by nanoprecipitation: drug loading and release studies of a water soluble drug.** *J Control Release* 1999, **57**:171-185.
22. Bisht S, Feldmann G, Soni S, Ravi R, Karikar C, Maitra A, Maitra A: **Polymeric nanoparticle-encapsulated curcumin ("nanocurcumin"): a novel strategy for human cancer therapy.** *J Nanobiotechnology* 2007, **5**:3.
23. Dong S, Roman M: **Fluorescently labeled cellulose nanocrystals for bioimaging applications.** *J Am Chem Soc* 2007, **129**:13810-13811.
24. Gavert N, Ben-Ze'ev A: **beta-Catenin signaling in biological control and cancer.** *J Cell Biochem* 2007, **102**:820-828.
25. Wheelock MJ, Johnson KR: **Cadherin-mediated cellular signaling.** *Curr Opin Cell Biol* 2003, **15**:509-514.
26. Gatcliffe TA, Monk BJ, Planutis K, Holcombe RF: **Wnt signaling in ovarian tumorigenesis.** *Int J Gynecol Cancer* 2008, **18**:954-962.
27. Sarrio D, Moreno-Bueno G, Sanchez-Estevéz C, Banon-Rodríguez I, Hernandez-Cortes G, Hardisson D, Palacios J: **Expression of cadherins and catenins correlates with distinct histologic types of ovarian carcinomas.** *Hum Pathol* 2006, **37**:1042-1049.
28. Dehner M, Hadjihannas M, Weiske J, Huber O, Behrens J: **Wnt signaling inhibits Forkhead box O3a-induced transcription and apoptosis through up-regulation of serum- and glucocorticoid-inducible kinase 1.** *J Biol Chem* 2008, **283**:19201-19210.
29. Huang M, Wang Y, Sun D, Zhu H, Yin Y, Zhang W, Yang S, Quan L, Bai J, Wang S, et al: **Identification of genes regulated by Wnt/beta-catenin pathway and involved in apoptosis via microarray analysis.** *BMC Cancer* 2006, **6**:221.
30. Yang F, Zeng Q, Yu G, Li S, Wang CY: **Wnt/beta-catenin signaling inhibits death receptor-mediated apoptosis and promotes invasive growth of HNSCC.** *Cell Signal* 2006, **18**:679-687.
31. Liu M, Yang S, Wang Y, Zhu H, Yan S, Zhang W, Quan L, Bai J, Xu N: **EB1 acts as an oncogene via activating beta-catenin/TCF pathway to promote cellular growth and inhibit apoptosis.** *Mol Carcinog* 2009, **48**:212-219.

32. Anand P, Nair HB, Sung B, Kunnumakkara AB, Yadav VR, Tekmal RR, Aggarwal BB: **Design of curcumin-loaded PLGA nanoparticles formulation with enhanced cellular uptake, and increased bioactivity in vitro and superior bioavailability in vivo.** *Biochem Pharmacol* 2010, **79**:330-338.
33. Shaikh J, Ankola DD, Beniwal V, Singh D, Kumar MN: **Nanoparticle encapsulation improves oral bioavailability of curcumin by at least 9-fold when compared to curcumin administered with piperine as absorption enhancer.** *Eur J Pharm Sci* 2009, **37**:223-230.
34. Ponnusamy MP, Venkatraman G, Singh AP, Chauhan SC, Johansson SL, Jain M, Smith L, Davis JS, Remmenga SW, Batra SK: **Expression of TAG-72 in ovarian cancer and its correlation with tumor stage and patient prognosis.** *Cancer Lett* 2007, **251**:247-257.
35. Morris PG, Fornier MN: **Microtubule active agents: beyond the taxane frontier.** *Clin Cancer Res* 2008, **14**:7167-7172.
36. Perez EA: **Impact, mechanisms, and novel chemotherapy strategies for overcoming resistance to anthracyclines and taxanes in metastatic breast cancer.** *Breast Cancer Res Treat* 2009, **114**:195-201.
37. Krishna R, Mayer LD: **Multidrug resistance (MDR) in cancer. Mechanisms, reversal using modulators of MDR and the role of MDR modulators in influencing the pharmacokinetics of anticancer drugs.** *Eur J Pharm Sci* 2000, **11**:265-283.
38. Chendil D, Ranga RS, Meigooni D, Sathishkumar S, Ahmed MM: **Curcumin confers radiosensitizing effect in prostate cancer cell line PC-3.** *Oncogene* 2004, **23**:1599-1607.
39. Javvadi P, Segan AT, Tuttle SW, Koumenis C: **The chemopreventive agent curcumin is a potent radiosensitizer of human cervical tumor cells via increased reactive oxygen species production and overactivation of the mitogen-activated protein kinase pathway.** *Mol Pharmacol* 2008, **73**:1491-1501.
40. Chan MM, Fong D, Soprano KJ, Holmes WF, Heverling H: **Inhibition of growth and sensitization to cisplatin-mediated killing of ovarian cancer cells by polyphenolic chemopreventive agents.** *J Cell Physiol* 2003, **194**:63-70.
41. Chirnomas D, Taniguchi T, de la Vega M, Vaidya AP, Vasserman M, Hartman AR, Kennedy R, Foster R, Mahoney J, Seiden MV, D'Andrea AD: **Chemosenitization to cisplatin by inhibitors of the Fanconi anemia/BRCA pathway.** *Mol Cancer Ther* 2006, **5**:952-961.
42. Montopoli M, Ragazzi E, Frolidi G, Caparrotta L: **Cell-cycle inhibition and apoptosis induced by curcumin and cisplatin or oxaliplatin in human ovarian carcinoma cells.** *Cell Prolif* 2009, **42**:195-206.
43. Frenzel A, Grespi F, Chmielewski W, Villunger A: **Bcl2 family proteins in carcinogenesis and the treatment of cancer.** *Apoptosis* 2009, **14**:584-596.
44. Lopez-Lazaro M: **Anticancer and carcinogenic properties of curcumin: considerations for its clinical development as a cancer chemopreventive and chemotherapeutic agent.** *Mol Nutr Food Res* 2008, **52 Suppl 1**:S103-127.
45. Hsu CH, Cheng AL: **Clinical studies with curcumin.** *Adv Exp Med Biol* 2007, **595**:471-480.
46. Sharma RA, Euden SA, Platton SL, Cooke DN, Shafayat A, Hewitt HR, Marczyklo TH, Morgan B, Hemingway D, Plummer SM, et al: **Phase I clinical trial of oral curcumin:**

- biomarkers of systemic activity and compliance. *Clin Cancer Res* 2004, **10**:6847-6854.**
47. Ireson C, Orr S, Jones DJ, Verschoyle R, Lim CK, Luo JL, Howells L, Plummer S, Jukes R, Williams M, et al: **Characterization of metabolites of the chemopreventive agent curcumin in human and rat hepatocytes and in the rat in vivo, and evaluation of their ability to inhibit phorbol ester-induced prostaglandin E2 production.** *Cancer Res* 2001, **61**:1058-1064.
 48. Ireson CR, Jones DJ, Orr S, Coughtrie MW, Boocock DJ, Williams ML, Farmer PB, Steward WP, Gescher AJ: **Metabolism of the cancer chemopreventive agent curcumin in human and rat intestine.** *Cancer Epidemiol Biomarkers Prev* 2002, **11**:105-111.
 49. Singh R, Lillard JW, Jr.: **Nanoparticle-based targeted drug delivery.** *Exp Mol Pathol* 2009, **86**:215-223.
 50. Emerich DF, Thanos CG: **Targeted nanoparticle-based drug delivery and diagnosis.** *J Drug Target* 2007, **15**:163-183.
 51. Byrne JD, Betancourt T, Brannon-Peppas L: **Active targeting schemes for nanoparticle systems in cancer therapeutics.** *Adv Drug Deliv Rev* 2008, **60**:1615-1626.
 52. Davis ME, Chen ZG, Shin DM: **Nanoparticle therapeutics: an emerging treatment modality for cancer.** *Nat Rev Drug Discov* 2008, **7**:771-782.
 53. Kukowska-Latallo JF, Candido KA, Cao Z, Nigavekar SS, Majoros IJ, Thomas TP, Balogh LP, Khan MK, Baker JR, Jr.: **Nanoparticle targeting of anticancer drug improves therapeutic response in animal model of human epithelial cancer.** *Cancer Res* 2005, **65**:5317-5324.

Figure legends:

Figure 1. Curcumin pre-treatment effectively lowers the cisplatin dose needed for inhibiting growth of cisplatin resistant A2780CP ovarian cancer cells. (A) Design of treatment method for curcumin sensitization followed by cisplatin treatment. Cisplatin resistant ovarian cancer cells (A2780CP) were either treated with curcumin or cisplatin alone for 48 hrs, or pre-treated with curcumin for 6 hrs followed by cisplatin for an additional 42 hrs. **(B) Curcumin pre-treatment followed by cisplatin exposure decreases cell proliferation at lower doses of cisplatin.** A2780CP cells were treated with either 2.5-40 μ M of curcumin (CUR) or cisplatin (CIS) alone for 48 hrs or pre-treated with 10 or 20 μ M curcumin for 6 hrs followed by 2.5-40 μ M of cisplatin treatment for 42 hrs (CUR + CIS). Cell proliferation was determined by MTS assay and normalized to control cells treated with appropriate amounts of vehicle (DMSO or DMSO-PBS). Data represent mean \pm SE of 6 repeats for each treatment and the experiment was repeated three times. **(C) Phase contrast microscopic analysis reveals curcumin sensitization to cisplatin.** Phase contrast images of A2780CP cells treated with vehicle (DMSO, control), 2.5 μ M CIS for 48 hrs, 20 μ M CUR for 48 hrs, and 20 μ M CUR for 6 hrs followed by 2.5 μ M CIS for 42 hrs. Bar equals 100 microns.

Figure 2. Curcumin pre-treatment followed by cisplatin exposure reduces the clonogenic potential of A2780CP cells. A2780CP cells were treated with the indicated amounts of curcumin or cisplatin alone or pre-treated with curcumin for 6 hrs followed by cisplatin and allowed to grow for 8 days. **(A)** Representative images of colony forming assays. **(B)** Colonies were counted and expressed as a percent of the DMSO vehicle control. Data represent mean of 3

repeats for each treatment (Mean \pm SE; * $p < 0.017$, compared to the same cisplatin dose without curcumin).

Figure 3. Curcumin pre-treatment sensitizes cells to radiation exposure and reduces the clonogenic potential of A2780CP cells. A2780CP cells were treated with the indicated amounts of curcumin or radiation alone or pre-treated with curcumin for 6 hrs followed by radiation exposure and allowed to grow for 8 days. **(A)** Representative images of colony forming assays. **(B)** Colonies were counted and expressed as a percent of each respective dose of radiation. Data represent mean of 3 repeats for each treatment (Mean \pm SE; * $p < 0.017$, compared to the same dose of curcumin with no radiation exposure).

Figure 4. Curcumin treatment alters the expression of pro-survival and pro-apoptosis related proteins. (A) Curcumin decreases the expression of Bcl2 family of pro-survival proteins during 6 hr pre-treatment. A2780CP cells were treated with 20 μ M curcumin for 6 hrs and protein lysates were collected and analyzed by immunoblotting for Bcl-x1, Mcl-1 and β -actin. Appropriate bands were quantified by densitometry, normalized to β -actin, scaled to the DMSO control and expressed as relative expression levels (number beneath the blots). **(B) Curcumin pre-treatment followed by low dose cisplatin increases percent of Annexin V positive cells.** A2780CP cells treated as indicated with vehicle (DMSO), curcumin (20 μ M) or cisplatin (5 μ M) only or pre-treated with curcumin (20 μ M) followed by cisplatin (5 μ M) treatment. After 48 hrs, adherent and attached cells were stained with Annexin V-PE and analyzed by Flow Cytometry. Representative histograms are shown for 1 of 3 similar experiments. **(C and D) Curcumin pre-treatment promotes the induction of apoptosis by**

cisplatin. A2780CP cells were treated as indicated for a total of 48 hrs and protein lysates were collected and analyzed by immunoblotting for caspase 9 and PARP. **(D)** Bands for full length and cleaved PARP were quantified by densitometry, normalized to β -actin and calculated as a ratio of cleaved PARP to full length PARP. Data represent mean of 3 repeats for each treatment (Mean \pm SE, * $p < 0.017$, compared to curcumin only)

Figure 5. Curcumin inhibits nuclear β -catenin signaling. (A) Curcumin inhibits β -catenin transcription activity. A2780CP cells were transiently transfected with TOPFlash or FOPFlash and co-transfected with Renilla luciferase to determine β -catenin/TCF transcription activity. The cells were treated with 20 μ M curcumin, 5 μ M cisplatin or a 6 hr pre-treatment with 20 μ M curcumin followed by treatment with 5 μ M cisplatin. After 24 hrs of incubation, cell lysates were collected and probed for luciferase activity. Treatment of A2780CP cell line with 20 μ M curcumin resulted in over a 60% reduction in β -catenin activity (Mean \pm SE, $n=3$, * p value $p < 0.017$, compared to control). **(B) Curcumin treatment reduces overall β -catenin and c-Myc protein levels.** A2780CP cell lines were treated as in (A), protein lysates were collected and analyzed by immunoblotting for β -catenin, c-Myc and β -actin. Protein bands were quantified by densitometry, normalized to β -actin, scaled to the DMSO control and expressed as relative expression levels (number beneath the blots). Curcumin treatment caused a 50% reduction in β -catenin and c-Myc levels.

Figure 6. Characterization of PLGA-nanoparticle (NP) containing curcumin (Nano-CUR) and its *in vitro* therapeutic efficacy. (A and B) Nano-CUR particles are an appropriate size of ~70 nm. Nano-CUR size was determined by **(A)** dynamic light scattering (DLS) and **(B)**

transmission electron microscopy (TEM). **(C) Nano-CUR formulation demonstrates sustained release of curcumin.** Cumulative release of curcumin from PLGA NPs was determined by UV spectrophotometer at 450 nm over a period of 18 days. **(D) Nano-CUR effectively inhibits the growth of cisplatin resistant ovarian cancer cells.** A2780CP cells were treated with Nano-CUR (5-80 μ M) or PLGA NPs without curcumin (NPs control) for 48 hrs. Cell proliferation was determined by MTS assay and normalized to control cells treated with vehicle (PBS). **(E) A2780CP cells internalize PLGA-NPs.** A2780CP cells were incubated with FITC-PLGA NPs for 6 hrs and analyzed by fluorescent microscopy. Original magnifications 400X. Inset image represents PLGA NPs no FITC. **(F) Strategy used for antibody conjugation of PLGA-NP for targeted delivery of curcumin to ovarian cancer cells.** **(G) PLGA-NPs can be conjugated with anti-TAG-72 MAb (CC49).** PLGA-NPs were incubated with anti-TAG-72 MAb. Nano-immunoconjugates were run on 10% SDS-PAGE, transferred to the PVDF membrane and were probed with an anti-mouse secondary antibody as indicated.

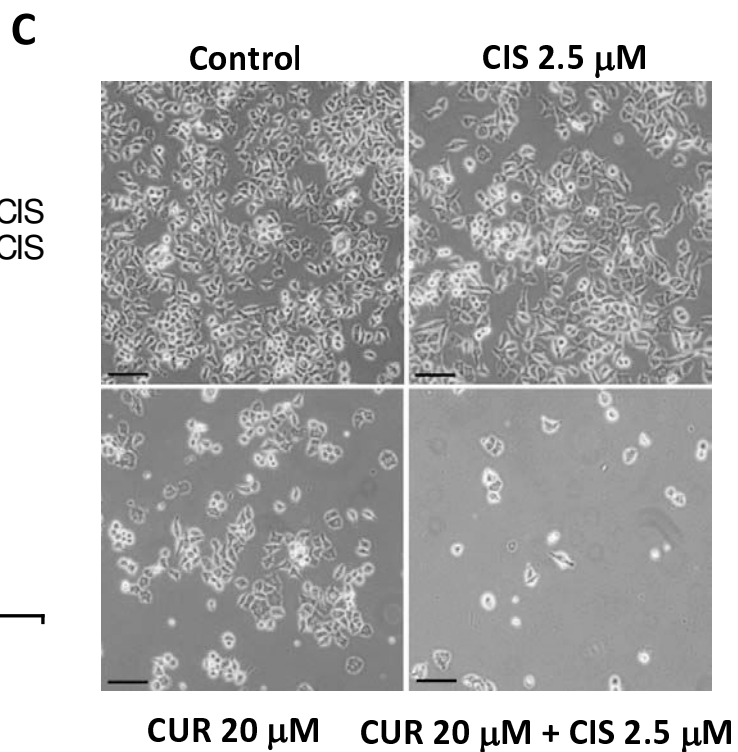
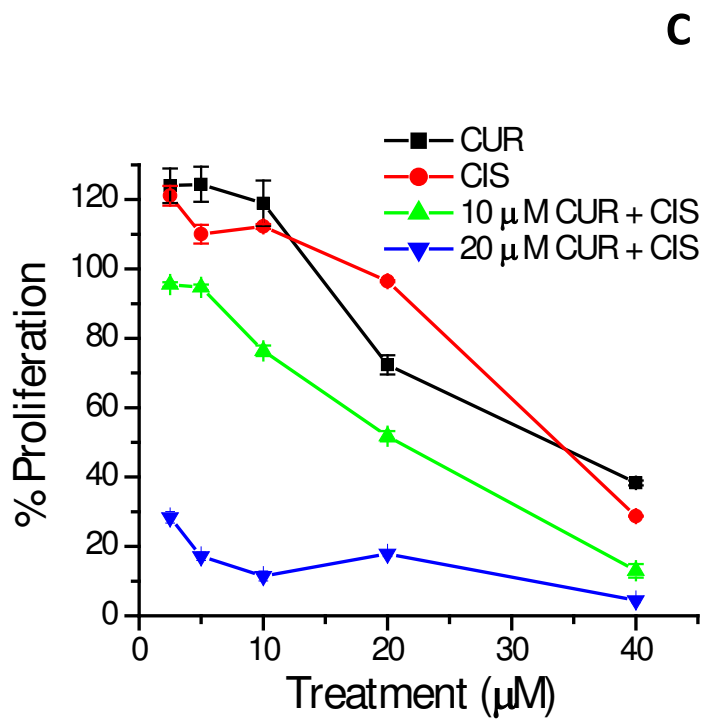
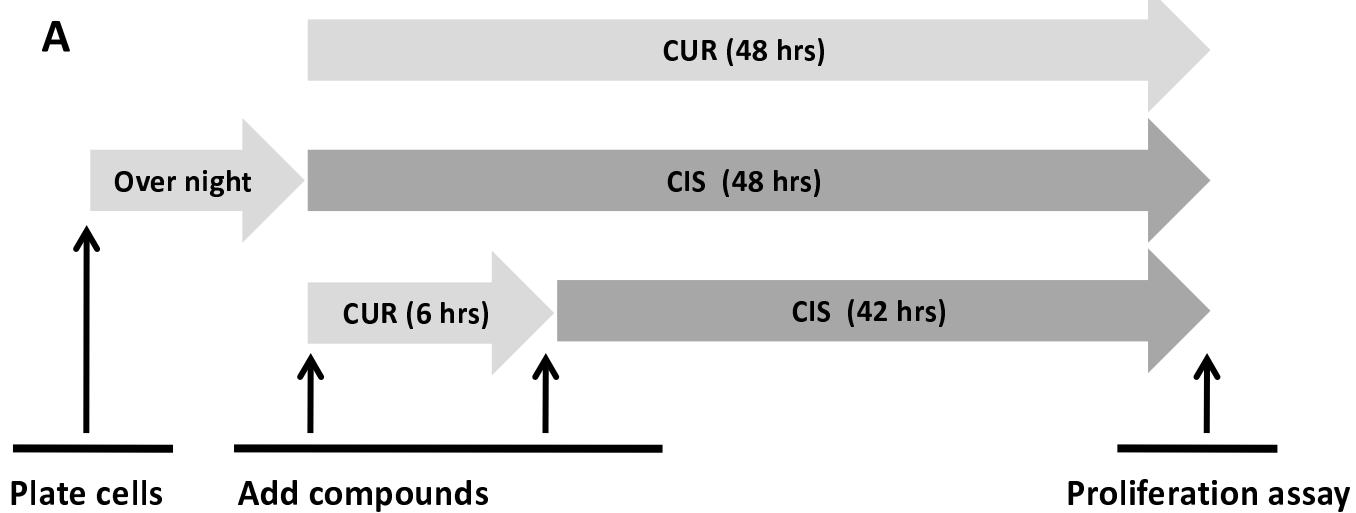


Figure 1

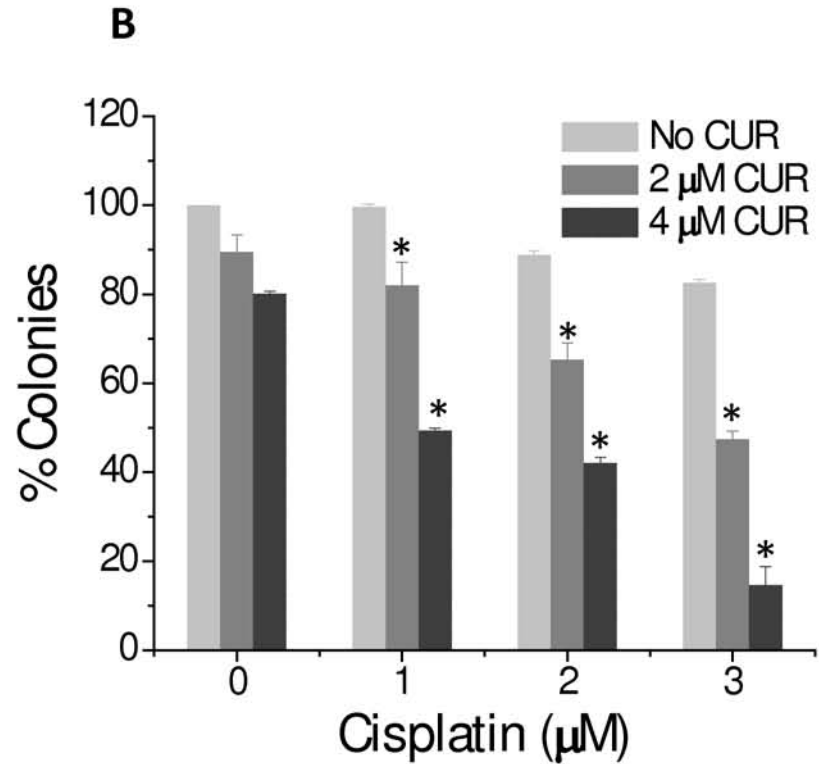
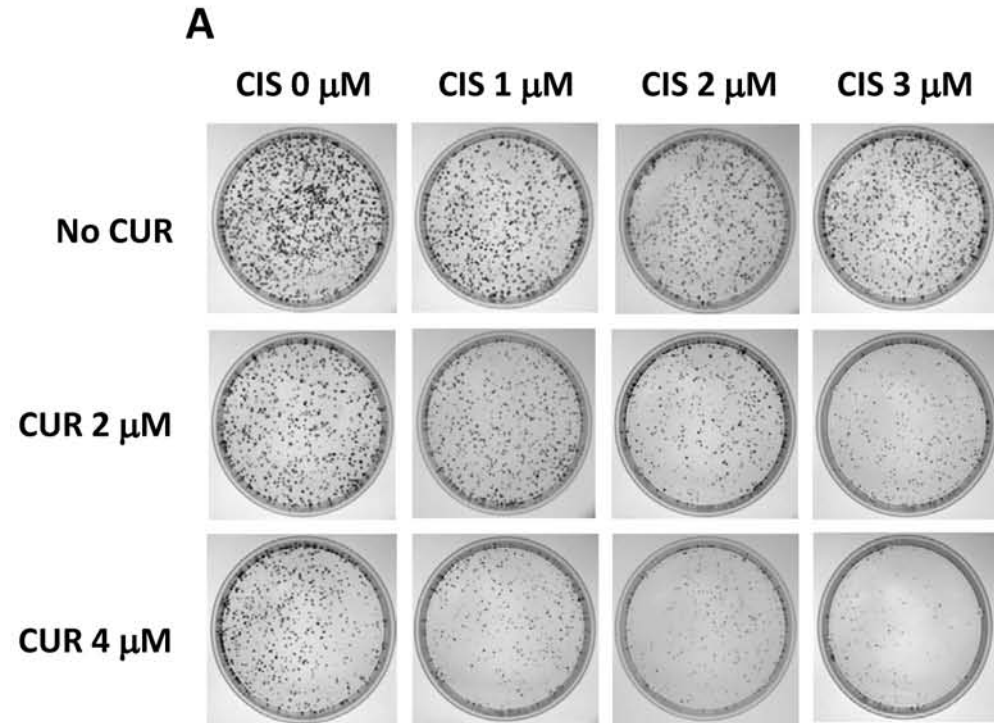


Figure 2

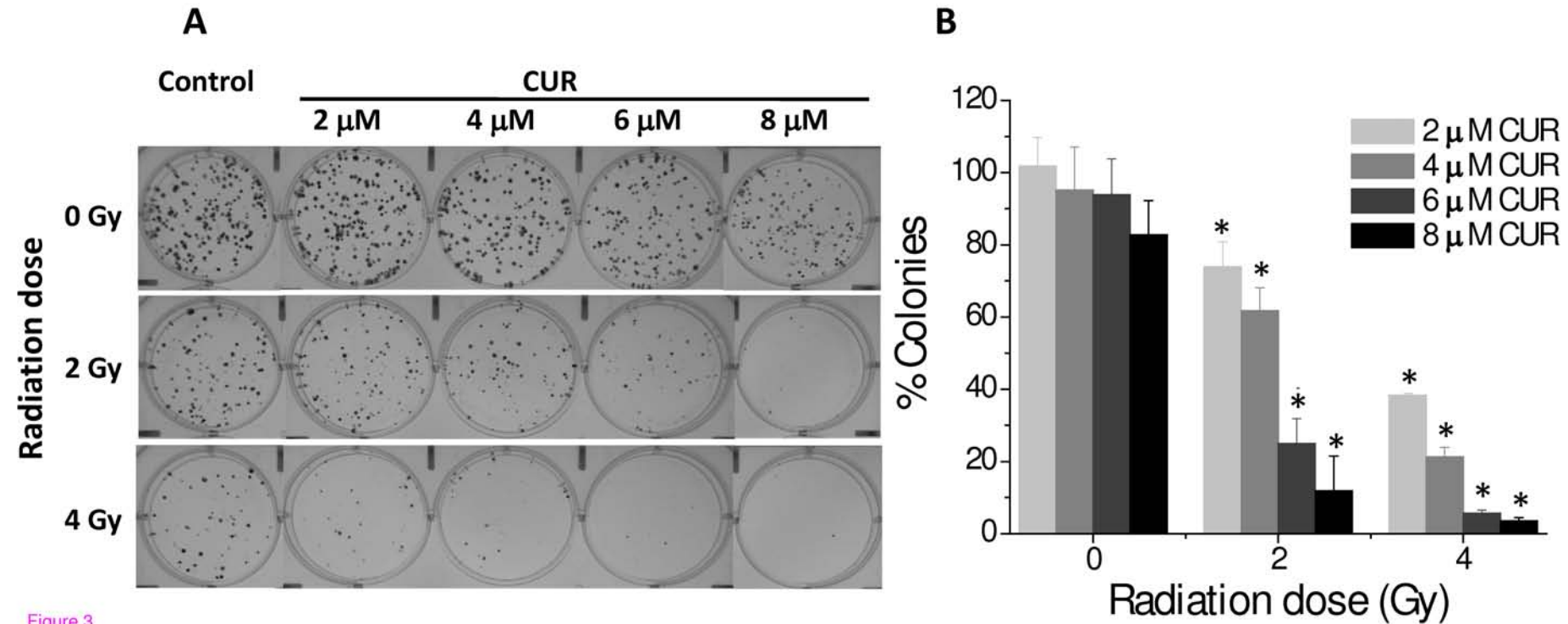


Figure 3

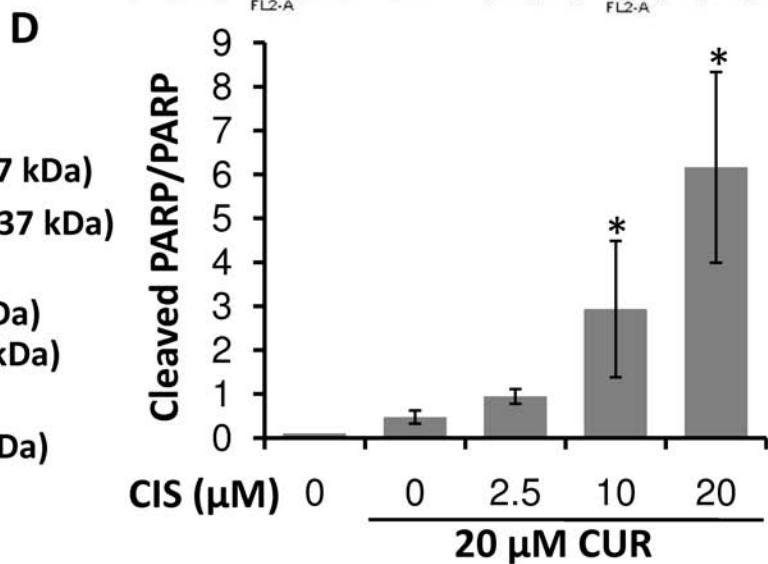
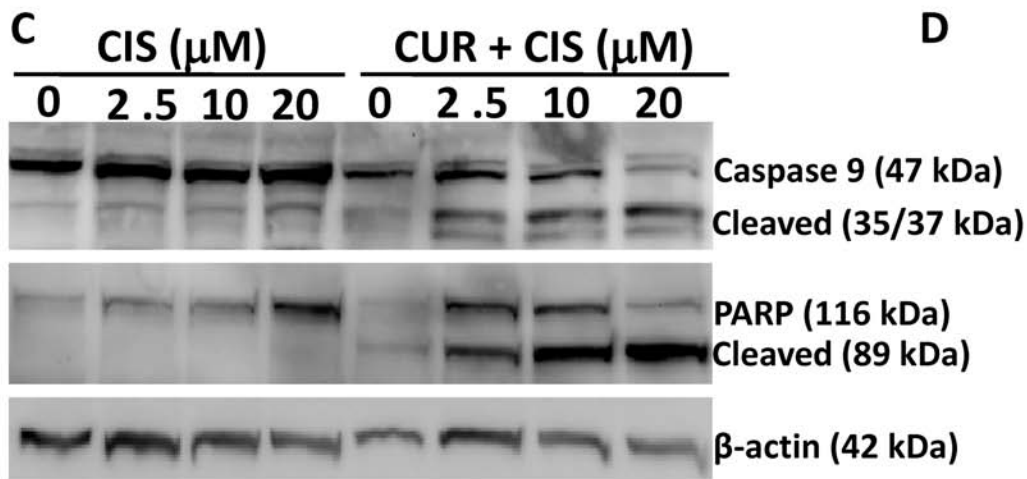
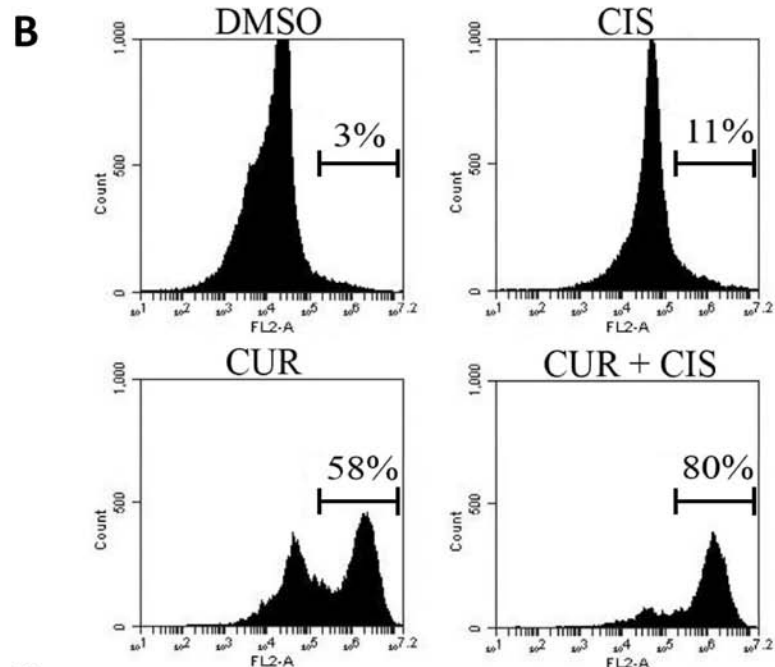
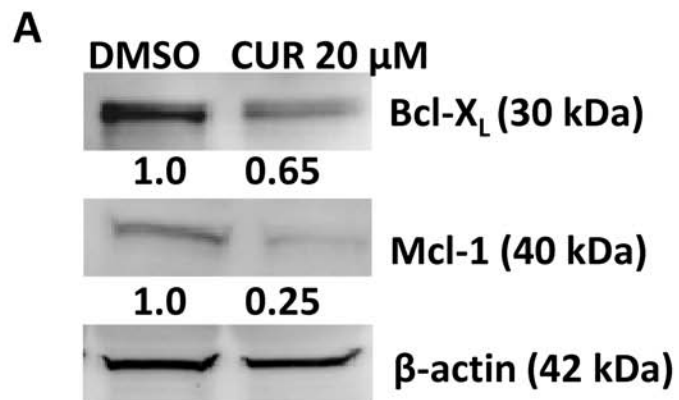


Figure 4

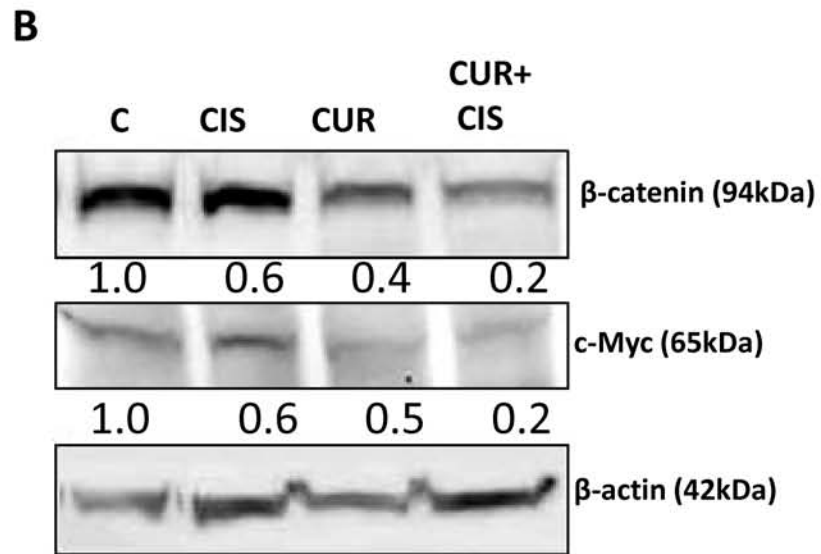
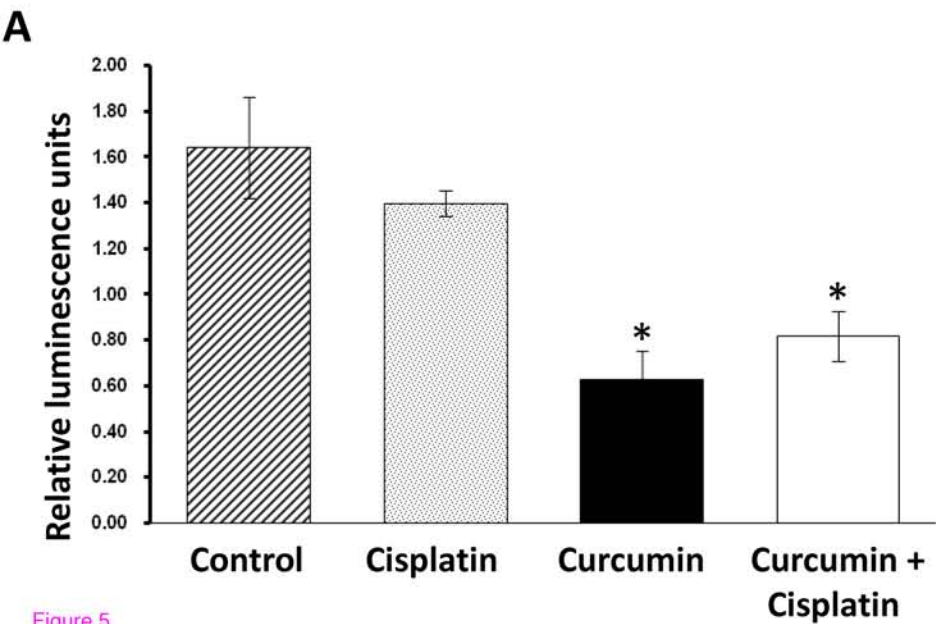


Figure 5

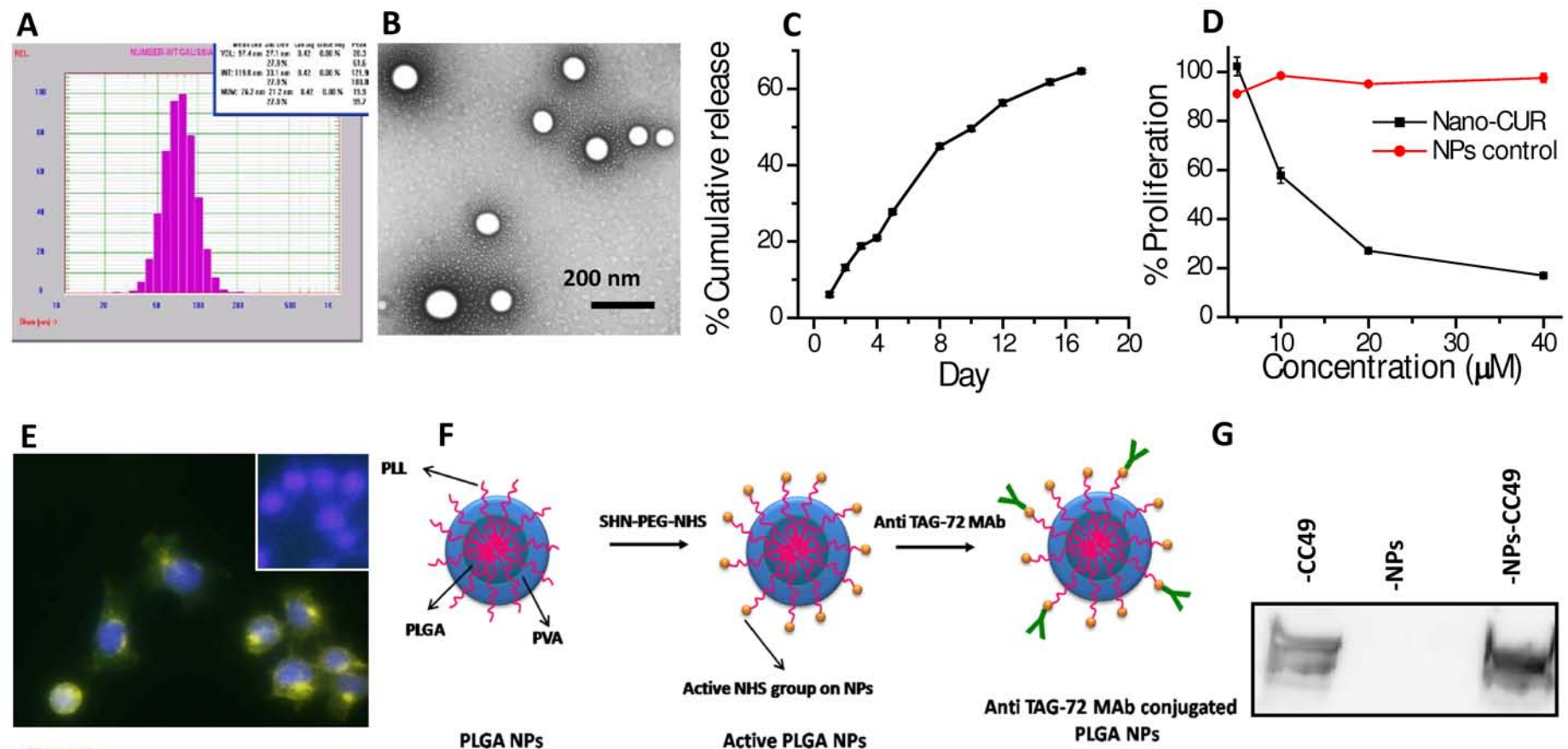


Figure 6

Poly(β -cyclodextrin)-Curcumin Self-assembly : A Novel Approach to Improve Curcumin Delivery and its Therapeutic Efficacy in Prostate Cancer Cells

Murali Mohan Yallapu ¹, Meena Jaggi ^{1,2}, Subhash C. Chauhan ^{1,2*}

¹Cancer Biology Research Center, Sanford Research/USD, 1400 W. 22nd Street, Sioux Falls, SD 57105, USA

²Department of OB/GYN and Basic Biomedical Science Division, Sanford School of Medicine, University of South Dakota, 1400 W. 22nd Street, Sioux Falls, SD 57105, USA

*Correspondence to Subhash C. Chauhan, PhD, Cancer Biology Research Center, Sanford Research/USD, 1400 W. 22nd Street, Sioux Falls, SD-57105, Phone: 605-328-0461, Fax: 605-328-0451

Email: chauhans@sanfordhealth.org (or) subhash.chauhan@usd.edu

Abstract

This study was designed to develop a novel poly(β -cyclodextrin)-curcumin (PCD-CUR) self-assembly approach for improved curcumin delivery to prostate cancer cells. Poly(β -cyclodextrin)-curcumin self-assemblies were prepared *via* the cooperation of host-guest chemistry and hydrogen-bonding interactions. These PCD-CUR self-assemblies were characterized in detail using Fourier Transform Infra-red (FTIR), Differential Scanning Calorimetry (DSC), Thermo-gravimetric Analysis (TGA), and Scanning and Transmission Electron Microscopic (SEM/TEM) analyses. We have proposed a putative self-assembly mechanism of poly(β -cyclodextrin)-curcumin complex formation. Intracellular uptake of these self-assemblies was evaluated by Flow cytometry and immunofluorescence microscopy analyses. Therapeutic efficacy of PCD-CUR self-assembly was determined by cell proliferation and colony formation assays using C4-2, DU145 and PC3 prostate cancer cells. The effect of PCD-CUR formulation on apoptosis related proteins was determined by immunoblotting. Physico-chemical characterization analyses confirmed the formation of PCD-CUR self-assemblies, which demonstrated excellent stability and solubility in physiological solutions. The PCD-CUR assemblies have shown improved uptake and exhibited a superior anti-cancer efficacy compared to free curcumin in cell proliferation and clonogenic assays in C4-2, DU145 and PC3 prostate cancer cells. These results suggest that PCD-CUR formulation could be a useful nanoscale system for improving curcumin delivery and its therapeutic efficacy in prostate cancer.

Key words: Curcumin, poly(β -cyclodextrin), drug delivery, self-assembly, nanoparticles, nano-assembly, cancer therapy, prostate cancer.

Introduction

Although chemotherapy is a successful approach in the management of cancers, severe side effects and genetic heterogeneity limit its use.^[1] The success of chemotherapy is not only dependent on the anti-cancer agent used, but also on a sufficient therapeutic index being administered to cancer cells. Nanotechnology can improve the overall clinical efficacy of chemotherapeutic agents by changing the biological disposition and enhancing the efficacy of therapeutic dose.^[2] Design of chemically flexible nano-carrier systems^[3] for this purpose often requires careful consideration of the properties of the therapeutic agents and the biology of the disease.

Alternatively, polymer assemblies in well-defined nanostructures such as micelles or nano-assemblies are of increased interest as a means for drug transport.^[4] A micro or nanogel self-assembly system can be obtained from the association of amphiphilic block co-polymers or complexation of oppositely charged molecules.^[5] These carriers allow encapsulation of a variety of biologically active molecules including anti-cancer drugs, enzymes, proteins (BSA) and DNA *via* hydrogen bonding or complexation.^[6] Polysaccharides modified by hydrophobic groups (for example, cholesteryl-group modified pullulans), can form instantaneous monodispersed nanogel structures of 20-30 nm by intermolecular self-aggregations.^[6a,7] Cyclodextrin (CD) or cyclodextrin polymer (PCD) based self-assemblies/inclusion complexation with various chemotherapeutic agents have resulted in well defined nano-structured drug delivery systems.^[8] The keen interest in developing cyclodextrin (α -, β -, γ -cyclodextrin) based drug delivery systems is due to cyclic bucket shaped oligosaccharides linked by α -1,4-glycosidic bonds which form macrocycles.^[9] A higher stability to drugs in these self-assemblies is achieved by a “lock and key” (host-guest) mechanism. β -cyclodextrin (CD) is a method of choice for encapsulation of

chemotherapeutic agents because of its semi-natural nature with extremely low toxicity. Additionally, it is known to provide enhanced drug delivery through biological membranes^[6a] and is being approved by the FDA.

Curcumin (CUR) is a yellow polyphenol compound found in the rhizome of the plant *Curcuma Longa* Linn. This compound has been widely used in traditional Ayurvedic and Chinese medicine. Curcumin has been reported to show anti-inflammatory, anti-microbial, anti-oxidant, anti-parasitic, anti-mutagenic and anti-cancer properties.^[10] Curcumin is also known for its cancer preventative and anti-cancer activities *via* influencing multiple cancer associated signaling pathways.^[11] Various animal models and human clinical studies have demonstrated the safety of curcumin even at dosages as high as 12 g per day.^[10d,12,13] However, oral administration of curcumin at a dose of 2 g kg⁻¹ to rats and humans resulted in maximum serum concentrations of only 1.35 (0.23 µg mL⁻¹ after 1 h in rats and 0.005 µg mL⁻¹ after 1 h in humans), indicative of poor pharmacokinetics.^[10d,12] Therefore, in spite of superior anti-cancer properties, curcumin suffers from low solubility in aqueous solution (~ 20 µg/mL), rapid degradation at physiological pH and poor bioavailability,^[14] which reflect its poor *in vivo* efficacy.^[15] In order to enhance its anti-cancer efficacy, different carriers (polymer nanoparticles, polymer micelles, surfactants, nanogels, etc.)^[16] have been employed to improve water solubility, stability and bioavailability characteristics. However, all these nano-carriers are suitable for the encapsulation of first line chemotherapeutic agents but not for second line chemotherapeutic agents such as curcumin.

In this study we have developed a novel formulation, poly(β-cyclodextrin)-curcumin (PCD-CUR) self-assembly, to improve curcumin's water solubility, stability and bioavailability for enhancing its anti-cancer efficacy to treat prostate cancer. Poly(β-cyclodextrin)-curcumin

complexes were prepared by supramolecular encapsulation or self-assembly (inclusion complexation), characterized by using spectral (FTIR, ¹H-NMR), thermal (DSC and TGA), X-ray diffraction and microscopic (SEM and TEM) analyses. The developed curcumin formulations showed an improved intracellular uptake in cancer cells compared to free curcumin. Additionally, the optimized curcumin formulation (PCD30) has exhibited superior anti-cancer efficacy in prostate cancer cells compared to free curcumin. This study suggests a new nano self-assembly approach for improved curcumin delivery and therapeutic efficacy in cancer treatment.

Materials and Methods

Chemicals and Cell Lines

β-cyclodextrin polymer or poly(β-cyclodextrin) (PCD) (Product No. C2485, Average molecular weight = 2,975 to 4,120; Molecular weight distribution = 2,000 to 15,000; Cyclodextrin content = 50 to 55%), curcumin (CUR) (≥95% purity, (E,E)-1,7-bis(4-Hydroxy-3-methoxyphenyl)-1,6-heptadiene-3,5-dione), acetone (≥99.5, ACS reagent grade), and dimethylsulfoxide (DMSO) (ACS reagent, UV spectrophotometry grade, ≥99.9%) were purchased from Sigma Chemical Co. (St Louis, MO, USA). Prostate cancer cells lines C4-2, DU145 and PC-3 cells were kindly provided by Dr. Meena Jaggi. These cells were maintained as monolayer cultures (C4-2 and PC-3) in RPMI-1640 medium or in MEM medium (DU145) (HyClone Laboratories, Inc., Logan, UT, USA) supplemented with 10% fetal bovine serum (Atlanta Biologicals, Lawrenceville, GA, USA) and 1% penicillin-streptomycin (Gibco BRL, Grand Island, NY, USA) at 37 °C in a humidified atmosphere (5% CO₂).

Preparation of PCD Curcumin Self-assembly

To prepare PCD curcumin self-assembly formulations, poly(β -cyclodextrin) (PCD) (40 mg) was dissolved in 8 mL deionized water in a 20 mL glass vial (Fisher Scientific, Pittsburg, PA, USA) containing a magnetic bar. Curcumin (2 mg, i.e., 5% (wt./wt.) CUR to PCD) dissolved in 500 μ L acetone was drop-wise added to PCD aqueous solutions while stirring at 400 rpm. The solution was stirred overnight, passed through a 0.45 μ m Millex PVDF Syringe driven filter unit (Millipore Corporation, Bedford, MA, USA), and the supernatant containing highly water soluble poly(β -cyclodextrin)-curcumin (PCD-CUR) self assembly, i.e., PCD5 (inclusion complex), was recovered by freeze drying (Labconco Freeze Dry System; -48 $^{\circ}$ C, 133×10^{-3} mBar; Labconco, Kansas City, MO, USA).

Similarly, PCD10 (40 mg of PCD + 4 mg of CUR), PCD20 (40 mg of PCD + 8 mg of CUR), and PCD30 (40 mg of PCD + 12 mg of CUR) self-assembly formulations were prepared and purified as mentioned above. All the PCD-CUR self-assemblies were stored at 4 $^{\circ}$ C until further use. The prepared PCD-CUR self-assemblies were designated as PCD5, PCD10, PCD20 and PCD30 based on the % of CUR employed in the preparations with respect to PCD.

Curcumin (CUR) Loading

In order to estimate the amount of curcumin present in PCD-CUR self-assemblies, 2-3 mg of PCD-CUR self-assemblies were dissolved in 1 mL dimethylsulfoxide (DMSO), gently shaken on a shaker (Labnet S 2030-RC, RPM 150, Labnet International, Woodbridge, NJ, USA) for 24 h at room temperature in the dark and centrifuged at 14,000 rpm (Centrifuge 5415D, Eppendorf AG, Hamburg, Germany). The supernatant was collected and diluted supernatant (20 μ L in 1 mL DMSO) was used for the estimations. The CUR concentrations were determined by a standard

UV-Vis spectrophotometer method (Biomate 3, Thermo Electron Corporation, Hudson, NH, USA) at 450 nm, as described earlier.^[16a] A standard plot of CUR in DMSO (0-10 µg/mL) was prepared under identical conditions. The CUR loading was calculated as follows: *CUR loading* = *CUR recovered in PCD-CUR self-assembly/PCD-CUR assembly recovered*.

***In vitro* Stability of PCD-CUR Self-assemblies**

In vitro stability of self-assemblies was carried out in physiological buffer solution (1XPBS, 0.01 M PBS, pH 7.4). For this study, ~ 10 mg of CUR containing PCD-CUR self-assemblies (PCD5, PCD10, PCD20 and PCD30) were dispersed in 5 mL of PBS and incubated at 37 °C under gentle shaking on a shaker (Labnet S 2030-RC, RPM 150, Labnet International, Woodbridge, NJ, USA). The CUR retention was determined at different time intervals using UV-Vis spectrophotometer as described in CUR loading experiments. The % curcumin retention was calculated using the following equation: *% CUR retention* = $[(CUR\ in\ assembly - Released\ curcumin) / CUR\ in\ assembly] \times 100$.

Characterization

The Fourier Transform Infrared (FTIR) spectra of PCD, CUR and PCD-CUR self-assemblies were recorded employing a Smiths Detection IlluminatIR FT-IR microscope (Danbury, CT, USA) with diamond ATR objective. FTIR spectra of samples were acquired by placing self-assembly powder on the tip of the ATR objective. Data was acquired between 4000–750 cm⁻¹ at a scanning speed of 4 cm⁻¹ for 32 scans. The average data of 32 scans was presented as FTIR spectra. The ¹H-NMR spectra were obtained in DMSO-*d*₆ using the Bruker Avance DRX 500 MHz NMR spectrophotometer. The following parameters were used during the NMR

experiments: number of scans, 64; relaxation delay, 1.0 s; and pulse degree, 25 °C. The chemical shifts are presented in terms of ppm with tetramethylsilane (TMS) as the internal reference.

The Differential scanning calorimeter (DSC) and Thermo-gravimetric analyzer (TGA) analysis of PCD, CUR and PCD-CUR self-assemblies were performed on a TA Instruments Q200 DSC or TA Instruments Q50 TGA (TA Instruments, New Castle, Delaware, USA) at The Applied Polymer Research Center, The University of Akron (Project # 139-10APRC). The cell constant calibration method was employed to study the DSC patterns of the samples from 25 °C to 300 °C at a heating ramp of 10 °C, under a constant flow (100 mL/min) of nitrogen gas. TGA study was conducted from 25 °C to 700 °C at a heating ramp of 10 °C, under a constant flow (100 mL/min) of nitrogen gas. This study followed the 20STD800 standard rubber analysis method. X-ray diffraction (XRD) patterns of PCD, CUR and PCD-CUR self-assemblies were recorded employing a D/Max – B Rigaku diffractometer (Rigaku Americas Corp, Woodlands, TX, USA) using Cu radiation at $\lambda = 0.1546$ nm, running at 40 kV and 40 mA. The samples were mounted on double sided silicone tape and measurements were performed at 2θ from 20 to 50°.

The transmission electron microscope images were taken on a JEOL-1210 transmission electron microscope (JEOL, Tokyo, Japan) operating at 60 kV. Approximately 10-20 μ L of the diluted dispersions of PCD-CUR self-assemblies was placed on a 200 mesh formvar-coated copper TEM grid (grid size: 97 μ m) (Ted Pella Inc., Redding, CA, USA), excess solution was removed using a piece of fine filter paper, and the samples were allowed to dry in air overnight prior to [imaging](#) under TEM.

CUR and PCD-CUR Self-assemblies Cellular Uptake

To visually compare the uptake of CUR and PCD-CUR *self-assembly* (PCD30) in prostate cancer cells, 5×10^5 cells were seeded in 6-well plates in 2 mL medium. After cells were attached, media was replaced with 10 μ g free CUR or equivalent CUR containing PCD-CUR *self-assembly* (PCD30). After 6 h, cells were washed with PBS and examined under an Olympus BX 51 fluorescence microscope (Olympus, Center Valley, PA).

CUR cellular uptake was quantified using an Acuri C6 flow cytometer (Accuri Cytometers, Inc., Ann Arbor, MI, USA) by determining the fluorescence levels in FL1 channel (488 excitation, Blue laser, 530 ± 15 nm, FITC/GFP). Briefly, DU145 cells (5×10^5) were seeded in 6-well plates (2 mL medium), and allowed to attach overnight. Cells were then treated with 10 μ g CUR or equivalent PCD-CUR complexes (PCD5, PCD10, PCD20 and PCD30) in each well. After 1 or 2 days the cells were washed twice with 1X PBS, trypsinized, centrifuged and collected in 2 mL media. These cell suspensions (50 μ L) were injected into a flow cytometer to determine the fluorescence levels.

***In vitro* Cytotoxicity (MTS Assay)**

C4-2, DU145 and PC-3 prostate cancer cells (5000 cells/well in 100 μ L media) were cultured in RPMI-1640/MEM medium containing 10% FBS and 1% penicillin-streptomycin in 96-well plates and allowed to attach overnight. The media was replaced with fresh media containing different concentrations (2.5-40 μ M) of CUR and PCD-CUR *self-assembly* (PCD30). Equivalent amounts of DMSO or PCD in PBS were used as control. These plates were incubated at 37 °C for 2 days. After day 2, the media was replaced with fresh media and the anti-proliferative activity of CUR and PCD30 was determined using a standard 3-(4,5-dimethylthiazol-2yl)-2,5-diphenyltetrazolium bromide (MTS) based colorimetric assay (CellTiter 96 AQ_{eous}, Promega,

Madison, WI, USA). The reagent (25 μ L/well) was added to each well and plates were incubated for 3 h at 37 °C. The color intensity was measured at 492 nm using a microplate reader (BioMate 3 UV-Vis spectrophotometer, Thermo Electron Corporation, Hudson, NH, USA). The anti-proliferative activity of CUR and PCD30 treatments was calculated as a percentage of cell growth with respect to the DMSO and PCD in PBS controls. Representative phase contrast microscope images of cells were taken using an Olympus BX 41 microscope (Olympus, Center Valley, PA, USA) before adding MTS reagents.

Colony Formation Assay

C4-2, DU145 and PC3 prostate cancer cells (1000) were seeded in 2 mL media in 6-well plates and allowed 2-3 days to initiate the colonies. These cells were treated with different concentrations (2-10 μ M) of CUR or PCD30 over a period of 10-12 days. The plates were washed twice with 1X PBS, fixed in chilled methanol, stained with hematoxylin (Fisher Scientific, Fair Lawn, NJ, USA), washed with water and air dried. The number of colonies was counted by using MultimageTM Cabinet (Alpha Innotech Corporation, San Leandro, CA, USA) using AlphaEase Fc software. The % colonies were calculated using the number of colonies formed in treatment divided by number of colonies formed in DMSO or PCD in PBS controls.

Statistical Analysis. Values were processed using Microsoft Excel 2007 software and presented as mean \pm standard error of the mean (S.E.M.). Statistical analyses were performed using an unpaired, two tailed student t-test. The level of significance was set at * $p < 0.05$. All the graphs were plotted using Origin 6.1 software.

Results and Discussion

Poly(β -cyclodextrin) and Curcumin Self-assembly Formation

A number of investigations have been conducted to develop efficient drug delivery systems for cancer chemotherapy.^[17] These studies suggest that a successful formulation of a polymeric drug delivery carrier must be capable of encapsulating or loading the desired amounts of drug within its structures and deliver them in active form to the cancerous tissues. Apart from nanoparticles, inclusion complexes or self-assemblies of polymers with drug molecules have potential applications in drug delivery.^[18] Various groups have employed host-guest complexation between cyclodextrins and a wide range of guest molecules to create macromolecular networks (self-assemblies or inclusion complexes) for drug delivery applications.^[19]

In this study we developed poly(β -cyclodextrin)-curcumin (PCD-CUR) self-assemblies by following solvent evaporation technique (Figure 1A). This approach loads different amounts of curcumin (CUR) into the cavities of β -cyclodextrins containing repeating units in PCD. The loading capacity of CUR is increased when the ratio of CUR to PCD (Figure 2A) is increased. The order of loading capacity (μg of CUR/mg of PCD) is PCD5 (48.5) < PCD10 (115.2) < PCD20 (163.4) < PCD30 (223.2). From the drug loading experiments, it was confirmed that each cyclodextrin cavity of PCD is filled with 0.27% (PCD5), 0.65% (PCD10), 0.91% (PCD20), and 1.25% (PCD30) of curcumin molecules. This clearly indicates that PCD 30 formulation contained in each CD cavity is filled with either one or more than one CUR molecules (Figure 1). According to the drug loading results, CUR is encapsulated into the PCD structures up to 23 w/w% (PCD30 self-assembly) which is a considerably high amount compared to the majority of other nanoparticle-based formulations.^[16a, 16b, 20] Curcumin is known to have very low solubility in aqueous solution ($\sim 20 \mu\text{g/mL}$) and possesses rapid degradation characteristics.^[14, 16c, 21] The

developed PCD-CUR self-assemblies have shown enormous improvements in aqueous solubility and stability characteristics. These self-assemblies are highly soluble in water, i.e., > 1.6 mg of curcumin equivalent. This solubility is much higher compared to other CD-CUR inclusion complexes in water (0.6 mg/mL of CUR).^[14] The higher solubility characteristics may result from the better compatibility between PCD and CUR compounds. The higher compatibility of PCD and CUR in PCD-CUR complexes can provide an increased *in vitro* stability of CUR in aqueous medium. These PCD-CUR inclusion complexes have shown high *in vitro* stability at physiological pH conditions (7.4) (Figure 2B), whereas CUR did not show significant stability.^[14] The order of stability for 72 h was noticed as PCD30 (~ 88.7%) > PCD20 (~ 82.5%) ≥ PCD10 (~ 77.4%) > PCD5 (~ 71.2%). Only 11% of CUR was precipitated in the case of PCD30 while CUR precipitated almost 100%. The higher stability in PCD30 self-assembly may be due to nano-assembly formation in which curcumin is highly entrapped in the PCD chain networks.

Figure 1 and Figure 2

Physico-chemical Characterization of PCD-CUR Self-assemblies

The implementation of a drug after administration *in vivo* depends strictly on the physico-chemical characteristics of the parent drug and its chemical structure; thus physico-chemical characterization of drug encapsulated particles or self-assemblies becomes important.^[17] The pattern of self-assembly or drug carrier in terms of particle size is an important factor as it directs the physical characteristics, cellular uptake, distribution and release of encapsulated drug from the assemblies/nanoparticles.^[2, 17c] Therefore, our PCD-CUR self-assemblies were studied for their extensive physico-chemical characterization.

The FTIR spectra of PCD, CUR and PCD-CUR self-assembly are shown in Figure 3A. CUR exhibited an absorption band at 3496 cm^{-1} attributed to the phenolic O-H stretching vibration. Additionally, sharp absorption bands at 1605 cm^{-1} (stretching vibrations of benzene ring of CUR), 1502 cm^{-1} (C=O and C=C vibrations of CUR), 1435 cm^{-1} (olefinic C-H bending vibration), 1285 cm^{-1} (aromatic C-O stretching vibrations), and 1025 cm^{-1} (C-O-C stretching vibrations of CUR) were noticed. In the case of PCD, absorption bands were noticed at 3325 cm^{-1} and 1025 cm^{-1} due to the O-H stretching vibrations and C-O-C stretching vibrations. However, the PCD-CUR self-assembly showed a sharp peak belonging to CUR at 1025 cm^{-1} while the rest of the peaks were diminished, indicating typical inclusion complex patterns. In addition, the PCD-CUR self-assembly has shown all the peaks belonging to PCD as well as CUR peaks in $^1\text{H-NMR}$ spectra (Figure 3B) but the CUR peaks were shifted.^[21] X-ray diffraction patterns of PCD, CUR and PCD-CUR self-assembly are depicted in Figure 3C. CUR showed few characteristic crystalline peaks between 20 and 30 (21.26 , 23.35 , 24.68 and 26.54°) while PCD had no crystalline peaks. In the case of PCD-CUR self-assembly, both the crystalline peaks of CUR and the amorphous nature of PCD can be observed. Spectral and X-ray diffraction studies provide clear evidence of formation of PCD-CUR self-assembly.^[11d, 19a]

Figure 3

Thermal studies (DSC and TGA) can provide useful information in elucidating the physical state of drug(s) that exists in various polymers, complexes and nanoparticles.^[22] In particular, complexation of a drug and cyclodextrin or polymer results in the absence/shifting of endothermic peaks indicating a change in the crystal lattice, melting, boiling, or sublimation points.^[6a] Therefore, these measurements can provide both qualitative and quantitative

information of drug(s) present in the complexes. The DSC thermograms of PCD, CUR and PCD-CUR self-assembly are presented in Figure 4A. PCD (black line) and CUR (red line) have shown individual endothermic peaks at 92.6 °C and 172 °C, respectively, due to their melting temperature. In the case of PCD-CUR self-assembly, the prominent melting peak belonging to CUR at 172 °C was largely diminished and the PCD melting peak (green line) shifted lower from 92.6 to 87.5 °C. This was attributed to the drug molecules being completely included into the cavities of β -cyclodextrin of PCD. Further, this behavior is an indication of stronger interactions between CD cavities in PCD and CUR in solid state. A similar phenomenon was observed in various cyclodextrins and curcumin inclusion complexes.^[23]

The thermo-gravimetric curves of PCD (black line), CUR (red line) and CD-CUR inclusion complex (PCD30) (green line) shown in Figure 4B, illustrate a complete degradation of PCD chains at 700 °C (i.e., weight loss is 100%) while at 700 °C, curcumin is degraded only 68%. Unlike PCD, PCD-CUR formulation (PCD30) showed an improved thermal stability due to the presence of CUR (Figure 4B, green line). This is probably due to formation of CUR inclusion complexation with CD cavities of PCD.

Figure 4

It is well known that morphology of self-assemblies or inclusion complexes can be distinguished from their parent polymers and drug molecules by microscopy. To obtain precise information of their self-assembly structures in aqueous solution, TEM studies were performed for PCD-CUR self-assemblies (Figure 5). Because of a high disparity of PCD in aqueous media, smaller self-assemblies were exhibited (Figure 5A). However, CUR is barely dispersible in water, resulting in completely aggregated structures (Figure 5B). PCD5 illustrates smaller assemblies with larger

clusters (Figure 5C). This cluster formation changed with the increase of CUR in PCD self-assemblies or inclusion complexation (PCD10 to PCD 30, Figure 5D-F). A higher concentration of CUR in PCD complexation leads to the formation of a nano-assembly containing particles ~ 250 nm.

Figure 5

It is evident from the TEM analysis that the nano- or self-assembly process occurs between the β -cyclodextrin cavities of PCD and CUR *via* van der Waals interaction, hydrogen bonding and hydrophobic interactions. A possible nano-assembly mechanism was revealed for PCD-CUR (see Figure 1A, PCD30 structure). During this process, release of high energy water molecules from the cavity of CD occurs and curcumin enters the molecule. The feasibility of the entire process was reported for various binary complexes of curcumin with the hydrophobic molecule of CD.^[23]

From this study, there is a clear confirmation of PCD-CUR self-assemblies formation *via* inclusion complexation mechanism. This inclusion complexation of β -cyclodextrin and curcumin is highly favored by Gibbs' free energy process^[23] and supports the notion that β -CD cavities in PCD solutions offer a positive environment for curcumin (CUR) self-assembly. The lyophilic cavities of β -CD in PCD chains protect the guest molecule (CUR) from the aqueous environment, while the polar outer surface of the β -CD molecule provides a stabilization effect. These additional characteristics of β -CD repeating units in PCD suggest that pharmaceutical preparations could be utilized for efficient delivery of curcumin to cancer cells.

PCD-CUR Self-assemblies Improved Curcumin's Cellular Uptake in Prostate Cancer Cells

An ideal drug delivery system for cancer therapy should prolong drug presence in the circulation and releases the drugs at tumor sites.^[24] When characterizing the cellular uptake and distribution of CUR or CUR in PCD-CUR self-assemblies in human prostate cancer cell lines, the inherent fluorescence property of CUR was taken into account. Characterization of cell surface by fluorescence microscopy indicated improved fluorescence intensity in the cells treated with PCD-CUR self-assemblies compared to free CUR treated cells (Figure 6A), whereas cancer cells treated with DMSO or PCD did not show any fluorescence in the cells (Figure 6A). To determine the exact internalization capacity of various PCD-CUR self-assemblies, FACS analysis was performed. For this study, DU145 cells were incubated with 10 μ g CUR or PCD-CUR self-assemblies for 1 or 2 days. A significant increase in CUR accumulation in DU145 cancer cells was observed in PCD-CUR self-assemblies compared to free CUR treatment (Figure 6B).

Figure 6

A similar improved uptake characteristic has been shown in other studies for curcumin encapsulated polymer nanoparticles, nanogels and polymeric micelles in different cancer cells.^[16a, 25] The uptake phenomenon in DU145 prostate cancer cells increased from PCD5 to PCD30 self-assemblies. A 3-4 fold increased uptake of CUR was noticed in PCD20 or PCD30 treated cells compared to free CUR. This reveals that only a certain number of PCD-CUR self-assemblies are capable of entering the cells. On the other hand, PCD-CUR self-assemblies which are nanometer scale particles or assemblies **not only** have **better** access to cells **but are** retained at a higher rate because of “enhanced permeation and retention” effect.^[26] The lower cellular

accumulation of free CUR by cancer cells might be due to either rapid degradation or precipitation in the media.^[14] These results suggested that overall, PCD30 self-assembly had a better uptake in DU145 cells and therefore it was speculated that PCD30 self-assembly will exhibit enhanced cytotoxicity effects compared to free CUR or other PCD-CUR self-assemblies (PCD5, PCD10 and PCD20). Therefore, PCD30 self-assembly was utilized for *in vitro* growth assays (MTS assay and clonogenic assay) in human prostate cancer cell lines.

PCD-CUR Self-assembly Enhanced Anti-cancer Efficacy of Curcumin

The cytotoxicity activity of free CUR or PCD-CUR self-assembly (PCD30) was evaluated in different prostate cancer cell lines (C4-2, DU145 and PC3 cell lines) by MTS cell viability assay. In all cell lines, both free CUR and PCD30 have shown dose dependant anti-proliferative effects (2.5-40 μM) while DMSO or PCD treatments used as controls for free CUR and PCD30, respectively, did not show any effects on cell growth (Figure 7A). The IC_{50} (50% cell growth inhibitory concentration) of curcumin loaded poly(β -cyclodextrin) (PCD 30) was found to be 12.5, 15.9, 16.1 μM for C4-2, DU145, and PC3 cancer cells, respectively, whereas free curcumin IC_{50} values were 19.6, 19.25, 19.4 μM for C4-2, DU145, and PC3 cancer cells, respectively. This data suggest that PCD30 is more efficient for the suppression of prostate cancer cell growth compared to other PCD formulations and free CUR. This effect can also be observed in phase contrast microscopy images (Figure 7B). From these images, it is evident that CUR treatment has shown a moderate decrease in cell growth, while CD30 not only reduced cell growth to a greater extent but also caused apoptosis related cell morphology changes in prostate cancer cells. Based on the morphological changes caused by PCD-CUR, we have investigated the pattern of

Poly(ADP-ribose) polymerase (PARP) cleavage pattern. PARP is a protein involved in a number of cellular processes including DNA repair and programmed cell death. It has been shown that PARP cleavage is the onset of apoptosis in several cell model systems.^[27] Cleavage of PARP is an indicator of DNA damage and apoptosis in response to a diverse range of cytotoxic insults.^[28] Prostate cancer cells treated with 20 μ M CUR or equivalent amounts of PCD30 showed considerable cleavage of full length PARP (116 kDa) into cleaved PARP (86 kDa), which indicates the cancer cells are undergoing cell death *via* apoptosis pathway (Figure 7C). The PARP cleavage caused by PCD30 is greater than free curcumin treatment, indicating improved efficacy of PCD30 formulation for prostate cancer therapy.

Figure 7

It is also important to evaluate long-term anti-cancer efficacy of the developed drug(s) or drug(s) formulations. Therefore, the long term anti-cancer efficacy of PCD30 formulation was evaluated employing a colony forming assay (Clonogenic assay). We tested the anti-cancer effects of free CUR and PCD30 formulation in C4-2, DU145 and PC3 cancer cell lines at equivalent doses of 2-10 μ M. Equivalent quantities of DMSO or PCD were used as controls for CUR and PCD30, respectively. Measurement of the density of colonies showed a significant improvement in the therapeutic efficacy of PCD30 formulation in all three cell lines compared to free CUR (Figure 8). Collectively, the presented data demonstrate an enhanced anti-cancer therapeutic efficacy of PCD30 formulation compared to free curcumin *via* improving cellular uptake of curcumin in prostate cancer cells.

Figure 8

Conclusion

We have developed a novel PCD-curcumin (PCD-CUR) self-assembly through the inclusion complexation mechanism which improves curcumin delivery and enhances its therapeutic efficacy for prostate cancer treatment. The PCD-CUR self-assemblies were able to effectively cross cellular barriers and enter into the intracellular region of the cancer cells. The PCD-CUR self-assembly (PCD30) exhibits enhanced anti-cancer activity compared to free curcumin. Therefore, the PCD30 formulation can be used for improving curcumin bioavailability and delivery in tumors for effective prostate cancer treatment.

Acknowledgements

The authors thank Cathy Christopherson (Sanford Research/USD) for editorial assistance. We also thank Dr. Diane Maher, Dr. Vasudha Sundram and Mara Ebeling (Sanford Research/USD) for their suggestions throughout the study. This work was supported in part by a Sanford Research/USD grant and Department of Defense Grants awarded to SCC (PC073887) and MJ (PC073643). We acknowledge Prof. Daniel Engebretson and Tyler Remund (Biomedical Engineering, University of South Dakota, Sioux Falls), Robert Japs (Sanford Health), Sara Basiaga (Department of Chemistry, UN-Lincoln), Shah Valloppilly (Nebraska Center for Materials and Nanoscience, UN-Lincoln) and Crittenden J. Ohlemacher (Applied Polymer Research Center, University of Akron) for their help in characterization of our samples.

References

- [1] [1a] B. A. Chabner, T. G. Roberts, Jr., *Nat. Rev. Cancer*. **2005**, *5*, 65; [1b] A. Sanchez-Munoz, E. Perez-Ruiz, N. Ribelles, A. Marquez, E. Alba, *Expert Rev Anticancer. Ther.* **2008**, *8*, 1907.
- [2] J. K. Vasir, V. Labhassetwar, *Technol. Cancer. Res. Treat.* **2005**, *4*, 363.
- [3] [3a] S. S. Davis, *Trends Biotechnol.* **1997**, *15*, 217; [3b] A. de la Zerda, S. S. Gambhir, *Nat. Nanotechnol.* **2007**, *2*, 745; [3c] B. Mishra, B. B. Patel, S. Tiwari, *Nanomedicine: Nanotechnology, Biology and Medicine*, **2009**, *6*, 1024.
- [4] [4a] K. A. Janes, P. Calvo, M. J. Alonso, *Adv. Drug. Deliv. Rev.* **2001**, *47*, 83; [4b] R. Kumar, M. H. Chen, V. S. Parmar, L. A. Samuelson, J. Kumar, R. Nicolosi, S. Yoganathan, A. C. Watterson, *J. Am. Chem. Soc.* **2004**, *126*, 10640; [4c] N. Nishiyama, K. Kataoka, *Pharmacol. Ther.* **2006**, *112*, 630; [4d] S. P. Zhao, L. M. Zhang, D. Ma, *J. Phys. Chem. B* **2006**, *110*, 12225.
- [5] [5a] Y. Ozawa, S. Sawada, N. Morimoto, K. Akiyoshi, *Macromol. Biosci.* **2009**, *9*, 694; [5b] C. M. Galmarini, G. Warren, E. Kohli, A. Zeman, A. Mitin, S. V. Vinogradov, *Mol. Cancer. Ther.* **2008**, *7*, 3373; [5c] R. L. Hong, W. H. Spohn, M. C. Hung, *Clin. Cancer. Res.* **1999**, *5*, 1884.
- [6] [6a] G. Horvath, T. Premkumar, A. Boztas, E. Lee, S. Jon, K. E. Geckeler, *Mol. Pharm.* **2008**, *5*, 358; [6b] J. Hu, S. Yu, P. Yao, *Langmuir* **2007**, *23*, 6358; [6c] S. Kazakov, K. Levon, *Curr. Pharm. Des.* **2006**, *12*, 4713; [6d] O. M. Koo, I. Rubinstein, H. Onyuksel, *Nanomedicine* **2005**, *1*, 193; [6e] N. Morimoto, T. Endo, M. Ohtomi, Y. Iwasaki, K. Akiyoshi, *Macromol. Biosci.* **2005**, *5*, 710; [6f] T. Hirakura, Y. Nomura, Y. Aoyama, K. Akiyoshi, *Biomacromolecules* **2004**, *5*, 1804; [6g] Y. Nomura, M. Ikeda, N. Yamaguchi, Y.

- Aoyama, K. Akiyoshi, *FEBS Lett.* **2003**, 553, 271.
- [7] K. Akiyoshi, *Nippon Rinsho* **2006**, 64, 215.
- [8] [8a] J. Li, X. J. Loh, *Adv. Drug. Deliv. Rev.* **2008**, 60, 1000; [8b] S. Salmaso, A. Semenzato, S. Bersani, P. Matricardi, F. Rossi, P. Caliceti, *Int. J. Pharm.* **2007**, 345, 42.
- [9] J. Szejtli, *Chem. Rev.* **1998**, 98, 1743.
- [10] [10a] G. Bar-Sela, R. Epelbaum, M. Schaffer, *Curr. Med. Chem.* **2010**, 17, 190-197; [10b] J. S. Jurenka, *Altern. Med. Rev.* **2009**, 14, 141; [10c] R. K. Maheshwari, A. K. Singh, J. Gaddipati, R. C. Srimal, *Life Sci.* **2006**, 78, 2081; [10d] A. S. Strimpakos, R. A. Sharma, *Antioxid. Redox Signal.* **2008**, 10, 511; [10e] R. A. Sharma, W. P. Steward, A. J. Gescher, *Adv. Exp. Med. Biol.* **2007**, 595, 453.
- [11] [11a] B. K. Jaggi, S. C. Chauhan, M. Jaggi, *Proceedings of the South Dakota Academy of Science* **2007**, 86, 283; [11b] S. Karmakar, N. L. Banik, S. J. Patel, S. K. Ray, *Neurosci. Lett.* **2006**, 407, 53; [11c] S. Shishodia, H. M. Amin, R. Lai, B. B. Aggarwal, *Biochem. Pharmacol.* **2005**, 70, 700; [11d] G. Sa, T. Das, *Cell. Div.* **2008**, 3, 14; [11e] P. Anand, C. Sundaram, S. Jhurani, A. B. Kunnumakkara, B. B. Aggarwal, *Cancer. Lett.* **2008**, 267, 133; [11f] T. Dorai, B. B. Aggarwal, *Cancer. Lett.* **2004**, 215, 129.
- [12] H. Hatcher, R. Planalp, J. Cho, F. M. Torti, S. V. Torti, *Cell. Mol. Life Sci.* **2008**, 65, 1631.
- [13] R. G. Tunstall, R. A. Sharma, S. Perkins, S. Sale, R. Singh, P. B. Farmer, W. P. Steward, A. J. Gescher, *Eur. J. Cancer* **2006**, 42, 415.
- [14] Y. J. Wang, M. H. Pan, A. L. Cheng, L. I. Lin, Y. S. Ho, C. Y. Hsieh, J. K. Lin, *J. Pharm. Biomed. Anal.* **1997**, 15, 1867.
- [15] P. Anand, A. B. Kunnumakkara, R. A. Newman, B. B. Aggarwal, *Mol. Pharm.* **2007**, 4, 807.

- [16] [16a] S. Bisht, G. Feldmann, S. Soni, R. Ravi, C. Karikar, A. Maitra, A. Maitra, *J Nanobiotechnology* **2007**, 5, 3; [16b] J. Shaikh, D. D. Ankola, V. Beniwal, D. Singh, M. N. Kumar, *Eur. J. Pharm. Sci.* **2009**, 37, 223; [16c] H. H. Tonnesen, M. Masson, T. Loftsson, *Int. J. Pharm.* **2002**, 244, 127; [16d] Z. Wang, M. H. Leung, T. W. Kee, D. S. English, *Langmuir* **2009**; [16e] H. I. Ingolfsson, R. E. Koeppe, 2nd, O. S. Andersen, *Biochemistry* **2007**, 46, 10384; [16f] M. H. Leung, T. W. Kee, *Langmuir* **2009**, 25, 5773; [16g] K. Maiti, K. Mukherjee, A. Gantait, B. P. Saha, P. K. Mukherjee, *Int. J. Pharm.* **2007**, 330, 155; [16h] A. Safavy, K. P. Raisch, S. Mantena, L. L. Sanford, S. W. Sham, N. R. Krishna, J. A. Bonner, *J. Med. Chem.* **2007**, 50, 6284.
- [17] [17a] C. Khemtong, C. W. Kessinger, J. Gao, *Chem. Commun.* **2009**, 24, 3497; [17b] L. Jabr-Milane, L. van Vlerken, H. Devalapally, D. Shenoy, S. Komareddy, M. Bhavsar, M. Amiji, *J. Control. Release.* **2008**, 130, 121; [17c] L. E. van Vlerken, M. M. Amiji, *Expert Opin. Drug Deliv.* **2006**, 3, 205.
- [18] F. Hirayama, K. Uekama, *Adv. Drug Deliv. Rev.* **1999**, 36, 125.
- [19] [19a] Y. Zhou, D. Yan, *Chem. Commun.* **2009**, 1172; [19b] E. M. Todd, S. C. Zimmerman, *J. Am. Chem. Soc.* **2007**, 129, 14534; [19c] H. Amouri, C. Desmarets, A. Bettoschi, M. N. Rager, K. Boubekour, P. Rabu, M. Drillon, *Chemistry* **2007**, 13, 5401; [19d] B. W. Messmore, J. F. Hulvat, E. D. Sone, S. I. Stupp, *J. Am. Chem. Soc.* **2004**, 126, 14452; [19e] X. Shi, K. M. Barkigia, J. Fajer, C. M. Drain, *J. Org. Chem.* **2001**, 66, 6513; [19f] M. A. Wolfert, E. H. Schacht, V. Toncheva, K. Ulbrich, O. Nazarova, L. W. Seymour, *Hum. Gene Ther.* **1996**, 7, 2123.
- [20] C. Daniela, G. Marina, T. Michele, E. C. Maria, C. G. Emanuela, C. Giancarlo, *J. Incl. Phenom. Macrocycl. Chem.* **2009**, 65, 391.

- [21] M. B. A. Gloria, L. Peret-Almeida, R. J. Alves, L. Dufosse, A. P. F. Cherubino, *Food Res. Inter.* **2005**, *38*, 1039.
- [22] [22a] M. Uner, *Pharmazie* **2006**, *61*, 375; [22b] M. J. Santander-Ortega, D. Bastos-Gonzalez, J. L. Ortega-Vinuesa, M. J. Alonso, *J. Biomed. Nanotechnol.* **2009**, *5*, 45; [22c] C. Schulze Isfort, M. Rochnia, *Toxicol. Lett.* **2009**, *186*, 148; [22d] E. F. Craparo, G. Cavallaro, M. L. Bondi, D. Mandracchia, G. Giammona, *Biomacromolecules* **2006**, *7*, 3083; [22d] C. Lemarchand, R. Gref, S. Lesieur, H. Hommel, B. Vacher, A. Besheer, K. Maeder, P. Couvreur, *J. Control. Release.* **2005**, *108*, 97.
- [23] V. R. Yadav, S. Suresh, K. Devi, S. Yadav, *AAPS PharmSciTech* **2009**, *10*, 752.
- [24] [24a] B. McCormack, G. Gregoriadis, *J. Drug. Target.* **1994**, *2*, 449; [24b] P. Caliceti, S. Salmaso, A. Semenzato, T. Carofiglio, R. Fornasier, M. Fermeglia, M. Ferrone, S. Princl, *Bioconjug. Chem.* **2003**, *14*, 899; [24c] E. Bilensoy, A. A. Hincal, *Expert Opin. Drug Deliv.* **2009**, *6*, 1161.
- [25] [25a] A. Sahu, U. Bora, N. Kasoju, P. Goswami, *Acta Biomater.* **2008**, *4*, 1752; [25b] W. Tiyaboonchai, W. Tungpradit, P. Plianbangchang, *Int. J. Pharm.* **2007**, *337*, 299.
- [26] L. H. Reddy, *J. Pharm. Pharmacol.* **2005**, *57*, 1231.
- [27] A. J. McGowan, M. C. Ruiz-Ruiz, A. M. Gorman, A. Lopez-Rivas, T. G. Cotter, *FEBS Lett.* **1996**, *392*, 299.
- [28] [28a] G. De Murcia, J. M. De Murcia, *Trends Biochem. Sci* **1994**, *19*, 172; [28b] G. De Murcia, J. M. De Murcia, V. Mschreiber, *Bioassays* **1991**, *13*, 455.

Captions of the Figures

Figure 1. (A) Schematic representation of PCD-CUR self-assembly (inclusion complexation) formation.

Figure 2. (A) Curcumin loading into β -cyclodextrin cavities of PCD. Curcumin loading expressed as μg of curcumin present in mg of PCD-CUR inclusion complex. (B) Stability curves of PCD-CUR self-assemblies with time.

Figure 3. (A) FTIR spectra (B) $^1\text{H-NMR}$ spectra and (C) X-ray diffraction patterns of PCD, CUR, and PCD-CUR (PCD30) self-assemblies.

Figure 4. (A) DSC and (B) TGA curves of PCD, CUR, and PCD-CUR (PCD30) self-assemblies.

Figure 5. TEM analysis of PCD, CUR and PCD-CUR self-assemblies (PCD5, PCD10, PCD20 and PCD30).

Figure 6. Cellular uptake of CUR or PCD-CUR self-assemblies in prostate cancer cells. (A) Fluorescence images of C4-2, DU145 and PC3 prostate cancer cells treated with DMSO, PCD, CUR, or PCD-CUR self-assembly (PCD30). Original magnifications 200X. (B) Flow Cytometric analysis for cellular uptake of CUR and PCD-CUR self-assembly (PCD30) in DU145 cells. Data represents average of 3 repeats. * $p < 0.05$ represents significant difference from the curcumin uptake. Y axis: RFL represents relative fluorescence measured using FACS.

Figure 7. (A) Viability of prostate cancer cells with CUR and PCD-CUR self-assembly treatment. (B) Phase contrast microscopy images of 20 μM CUR or PCD30 treated prostate cancer cells. Note: PCD30 has been shown to have an improved therapeutic effect on prostate

cancer cells compared to free curcumin. Original Magnifications 200X. (C) Immunoblot analysis for PARP cleavage in curcumin or PCD30 treated prostate cancer cells. β -actin was used as an internal loading control. Note: PCD30 has shown enhanced PARP cleavage compared to curcumin.

Figure 8. (A) Representative photographs of colony formation assays of prostate cancer cells treated with CUR or PCD-CUR self-assembly (PCD30). (B) **Quantification** of colony densities in CUR and PCD30 treatment groups in three prostate cancer cell lines. Data represent mean of 3 repeats for each treatment (Mean \pm SE; * $p < 0.05$, compared to the same curcumin dose).

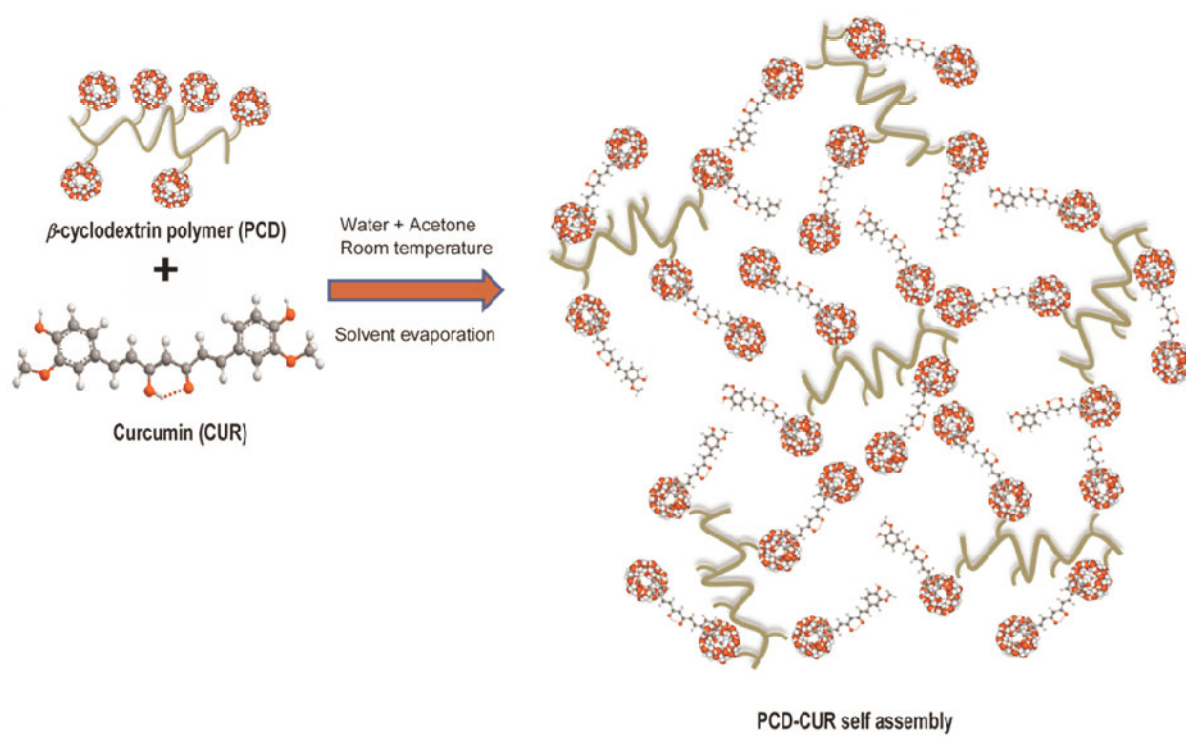


Figure 1

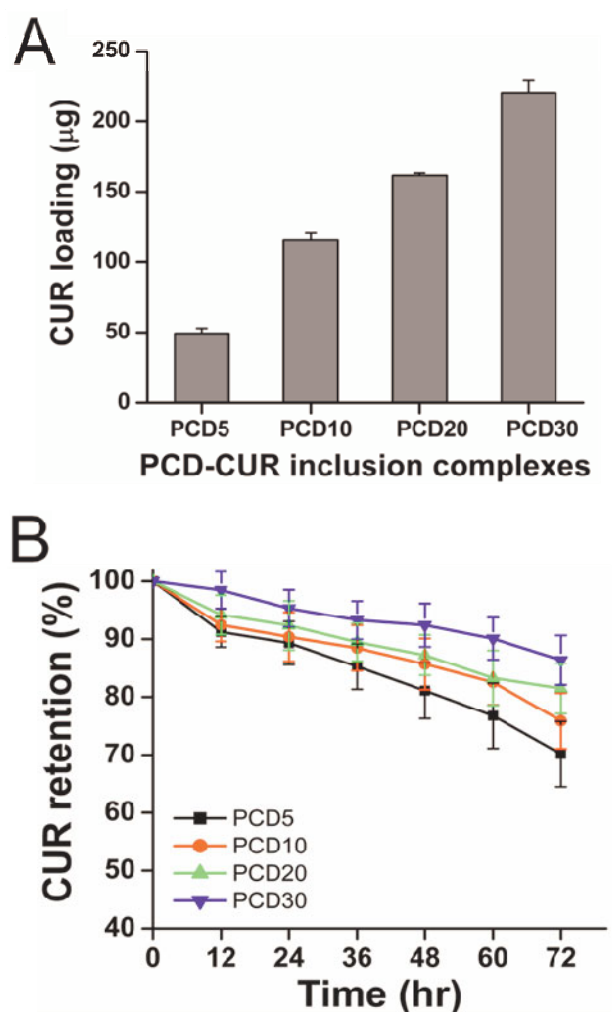


Figure 2

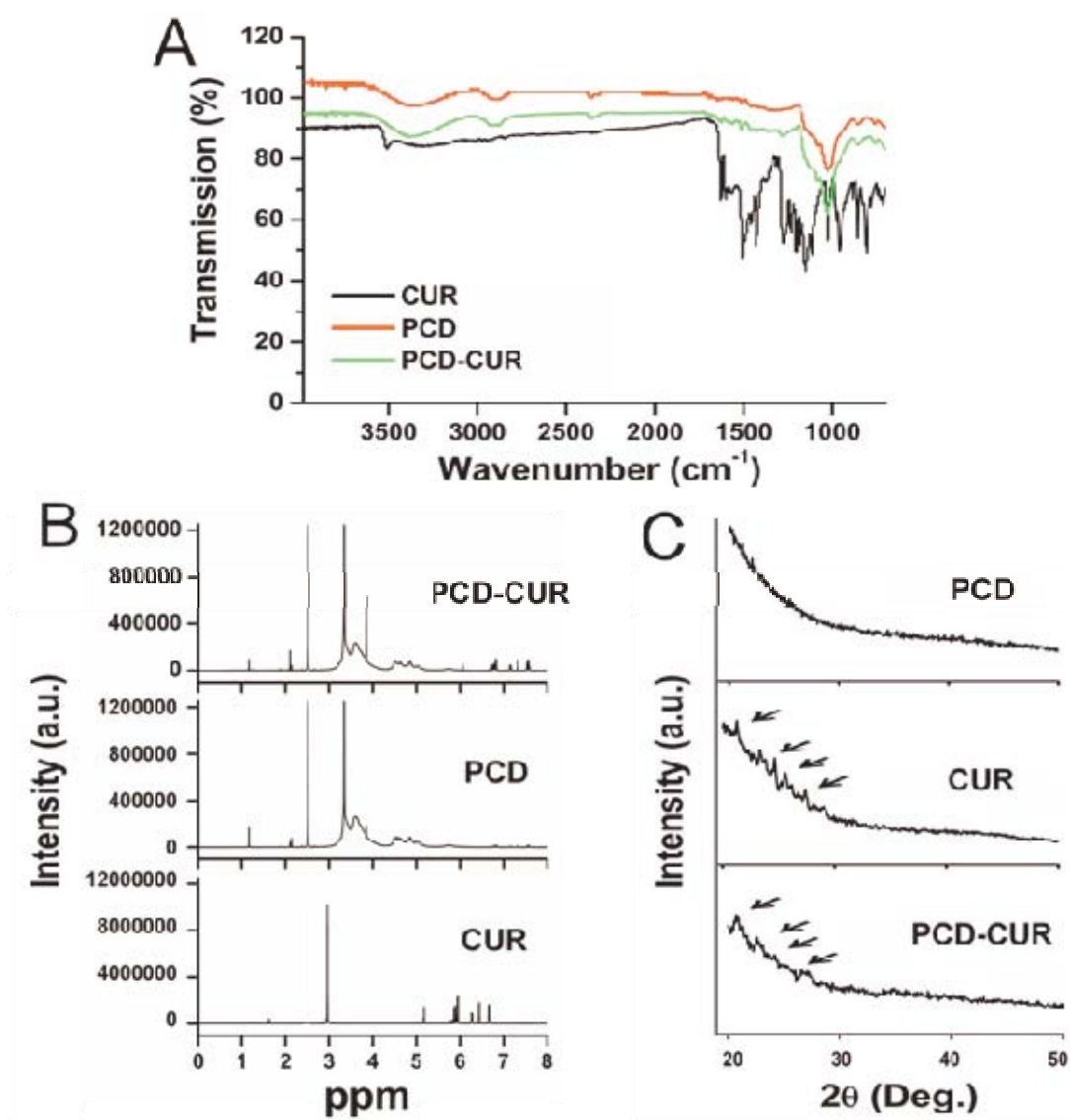


Figure 3

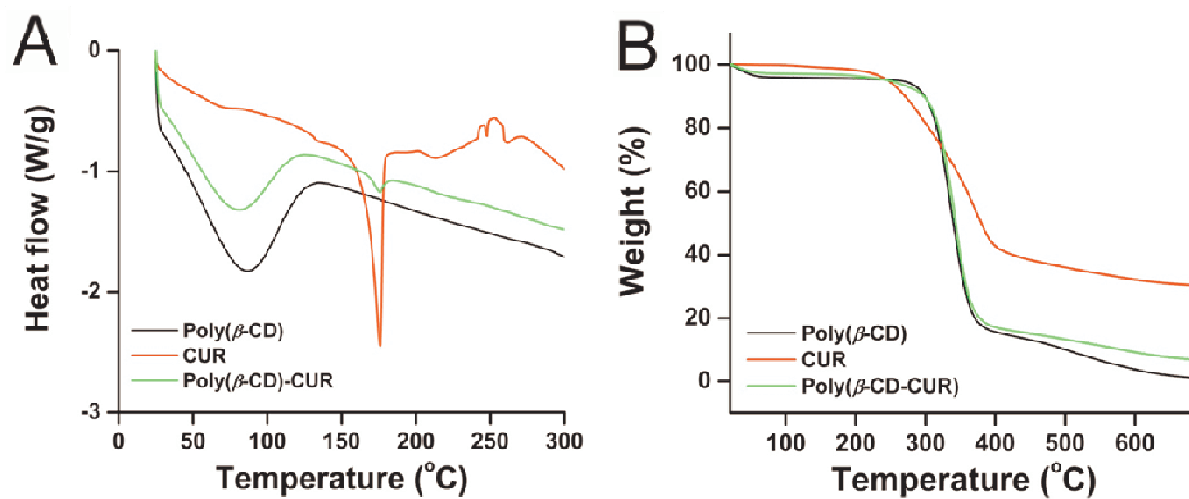


Figure 4

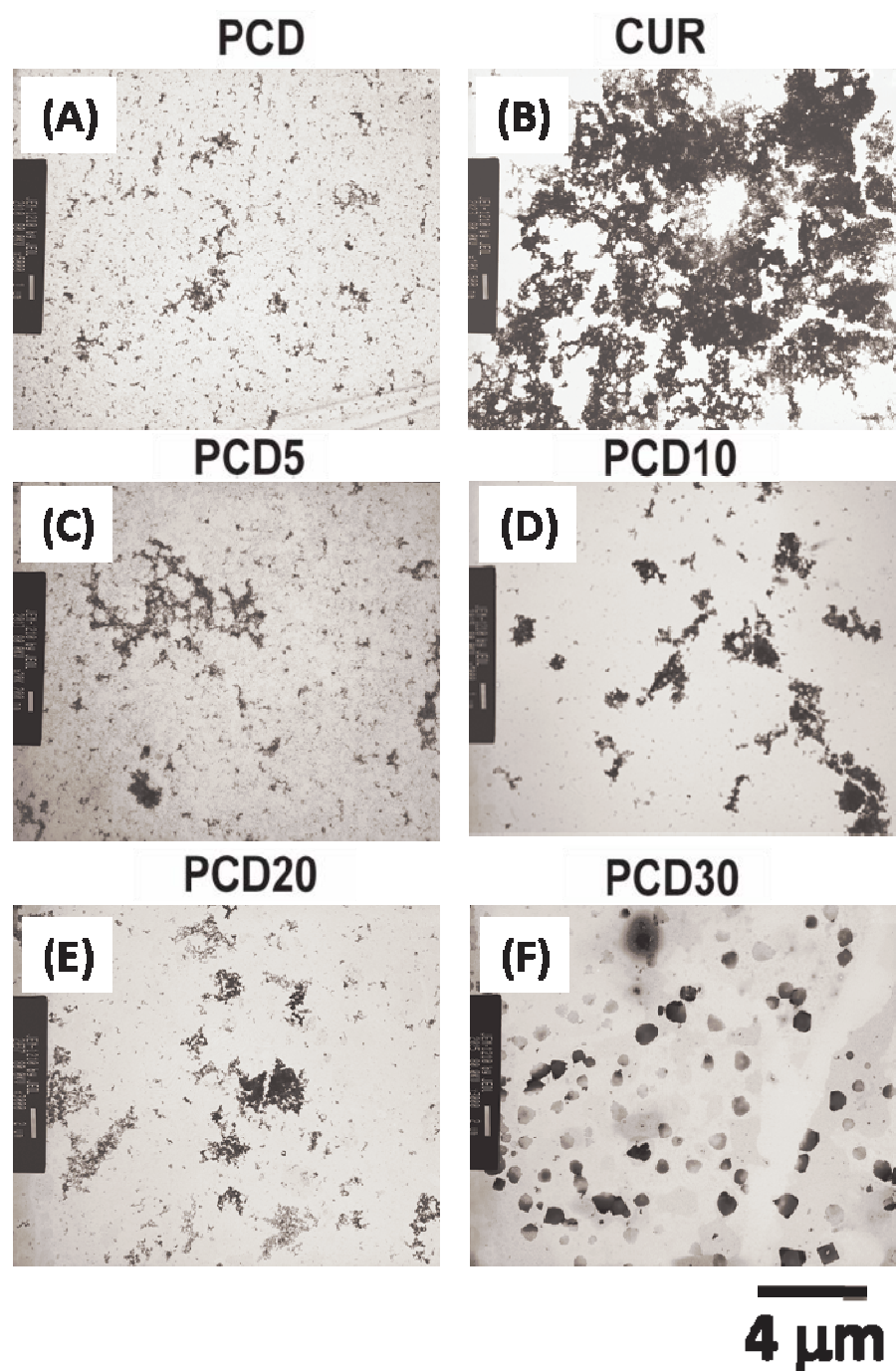


Figure 5

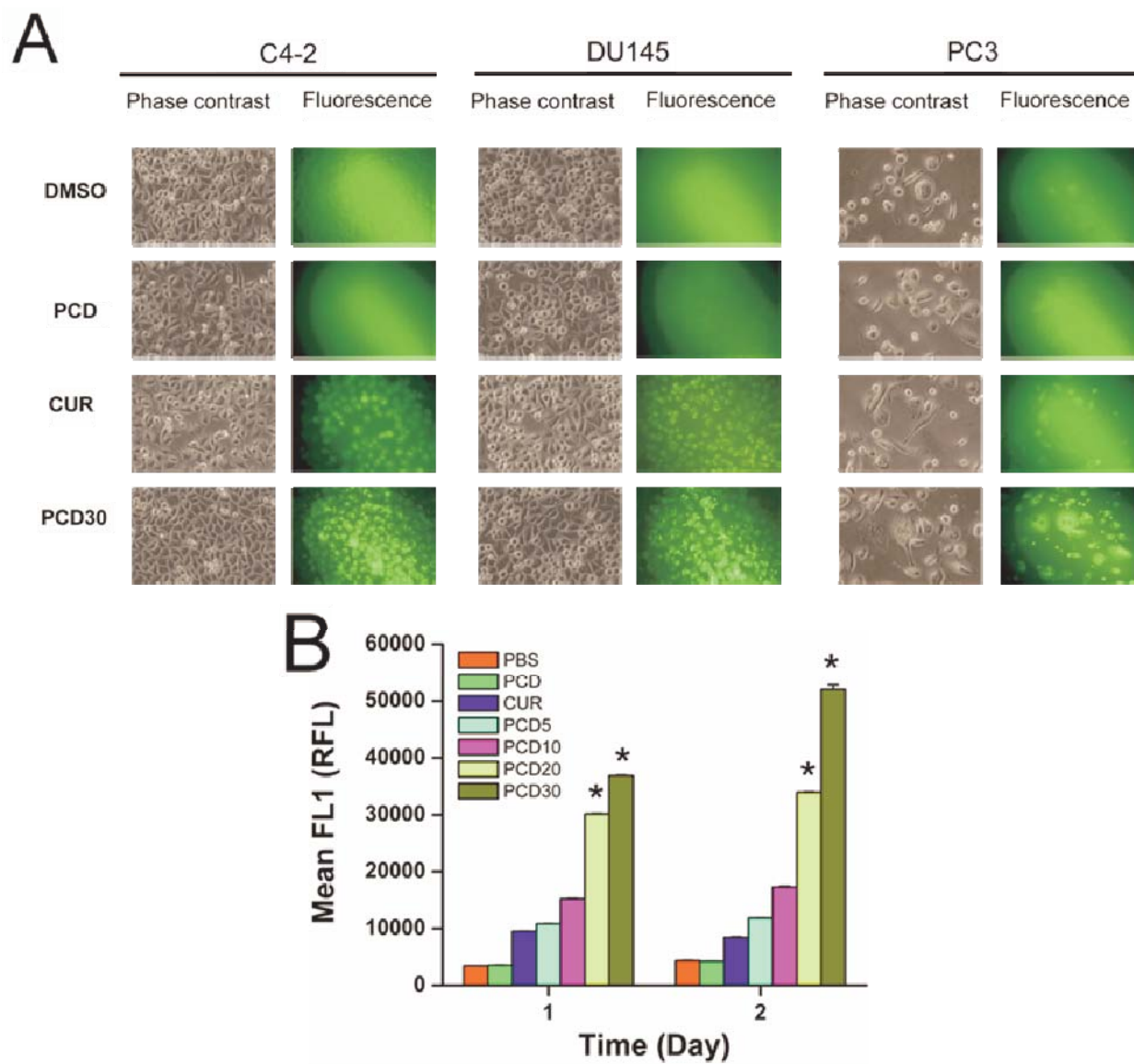


Figure 6

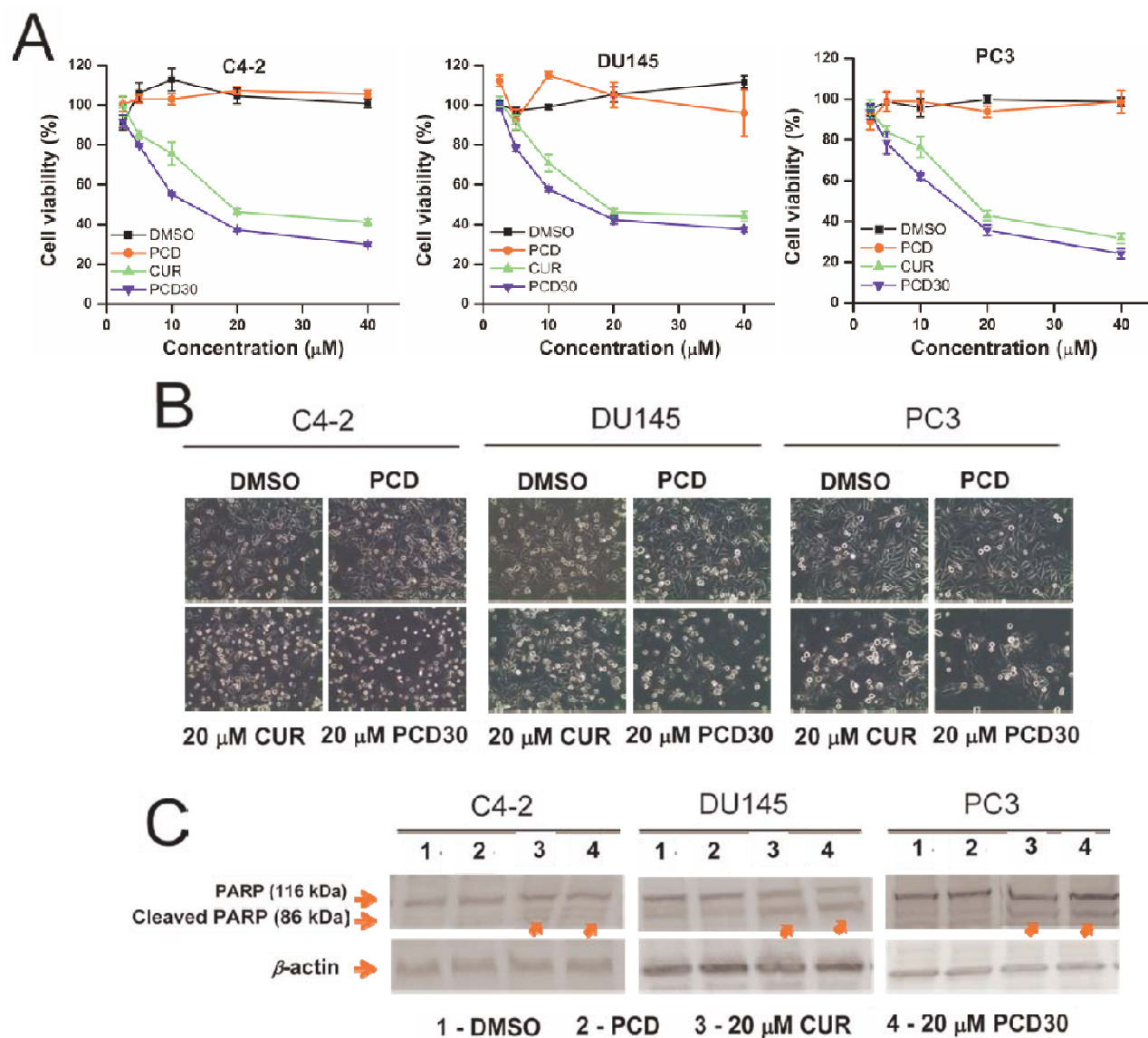


Figure 7

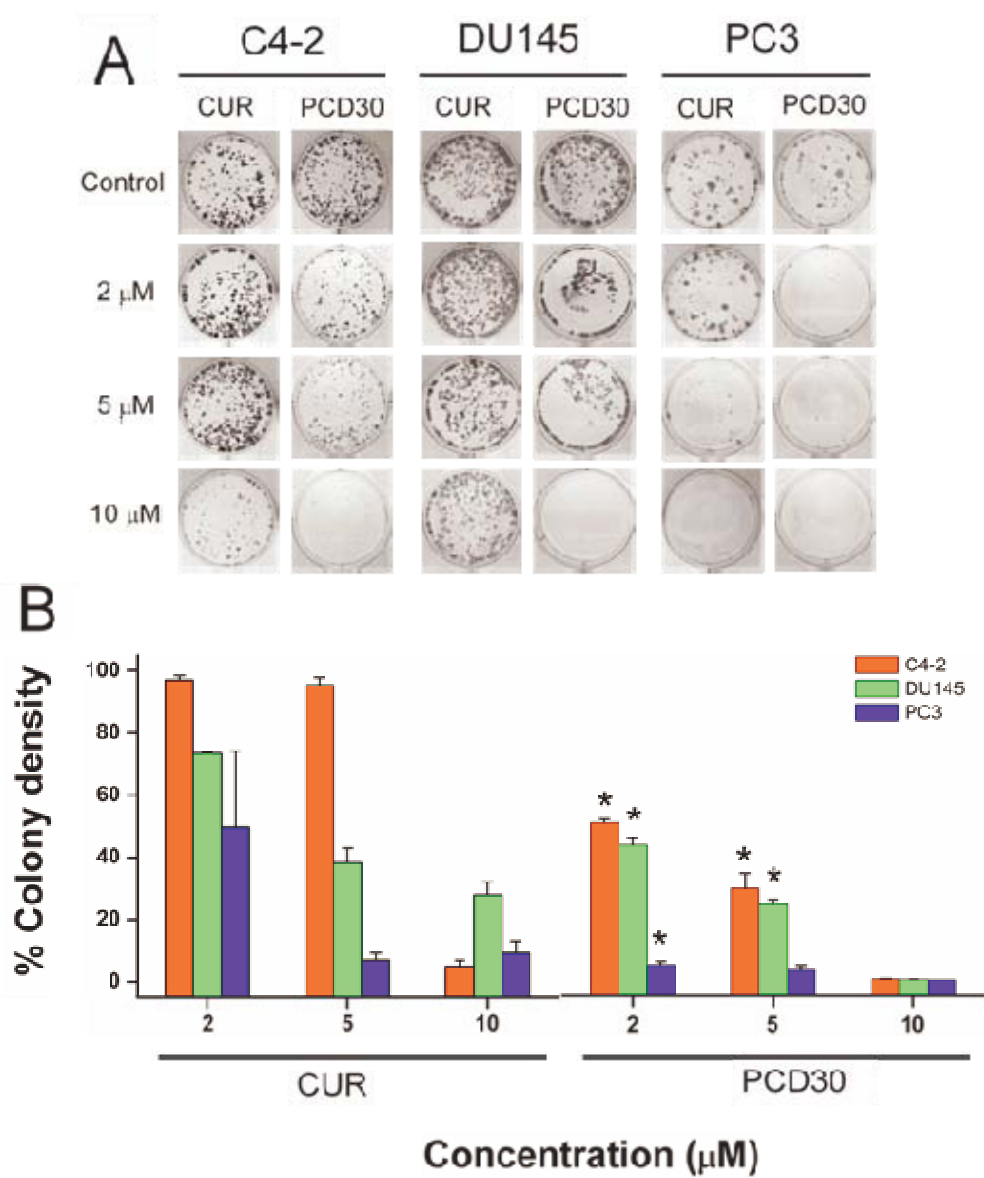
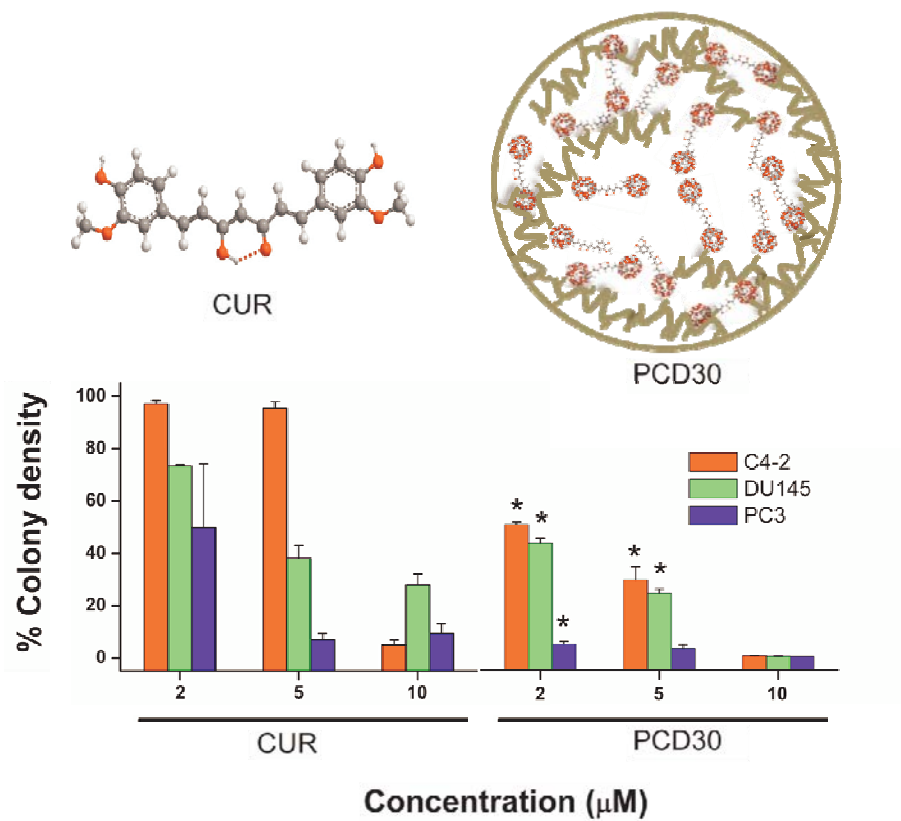


Figure 8

Text and Graphic for the 'Table of Contents'

We have successfully developed a poly(cyclodextrin)-curcumin self-assembly (PCD30) for improved curcumin drug delivery in prostate cancer cells.



Review

Open Access

Mucins in ovarian cancer diagnosis and therapy

Subhash C Chauhan*^{1,2}, Deepak Kumar³ and Meena Jaggi^{1,2}

Address: ¹Cancer Biology Research Center, Sanford Research/USD, Sioux Falls, SD, USA, ²Department of OB/GYN and Basic Biomedical Science Division, Sanford School of Medicine, Sioux Falls, SD, USA and ³Department of Biological and Environmental Sciences, University of the District of Columbia, Washington, DC, USA

Email: Subhash C Chauhan* - subhash.chauhan@usd.edu; Deepak Kumar - dkumar@udc.edu; Meena Jaggi - meena.jaggi@usd.edu

* Corresponding author

Published: 24 December 2009

Received: 4 September 2009

Journal of Ovarian Research 2009, **2**:21 doi:10.1186/1757-2215-2-21

Accepted: 24 December 2009

This article is available from: <http://www.ovarianresearch.com/content/2/1/21>

© 2009 Chauhan et al; licensee BioMed Central Ltd.

This is an Open Access article distributed under the terms of the Creative Commons Attribution License (<http://creativecommons.org/licenses/by/2.0>), which permits unrestricted use, distribution, and reproduction in any medium, provided the original work is properly cited.

Abstract

Ovarian cancer is the most lethal gynecologic malignancy and the five-year survival rate is only 35% after diagnosis. Epithelial ovarian cancer is a highly metastatic disease characterized by widespread peritoneal dissemination and ascites. The death incidences from ovarian cancer could be significantly lowered by developing new methods for the early diagnosis and treatment of this fatal disease. Several potential markers have been identified recently. However, mucins are the most promising markers for ovarian cancer diagnosis. Mucins are large extracellular, heavily glycosylated proteins and their aberrant expression has been implicated in the pathogenesis of a variety of cancers, including ovarian cancer. This review will summarize known facts about the pathological and molecular characteristics of ovarian cancer, the current status of ovarian cancer markers, as well as general information about mucins, the putative role of mucins in the progression of ovarian cancer and their potential use for the early diagnosis and treatment of this disease.

Ovarian Cancer

The life-time risk of having ovarian cancer is 1 in 70 women. This is the fifth leading cause of death for women in developing countries [1,2]. According to epidemiological studies, age is a common risk factor of ovarian cancer because the ovaries of post-menopausal women become smaller and folded. This folding results in deep cleft formations and formation of smaller cysts lined with ovarian surface epithelial (OSE) cells [3-6]. The other risk factors are: nulliparity, family history, history of fertility drug use and endocrine disorders. Multiparity, use of oral contraceptives, pregnancy and lactation all are associated with lower risk of ovarian cancer because of the decreased number of ovulation cycles [6-10]. Molecular alterations are also known to occur in ovarian cancer. These molecular alterations include mutation in the p53 gene which is known to be involved in DNA damage repair. Mutation in

BRCA1 and BRCA2 has also been reported in ovarian tumors [11-15]. Inactivation or downregulation of tumor suppressor genes and amplification of oncogenes is also a potential cause of ovarian cancer. In ovarian tumors, the downregulation of OVCA1 and OVCA2 (tumor suppressor genes present in normal ovary) is reported, while their functions in normal ovary are not well known [11,16]. In contrast, overexpression/amplification of certain oncogenes like C-MYC, RAS, AKT, EGFR (ErbB1 or HER1), HER2/neu (ErbB2), CSF1 C-MYC, etc., is also well known in ovarian tumors [3-5,11,14,17-20].

Ovarian Cancer Staging and Histological Types

Phenotypically, the following types of epithelial ovarian cancers (90%) are classified based on their expressed properties related to the epithelium of the fallopian tube (serous tumors), proliferative endometrium

(endometrioid), endocervix or colonic epithelium (mucinous tumors), gestational endometrium (clear cell carcinoma), or the urinogenital tract (transitional or Brenner tumors) (Table 1). The remaining 10% of ovarian tumors are gonadal-stromal tumors (6%), germ cell tumors (3%) and metastatic tumors (1%) [5] (Table 1). The histological classification of ovarian tumors suggests four different stages in ovarian cancer: stage I (tumors involve one or both the ovaries, 5 year survival 60-90%), stage II (tumors involve one or both ovaries with pelvic extension, 5 year survival 37-66%), stage III (tumors involve one or both ovaries with intraperitoneal metastasis outside the pelvis, retroperitoneal nodes or both, 5 year survival 5-50%) and stage IV (tumors involve one or both ovaries with distant metastases, i.e. to lungs or liver, 5 year survival 0-17%) [5,21] (Table 2). The majority (90%) of ovarian cancers are epithelial ovarian carcinomas (EOC) which are thought to arise from the ovarian surface epithelium (OSE). OSE is the outermost mesothelial (peritoneal) lining and least component of the normal ovary, with no unique feature or known major functions. In addition, the early changes and minor anomalies remain undetected in this tissue [3,5,20]. Due to the anatomic location and the lack of early symptoms, it has become a difficult task to differentiate normal OSE, metaplasia, benign epithelial tumors and borderline tumors. Ovarian cancer can be treated effectively if detected at an early stage; but unfortunately, at the present time most of the ovarian tumors are not diagnosed before an advanced stage (stage III and IV) primarily due to the lack of reliable biomarkers of early diagnosis. Since most ovarian cancers are of epithelial nature and mucins are considered to be the hallmark of epithelial cells, the expression profile of mucins may serve as a potential diagnostic/prognostic and therapeutic target. In this article, we have compiled available information on the expression profile of different mucins in ovarian tumors and their potential role in ovarian cancer diagnosis and treatment.

Mucins

Being that 90% of ovarian cancers are of epithelial origin, mucins may be attractive candidates for the detection of early stage ovarian cancer [1,2,5]. Mucins, large extracellu-

lar proteins, are heavily glycosylated with oligosaccharides and are generally known for providing protection to the epithelial tissues under normal physiological conditions [22-24]. Mucins are usually secreted by the epithelial tissues which remain in contact with relatively harsh environments such as airway epithelium, stomach epithelia, epithelial lining of intestine and ductal epithelial tissue of liver, pancreas, gall bladder, salivary gland, lachrymal gland, etc. In these tissues, epithelial cells are exposed to a variety of microorganisms, toxins, proteases, lipases, glycosidases and diverse microenvironment fluctuations that includes pH, ionic concentration, oxygenation, etc. [22-25]. All mucins share general characteristics. For example, they have repetitive domains of peptides rich in serine, threonine, and proline in their backbone. Serine and threonine are sites for O- and N-glycosylation. Presence of the tandem repeat domain which varies in number, length and O-glycosylation is the common structural feature of all mucins [23,26-29]. Their general structure and biochemical composition provides protection for the cell surface and specific molecular structures regulate the local microenvironment near the cell surface. In addition, mucins also communicate the information of the external environment to the epithelial cells via cellular signaling through membrane-anchored mucins [22-24,29]. It appears that mucins have the capability of serving as cell surface receptors and sensors and conducting signals in response to external stimuli for a variety of cellular responses like cell proliferation, cell growth, differentiation and apoptosis. These reports suggest that the aberrant expression of mucins may be implicated in the development and progression of ovarian cancer.

Type of Mucins

Currently, there are twenty known mucins which have been placed in two categories: secreted mucins (gel forming: MUC2 [30], MUC5AC [31], MUC5B [32], MUC6 [33], and non-gel forming: MUC7 [34] MUC8 [35] and MUC11[36]), and membrane bound mucins (MUC1[26], MUC3 [37], MUC4 [38], MUC9 [39], MUC10 [40], MUC12 [36], MUC13 [41], MUC16 [42,43], MUC17 [44], MUC18 [45] and MUC20 [46]).

Table 1: Classification of ovarian tumors

Epithelial ovarian tumors (90%) Mostly diagnosed after the age of 50.	Germ cell neoplasm (3%) Mostly diagnosed under the age of 30	Gonado-stromal tumors (6%) No particular pattern with age
Serous	Teratomas	Granulosa cell tumors
Mucinous	Mature cyst teratomas	Thecomas
Endometrioid	Immature teratomas	Fibrosarcomas
Clear cell	Dysgerminomas	Sertoli cell tumors
Transitional cell or Brenner tumors	Yolk sac tumors	Leydig cell tumors
	Embryonal carcinomas	

Metastatic tumors: Ovaries may have tumors due to secondary metastasis of stomach, colon, pancreas, appendix, breast, and hematopoietic system.

Table 2: Stage and Features of the Ovarian Tumors

Stage	Features	% 5 year Survival
Stage I	Tumor growth is limited to the one or both the ovaries	60-90
Stage II	Tumor growth in the one or both the ovaries with extension in the pelvis	37-66
Stage III	Tumor growth involves one or both ovaries with extension and intraperitoneal metastasis extended to the bowel, to the lining of the abdominal cavity, or to the lymph nodes	5-50
Stage IV	Tumor growth in one or both ovaries with distant metastases to other organs such as lungs liver or in the chest	0-17

Mucin Expression in Normal Ovary and Nonmalignant Ovarian Cell Lines

Goblet cells or glandular structures are not present in normal ovaries and, therefore, the normal ovarian tissues are not expected to express secretory mucins. Ovarian surface epithelium (OSE) expresses a mixed epithelo-mesenchymal phenotype and is the only compartment known to express mucins. MUC1 is the only well known mucin which is expressed by the OSE at a detectable level [3,4]. Cultured nonmalignant ovarian epithelial cell lines also express MUC1 (a membrane associated mucin) and MUC5AC (a secreted mucin) [47].

Mucin Expression in Ovarian Tumors

The expression of mucin genes by ovarian epithelial cells has not been studied in detail and only a few reports are

available to address this issue. Phenotypically, EOCs are among the most variable tumors of any organ in that they may express ovarian tumor cells structurally related to the epithelium of different organs [4]. It has been shown that malignant ovarian tumors often express more mucins than benign and borderline ovarian tumors. Different studies (Table 3) on the expression of mucins in ovarian tumors have shown overexpression of MUC1, MUC2, MUC3, MUC4, MUC5AC and MUC16 or CA125 [4,47-51]. In agreement with these studies, we also observed overexpression of MUC1, MUC4 and MUC16 in several ovarian tumors [52] with no or an undetectable level of MUC4 and MUC16 in normal ovarian tissues. In northern blot analysis a higher expression of MUC3 and MUC4 was reported in early stage ovarian tumor samples compared to the late stage ovarian tumor samples and it was pro-

Table 3: Comparative expression profile of mucins in different stages and histological types of ovarian cancer

Gene	Normal Ovary	Borderline (Mucinous)	Low Stage (Stage 1-2)	High Stage (Stage 3-4)	Detection method
MUC1	+/-	++	+ to +++ (in all histological types i.e. C, M, E, S)	+ to +++ (in all histological types i.e. C, M, E, S)	ISH, NB, IHC [47-50]
MUC2	ND	+++	+++ (all histological types, primarily in mucinous type)	+ to ++	ISH, NB, IHC [47-51]
MUC3	ND	+++ (primarily in intestinal phenotype)	+++ (E, M)	- to +	ISH, NB [47,48]
MUC4	-	+++ (primarily in endocervical phenotype)	+++ (all types i.e. C, M, E, S)	- to ++	ISH, NB, IHC [47,48]
MUC5AC	ND	++ (primarily in gastric surface cell or mucinous type)	++ (E, M, S)	++	ISH, NB, [47,48]
MUC5B	ND	++ (Express primarily in endocervical phenotype)	++ (C, S)	- to +	ISH, NB [47,48]
MUC13	ND	+	+++ (S, M)	++ (S, M)	OMA, TMA, IHC [53,97]
CA125/MUC16	-	- (express in non-mucinous borderline tumors)	- to +++ (rarely express in mucinous tumors)	+ to +++ (rarely express in mucinous tumors)	IHC [76-79]
MUC17	-	+	-	-	[44,97]

Note: C, M, E, and S are abbreviated for clear cell, mucinous, endometrioid and serous histological types of ovarian tumors, respectively. ISH, in-situ hybridization; NB, northern blotting; IHC, immunohistochemistry, TMA, tissue microarray, OMA, oligonucleotide microarray

posed that they provided a protective function in ovarian cancer [47]. However, in our study we did not see this correlation with MUC4 [52]. The overexpression of MUC1 in various types and stages of ovarian tumor samples is reported in several studies [47,49,50]. Recently, our laboratory has identified aberrant expression of a novel membrane anchored mucin, MUC13, in ovarian cancer. In this study, MUC13 expression was undetectable in normal and benign ovarian samples while 66% of epithelial ovarian cancer samples showed a significantly higher MUC13 expression. MUC13 was predominantly localized on the apical membrane and in the cytoplasm. Moreover, MUC13 expression was significantly ($p < 0.05$) higher in mucinous and Brenners type of samples compared to other histological types of ovarian cancer samples and adjacent normal ovary samples [53]. The expression pattern of certain membrane bound mucins in ovarian tumors is shown in Figure 1.

Pathological Roles of Mucins in Ovarian Cancer

The acquirement of an invasive phenotype is one of the pivotal features of malignant ovarian cells. In order to progress and metastasize, ovarian cancer cells must lose cell contacts with neighboring cells, traverse the basement membrane and migrate through stroma to reach blood vessels or the lymphatic system. Mucins may be implicated in the exfoliation, dissemination and invasion of the ovarian cancer cells due to the highly glycosylated extracellular domain, which may protrude up to 200-2000 nm above the cell surface [54-56]. The overexpression of mucins can effectively interfere with the function of cell adhesion molecules by steric blocking of the interaction of the cell surface molecules. MUC1 is known to suppress cell aggression and cell adhesion properties by interfering with the functions of E-cadherin and other cell adhesion molecules in MUC1 overexpressing breast cancer cells [54-56]. In addition to this, mucins may also be involved in the invasion of the basement membrane by modulating cell-matrix attachment because of their dif-

fused and basal localization in tumor cells. Mucins may also have an immunosuppressive effect by covering the surface of tumor cells and enabling access to the immune responsive cells [24,54-60]. The juxtamembrane domain of the membrane-bound mucins is known to promote cell proliferation by intercellular signaling mediated *via* one of their two/three EGF-like domains [24,55-61]. Moreover, the cytoplasmic tail of mucins like MUC1 is known to induce several cell signaling pathways, which promote the cell growth and proliferation in a variety of cancer cells [24,55-57,61-64]. Additionally, our recent study demonstrates that exogenous MUC13 expression induced morphological changes, including scattering of cells. These changes were abrogated through c-jun NH2-terminal kinase (JNK) chemical inhibitor (SP600125) or JNK2 siRNA. Moreover, a marked reduction in cell-cell adhesion and significant ($p < 0.05$) increases in cell motility, proliferation and tumorigenesis in a xenograft mouse model system were observed upon exogenous MUC13 expression. These cellular characteristics were correlated with up-regulation of HER2, p21-activated kinase1 (PAK1) and p38 protein expression [53]. Additionally, recent studies have shown the role of MUC16/CA125 in ovarian cancer metastasis. MUC16 mucin interacts with the glycosylphosphatidylinositol anchored glycoprotein mesothelin at high affinity and facilitates the peritoneal metastasis of ovarian cancer cells [65,66]. Moreover, MUC16/CA125 expression has been shown to inhibit the cytotoxic responses of human natural killer (NK) cells and downregulate CD16 activity in ovarian cancer cells. It has also been shown that MUC16/CA125 selectively binds to 30-40% of CD16⁺ NK cells in EOC patients. These studies suggest immunosuppressive properties of MUC16/CA125 [67]. These above mentioned findings demonstrate the aberrant expression of mucins in ovarian cancer and show that mucin expression may alter the cellular characteristics of ovarian cancer cells and also imply a significant role of mucins in the pathogenesis of ovarian cancer.

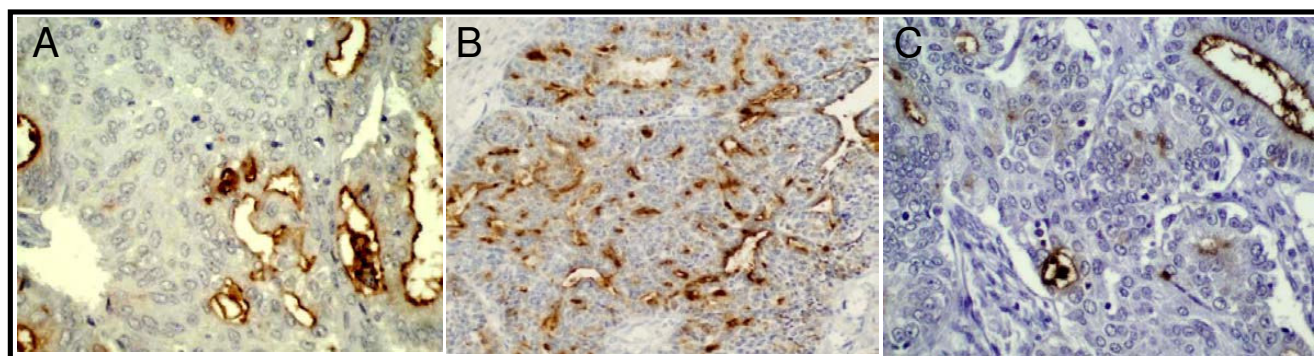


Figure 1
Expression of MUC1 (A), MUC13 (B) and MUC16/CA125 (C) trans-membrane mucins in ovarian tumors.

Mucins as Serum Marker of Ovarian Cancer

The structural characteristics of mucins suggest the presence of potential proteolytic cleavage sites in most mucin genes and several are known to cleave at the cell surface. Mucins, which are normally confined to the epithelial surfaces, become exposed to circulation and their overexpression may establish their potential as a tumor marker and/or diseased condition. Mucins already have shown their great potential as serum markers of ovarian and various other tumors. Aberrant O-glycosylation of mucins is particularly prominent in epithelial cancers. This feature has been termed "glycodynamics". These heterogeneously O-glycosylated mucins aberrantly enter the bloodstream in malignant conditions which provide diagnostic biomarkers for detection and monitoring of cancer. Although mucins are rapidly degraded by glycan-recognizing hepatic clearance receptors in the liver, small subsets of carcinoma mucins remained unrecognized by clearance systems. Thus, circulating cancer mucins used as clinical diagnostic markers likely represent only the clearance-resistant "tip of the iceberg" [68]. For example, O-glycans on circulating MUC16 recognized by antibody CA125 provide for diagnosis and monitoring of ovarian cancers [42]. CA125, an established serum marker of ovarian tumors, has been recently identified as a member of a mucin family and named MUC16 [42,43,69]. MUC16 is a large, heavily glycosylated transmembrane mucin. Several studies have shown the importance of CA125/MUC16 in ovarian cancer diagnosis. In fact, an elevated level of CA125/MUC16 is a gold standard non-invasive test for ovarian cancer diagnosis [70,71]. A decrease in CA125 can provide a surrogate marker to determine the response to chemotherapeutic drug(s) during the treatment procedure [72]. Moreover, antigens such as CA19-9, CA50, and CA242 are also the serum markers of various malignant conditions and are present on heavily glycosylated, high molecular weight mucins [22,73,74]. In breast cancers, serum MUC1 measured by CA15-3 is a well established assay and has been shown to correlate with the clinical course [75]. MUC1 and MUC4 are also known to be overexpressed in ovarian tumors. Despite having a great importance in ovarian cancer, CA125 does not display an elevated serum level in over 50% of the women with early stage tumors because this antigen is not expressed in most early stage ovarian tumors [1,76-79]. Additionally, an elevated level of CA125 was observed in some other (pancreatic, breast, liver, bladder and lung) cancers, benign conditions (diverticulitis, uterine fibroids, endometriosis, and ectopic pregnancy) and physiological conditions (pregnancy and menstruation). Therefore, the discovery of new serum tumor markers capable of complementing CA125 may allow for the development of a reliable test for the early stage diagnosis of ovarian cancer. Our recent and some previous studies showed the overexpression of MUC4 in a majority of early stage ovarian

tumors and a combined panel of MUC1, MUC4 and MUC16 dramatically increased the sensitivity of MUC16 staining test [52]. Additionally, a recent study suggests the overexpression of MUC4 in ovarian carcinoma cells present in peritoneal effusions [80]. Furthermore, our laboratory has recently identified the aberrant expression of a novel transmembrane mucin, MUC13, in ovarian tumor samples compared to normal/benign ovarian tissue samples [53]. Like other membrane-associated mucins, MUC4 and MUC13 also have a proteolytic cleavage site in its structure which may allow the cleavage of the extracellular part of MUC4 and MUC13 and their release in the blood stream [29]. A similar process occurs in case of MUC1 and MUC16. These data suggest that a combined panel of different mucins may improve sensitivity and accuracy of the currently used serum based diagnosis of ovarian cancer. Further, aberrant mucin expression may be immunogenic and may elicit a potent antibody response. This antibody response may also serve as a disease indicator. A recent study demonstrated the presence of MUC1 antibodies in blood plasma samples which was inversely correlated with risk of ovarian cancer [81]. These studies suggest that the aberrant expression of mucins holds great promise to serve as a surrogate marker of ovarian cancer and ovarian cancer prognosis.

Use of Mucins in Radioimmunodiagnosis (RID) and Radioimmunotherapy (RIT)

Monoclonal antibodies against mucins may have potential applications in improving the diagnosis and therapy of ovarian tumors, although very few published studies are available to address this issue, so far, and continued investigations are certainly required. The much higher expression of mucins (MUC1, MUC4, MUC5AC, MUC13 and MUC16) in ovarian tumors compared to the surrounding normal tissues can be exploited for the purpose of radioimmunodiagnosis (RID) and radioimmunotherapy (RIT). MUC1 monoclonal antibodies radiolabeled with γ -emitting radioisotopes like ^{99m}Tc and ^{111}In have been successfully used for the radioimmunodiagnosis of various malignancies [82]. As an extension of this technique, monoclonal antibodies to the mucins, radiolabeled with β -emitting isotopes such as ^{67}Cu , or ^{188}Re , may be employed for the irradiation of spreading tumor cells (radioimmunotherapy) while sparing normal cells [82-84]. At present, MUC1 and MUC16 are the best and only characterized mucins and monoclonal antibodies against MUC1 and MUC16 are under preclinical and clinical investigations for ovarian cancer treatment (Table 4). Therapeutic efficacy of anti-MUC1 MAb (HMFG1: anti-human milk fat globules) radiolabeled with ^{90}Y , ^{186}Re and ^{131}I was investigated in an OVCAR3 ovarian cancer xenograft model. These radiopharmaceuticals significantly improved survival in treated mice compared to control mice. Similarly, radiolabeled MUC16 MAbs also

Table 4: Some mucin-based and other emerging therapies for ovarian cancer treatment [88-94]

Antibody targeting	Vaccines		
	Antibody-based	Antigen-based	Cell-based
Anti-HER2/neu antibody (Herceptin) [In use]	Idiotypic vaccination with anti-MUC1 HMFG1 MAb [Phase I trial]	MUC1 presenting Immunogens [Phase I]	Fusions of ovarian carcinoma cells and dendritic cells (DC) [Preclinical]
⁹⁰ Y-labelled anti-MUC1 HMFG1 MAb [Phase I]	Anti-CA-125 B43.13 MAb vaccine (OvaRex) [Phase IIb]	Peptides derived from a folate binding protein [Phase I]	MUC1 RNA transfected dendritic cells [Preclinical]
¹³¹ I-labelled OC125 MAb [Phase I/II]	Anti-idiotypic antibody ACA-125 vaccine [Phase I/II]	Synthetic Lewis (y)-protein conjugate vaccine [Phase I]	Genetically engineered GM-CSF producing tumor cells
¹³¹ I-labelled MOv8 chimeric MAb [Phase I]		Her2/neu presenting peptides vaccines [Phase I]	Her2/neu and MUC1 peptide pulsed dendritic cells [Pilot study]
Nano-RIT with CA125 and anti-HER2 MAb [Under investigation]		Theratope STn-KLH cancer vaccine [Phase I]	Dendritic cells pulsed with tumor-lysate

caused significant delay in animal death. MUC13 is another potential mucin which is highly expressed on the surface of ovarian cancer cells, indicating its potential as a target for RID and RIT. An emerging concept in radioimmunotherapy is nano-radioimmunotherapy (Nano-RIT). In these studies radiolabeled antibodies are coupled with drug loaded liposomes or nanoparticles. This approach will overcome some of the major obstacles associated with conventional strategies and will improve tumor uptake and retention time of radioimmunoconjugates [85,86]. The radioimmunoconjugates can be safely administered *via* an intravenous route despite the fact they are mouse monoclonal antibodies and capable of inducing human anti-mouse antibody (HAMA) responses. However, this problem can be minimized in the future by using modern antibody engineering techniques [87].

Anti-Cancer Vaccines Based on Mucins

In recent years, projects associated with the development of tumor vaccines have received considerable attention (Table 4). A further possible approach involves the use of mucins as a vaccine and target for immune responses (Table 4) [88,89]. Three types of strategies can be employed for vaccine development: antibody-based, antigen-based and cell-based. As we mentioned earlier, certain membrane anchored mucins which are over/aberrantly expressed in ovarian cancer can be targeted for monoclonal antibody generation and anti-cancer vaccine development. Antibody generated against a tumor antigen can trigger potent antibody-dependent cellular cytotoxicity and T-cell response. Additionally, monoclonal antibodies can persuade anti-idiotypic antibodies that mimic the epitopes in tumor antigens and can elicit a potent anti-cancer response in patients. For an anti-cancer vaccine, synthetic peptide or DNA that encodes for a tumor anti-

gen can be administered to the patient and over time the patient will develop an immune response by activation of cytotoxic T cells. In a cell-based vaccine approach, tumor cells of the same patient (autologous) or a different patient (allogeneic) or dendritic cells (activated by cancer antigen) are administered to the cancer patient to stimulate the immune system. The induction of potential anti-MUC responses may provide potential benefits in targeting tumors overexpressing mucin antigens. MUC1 has been successfully used as a target for immuno-directed therapies and as a marker of disease progression [88-90]. The efficacy of the immune response to mucins or mucin peptides can be effectively augmented by conjugation of immune adjuvant and/or carrier proteins like Bacille Calmette-Guerin (BCG) and keyhole limpet hemocyanin (KLH). A cognate of the MUC1 peptide conjugated with KLH and *Quillaja saponaria* (QS-21) has entered into clinical trials for prostate cancer [91,92]. The use of naked DNA is another attractive and relatively simple approach for vaccination studies. MUC1 cDNA has been used as a cancer vaccine in mouse models and has been shown to result in long-term growth suppression of tumors [93,94]. Additionally, dendritic cells pulsed with mucin derived peptides were able to induce a potent cytotoxic T-cell response and provide therapeutic benefits [95,96]. For ovarian tumors, which are known to overexpress mucins, this may be a potential treatment approach with a better survival outcome.

Conclusions

The mucin gene family has considerable potential importance in the cell biology, diagnosis and treatment of ovarian malignancies. Various studies have shown the overexpression of MUC1, MUC2, MUC3, MUC4, MUC5AC and MUC16 in a variety of ovarian tumors. In

particular, a combined panel of MUC4, MUC5AC, and MUC16 may offer an effective and reliable diagnostic system and target for the management of various histological grades and types of ovarian cancer, although their biological functions are not clearly defined. The development of new molecular biology techniques will allow researchers to determine the biological role of mucins in the process of ovarian tumor progression and response to therapy. The gene locus of the majority of mucin genes has been identified and, therefore, may be a potential target for future gene-based therapies, including immunoliposome targeted techniques. The use of mucins as targets for radioimmunodiagnosis and radioimmunotherapy is also being explored and appears to be a potential approach for the diagnosis and treatment of ovarian tumors which overexpress mucins. The advancement in the area of antibody engineering techniques provides an opportunity to produce single-chain, divalent, tetravalent and humanized antibody constructs from murine monoclonal antibodies. These molecules will be significantly less immunogenic to the human host than their intact mouse Ig counterparts, and may allow repeated intravenous/intraperitoneal administrations of targeting radioconjugated molecules, improved tumor tissue penetration due to reduced physical size with a minimal or no risk of an HAMA response. In the light of available information, we conclude that switching of mucin genes occurs in ovarian cancer, which can be utilized for the early diagnosis and treatment of ovarian tumors.

Competing interests

The authors declare that they have no competing interests.

Authors' contributions

SCC drafted the manuscript. DK and MJ participated in substantial contribution to revising of the manuscript. All authors read and approved the final manuscript.

Acknowledgements

This work was supported by a Sanford Research/USD grant and Department of Defense Grants (PC073887) awarded to SCC and (PC073643) awarded to MJ. DK is supported by SC1 (CA141935) and U56 (CA101563) grants from NCI. We thank Cathy Christopherson for editorial assistance with the manuscript.

References

- Alexander-Sefre F, Menon U, Jacobs IJ: **Ovarian cancer screening.** *Hosp Med* 2002, **63**:210-213.
- Ozols RF: **Update on the management of ovarian cancer.** *Cancer J* 2002, **8**(Suppl 1):S22-30.
- Auersperg N, Edelson MI, Mok SC, Johnson SW, Hamilton TC: **The biology of ovarian cancer.** *Semin Oncol* 1998, **25**:281-304.
- Auersperg N, Ota T, Mitchell GW: **Early events in ovarian epithelial carcinogenesis: progress and problems in experimental approaches.** *Int J Gynecol Cancer* 2002, **12**:691-703.
- Auersperg N, Wong AS, Choi KC, Kang SK, Leung PC: **Ovarian surface epithelium: biology, endocrinology, and pathology.** *Endocr Rev* 2001, **22**:255-288.
- Daly M, Orams GI: **Epidemiology and risk assessment for ovarian cancer.** *Semin Oncol* 1998, **25**:255-264.
- Hankinson SE, Colditz GA, Hunter DJ, Willett WC, Stampfer MJ, Rosner B, Hennekens CH, Speizer FE: **A prospective study of reproductive factors and risk of epithelial ovarian cancer.** *Cancer* 1995, **76**:284-290.
- Eltabbakh GH, Piver MS, Hempling RE, Recio FO, Aiduk C: **Estrogen replacement therapy following oophorectomy in women with a family history of ovarian cancer.** *Gynecol Oncol* 1997, **66**:103-107.
- Hempling RE, Wong C, Piver MS, Natarajan N, Mettlin CJ: **Hormone replacement therapy as a risk factor for epithelial ovarian cancer: results of a case-control study.** *Obstet Gynecol* 1997, **89**:1012-1016.
- Rossing MA, Daling JR, Weiss NS, Moore DE, Self SG: **Ovarian tumors in a cohort of infertile women.** *N Engl J Med* 1994, **331**:771-776.
- Lynch HT, Casey MJ, Lynch J, White TE, Godwin AK: **Genetics and ovarian carcinoma.** *Semin Oncol* 1998, **25**:265-280.
- Lynch HT, Casey MJ, Shaw TG, Lynch JF: **Hereditary Factors in Gynecologic Cancer.** *Oncologist* 1998, **3**:319-338.
- Lynch HT, Lemon S, Lynch J, Casey MJ: **Hereditary gynecologic cancer.** *Cancer Treat Res* 1998, **95**:1-102.
- Mackey SE, Creasman WT: **Ovarian cancer screening.** *J Clin Oncol* 1995, **13**:783-793.
- Berman DB, Wagner-Costalas J, Schultz DC, Lynch HT, Daly M, Godwin AK: **Two distinct origins of a common BRCA1 mutation in breast-ovarian cancer families: a genetic study of 15 185delAG-mutation kindreds.** *Am J Hum Genet* 1996, **58**:1166-1176.
- Schultz DC, Vanderveer L, Berman DB, Hamilton TC, Wong AJ, Godwin AK: **Identification of two candidate tumor suppressor genes on chromosome 17p13.3.** *Cancer Res* 1996, **56**:1997-2002.
- Berchuck A: **Biomarkers in the ovary.** *J Cell Biochem Suppl* 1995, **23**:223-226.
- Wenham RM, Lancaster JM, Berchuck A: **Molecular aspects of ovarian cancer.** *Best Pract Res Clin Obstet Gynaecol* 2002, **16**:483-497.
- Wenham RM, Schildkraut JM, McLean K, Calingaert B, Bentley RC, Marks J, Berchuck A: **Polymorphisms in BRCA1 and BRCA2 and risk of epithelial ovarian cancer.** *Clin Cancer Res* 2003, **9**:4396-4403.
- Wong AS, Auersperg N: **Ovarian surface epithelium: family history and early events in ovarian cancer.** *Reprod Biol Endocrinol* 2003, **1**:70.
- Friedlander ML: **Prognostic factors in ovarian cancer.** *Semin Oncol* 1998, **25**:305-314.
- Gendler SJ, Spicer AP: **Epithelial mucin genes.** *Annu Rev Physiol* 1995, **57**:607-634.
- Gum JR Jr: **Mucin genes and the proteins they encode: structure, diversity, and regulation.** *Am J Respir Cell Mol Biol* 1992, **7**:557-564.
- Hollingsworth MA, Swanson BJ: **Mucins in cancer: protection and control of the cell surface.** *Nat Rev Cancer* 2004, **4**:45-60.
- Forstner JF: **Intestinal mucins in health and disease.** *Digestion* 1978, **17**:234-263.
- Gendler SJ, Lancaster CA, Taylor-Papadimitriou J, Duhig T, Peat N, Burchell J, Pemberton L, Lalani EN, Wilson D: **Molecular cloning and expression of human tumor-associated polymorphic epithelial mucin.** *J Biol Chem* 1990, **265**:15286-15293.
- Gupta R, Jentoft N: **Subunit structure of porcine submaxillary mucin.** *Biochemistry* 1989, **28**:6114-6121.
- Timpte CS, Eckhardt AE, Abernethy JL, Hill RL: **Porcine submaxillary gland apomucin contains tandemly repeated, identical sequences of 81 residues.** *J Biol Chem* 1988, **263**:1081-1088.
- Moniaux N, Escande F, Porchet N, Aubert JP, Batra SK: **Structural organization and classification of the human mucin genes.** *Front Biosci* 2001, **6**:D1192-1206.
- Gum JR Jr, Hicks JW, Toribara NW, Siddiki B, Kim YS: **Molecular cloning of human intestinal mucin (MUC2) cDNA. Identification of the amino terminus and overall sequence similarity to prepro-von Willebrand factor.** *J Biol Chem* 1994, **269**:2440-2446.
- Escande F, Aubert JP, Porchet N, Buisine MP: **Human mucin gene MUC5AC: organization of its 5'-region and central repetitive region.** *Biochem J* 2001, **358**:763-772.
- Desseyn JL, Buisine MP, Porchet N, Aubert JP, Laine A: **Genomic organization of the human mucin gene MUC5B. cDNA and**

- genomic sequences upstream of the large central exon. *J Biol Chem* 1998, **273**:30157-30164.
33. Toribara NW, Ho SB, Gum E, Gum JR Jr, Lau P, Kim YS: **The carboxyl-terminal sequence of the human secretory mucin, MUC6. Analysis Of the primary amino acid sequence.** *J Biol Chem* 1997, **272**:16398-16403.
 34. Bobek LA, Tsai H, Biesbrock AR, Levine MJ: **Molecular cloning, sequence, and specificity of expression of the gene encoding the low molecular weight human salivary mucin (MUC7).** *J Biol Chem* 1993, **268**:20563-20569.
 35. Seong JK, Koo JS, Lee WJ, Kim HN, Park JY, Song KS, Hong JH, Yoon JH: **Upregulation of MUC8 and downregulation of MUC5AC by inflammatory mediators in human nasal polyps and cultured nasal epithelium.** *Acta Otolaryngol* 2002, **122**:401-407.
 36. Williams SJ, McGuckin MA, Gotley DC, Eyre HJ, Sutherland GR, Antalis TM: **Two novel mucin genes down-regulated in colorectal cancer identified by differential display.** *Cancer Res* 1999, **59**:4083-4089.
 37. Pratt WS, Crawley S, Hicks J, Ho J, Nash M, Kim YS, Gum JR, Swallow DM: **Multiple transcripts of MUC3: evidence for two genes, MUC3A and MUC3B.** *Biochem Biophys Res Commun* 2000, **275**:916-923.
 38. Moniaux N, Nollet S, Porchet N, Degand P, Laine A, Aubert JP: **Complete sequence of the human mucin MUC4: a putative cell membrane-associated mucin.** *Biochem J* 1999, **338**(Pt 2):325-333.
 39. Lapensee L, Paquette Y, Bleau G: **Allelic polymorphism and chromosomal localization of the human oviductin gene (MUC9).** *Fertil Steril* 1997, **68**:702-708.
 40. Melnick M, Chen H, Zhou Y, Jaskoll T: **An alternatively spliced Muc10 glycoprotein ligand for putative L-selectin binding during mouse embryonic submandibular gland morphogenesis.** *Arch Oral Biol* 2001, **46**:745-757.
 41. Williams SJ, Wreschner DH, Tran M, Eyre HJ, Sutherland GR, McGuckin MA: **Muc13, a novel human cell surface mucin expressed by epithelial and hemopoietic cells.** *J Biol Chem* 2001, **276**:18327-18336.
 42. Yin BW, Dnistrian A, Lloyd KO: **Ovarian cancer antigen CA125 is encoded by the MUC16 mucin gene.** *Int J Cancer* 2002, **98**:737-740.
 43. Yin BW, Lloyd KO: **Molecular cloning of the CA125 ovarian cancer antigen: identification as a new mucin, MUC16.** *J Biol Chem* 2001, **276**:27371-27375.
 44. Gum JR Jr, Crawley SC, Hicks JW, Szymkowski DE, Kim YS: **MUC17, a novel membrane-tethered mucin.** *Biochem Biophys Res Commun* 2002, **291**:466-475.
 45. Mills L, Tellez C, Huang S, Baker C, McCarty M, Green L, Gudas JM, Feng X, Bar-Eli M: **Fully human antibodies to MCAM/MUC18 inhibit tumor growth and metastasis of human melanoma.** *Cancer Res* 2002, **62**:5106-5114.
 46. Higuchi T, Orita T, Nakanishi S, Katsuya K, Watanabe H, Yamasaki Y, Waga I, Nanayama T, Yamamoto Y, Munger W, Sun H, Falk R, Jennette J, Alcorta D, Li H, Yamamoto T, Saito Y, Nakamura M: **Molecular cloning, genomic structure, and expression analysis of MUC20, a novel mucin protein, up-regulated in injured kidney.** *J Biol Chem* 2004, **279**:1968-1979.
 47. Giuntoli RL, Rodriguez GC, Whitaker RS, Dodge R, Voinow JA: **Mucin gene expression in ovarian cancers.** *Cancer Res* 1998, **58**:5546-5550.
 48. Boman F, Buisine MP, Wacrenier A, Querleu D, Aubert JP, Porchet N: **Mucin gene transcripts in benign and borderline mucinous tumours of the ovary: an in situ hybridization study.** *J Pathol* 2001, **193**:339-344.
 49. Dong Y, Walsh MD, Cummings MC, Wright RG, Khoo SK, Parsons PG, McGuckin MA: **Expression of MUC1 and MUC2 mucins in epithelial ovarian tumours.** *J Pathol* 1997, **183**:311-317.
 50. Feng H, Ghazizadeh M, Konishi H, Araki T: **Expression of MUC1 and MUC2 mucin gene products in human ovarian carcinomas.** *Jpn J Clin Oncol* 2002, **32**:525-529.
 51. Hanski C, Hofmeier M, Schmitt-Graff A, Riede E, Hanski ML, Borchard F, Sieber E, Niedobitek F, Foss HD, Stein H, Riecken EO: **Overexpression or ectopic expression of MUC2 is the common property of mucinous carcinomas of the colon, pancreas, breast, and ovary.** *J Pathol* 1997, **182**:385-391.
 52. Chauhan SC, Singh AP, Ruiz F, Johansson SL, Jain M, Smith LM, Moniaux N, Batra SK: **Aberrant expression of MUC4 in ovarian carcinoma: diagnostic significance alone and in combination with MUC1 and MUC16 (CA125).** *Mod Pathol* 2006, **19**:1386-1394.
 53. Chauhan SC, Vannatta K, Ebeling MC, Vinayek N, Watanabe A, Pandey KK, Bell MC, Koch MD, Aburatani H, Lio Y, Jaggi M: **Expression and functions of transmembrane mucin MUC13 in ovarian cancer.** *Cancer Res* 2009, **69**:765-774.
 54. Kondo K, Kohno N, Yokoyama A, Hiwada K: **Decreased MUC1 expression induces E-cadherin-mediated cell adhesion of breast cancer cell lines.** *Cancer Res* 1998, **58**:2014-2019.
 55. Wesseling J, Valk SW van der, Hilken J: **A mechanism for inhibition of E-cadherin-mediated cell-cell adhesion by the membrane-associated mucin episialin/MUC1.** *Mol Biol Cell* 1996, **7**:565-577.
 56. Wesseling J, Valk SW van der, Vos HL, Sonnenberg A, Hilken J: **Episialin (MUC1) overexpression inhibits integrin-mediated cell adhesion to extracellular matrix components.** *J Cell Biol* 1995, **129**:255-265.
 57. Kohlgref KG, Gawron AJ, Higashi M, Meza JL, Burdick MD, Kitajima S, Kelly DL, Caffrey TC, Hollingsworth MA: **Contribution of the MUC1 tandem repeat and cytoplasmic tail to invasive and metastatic properties of a pancreatic cancer cell line.** *Cancer Res* 2003, **63**:5011-5020.
 58. Komatsu M, Carraway CA, Fregien NL, Carraway KL: **Reversible disruption of cell-matrix and cell-cell interactions by overexpression of sialomucin complex.** *J Biol Chem* 1997, **272**:33245-33254.
 59. Komatsu M, Tatum L, Altman NH, Carothers Carraway CA, Carraway KL: **Potential of metastasis by cell surface sialomucin complex (rat MUC4), a multifunctional anti-adhesive glycoprotein.** *Int J Cancer* 2000, **87**:480-486.
 60. Komatsu M, Yee L, Carraway KL: **Overexpression of sialomucin complex, a rat homologue of MUC4, inhibits tumor killing by lymphokine-activated killer cells.** *Cancer Res* 1999, **59**:2229-2236.
 61. Kashiwagi H, Kijima H, Dowaki S, Ohtani Y, Tobita K, Yamazaki H, Nakamura M, Ueyama Y, Tanaka M, Inokuchi S, Makuuchi H: **MUC1 and MUC2 expression in human gallbladder carcinoma: a clinicopathological study and relationship with prognosis.** *Oncol Rep* 2001, **8**:485-489.
 62. Li Y, Kufe D: **The Human DF3/MUC1 carcinoma-associated antigen signals nuclear localization of the catenin p120(ctn).** *Biochem Biophys Res Commun* 2001, **281**:440-443.
 63. Li Y, Kuwahara H, Ren J, Wen G, Kufe D: **The c-Src tyrosine kinase regulates signaling of the human DF3/MUC1 carcinoma-associated antigen with GSK3 beta and beta-catenin.** *J Biol Chem* 2001, **276**:6061-6064.
 64. Li Y, Ren J, Yu W, Li Q, Kuwahara H, Yin L, Carraway KL, Kufe D: **The epidermal growth factor receptor regulates interaction of the human DF3/MUC1 carcinoma antigen with c-Src and beta-catenin.** *J Biol Chem* 2001, **276**:35239-35242.
 65. Rump A, Morikawa Y, Tanaka M, Minami S, Umesaki N, Takeuchi M, Miyajima A: **Binding of ovarian cancer antigen CA125/MUC16 to mesothelin mediates cell adhesion.** *J Biol Chem* 2004, **279**:9190-9198.
 66. Gubbels JA, Belisle J, Onda M, Rancourt C, Migneault M, Ho M, Bera TK, Connor J, Sathyanarayana BK, Lee B, Pastan I, Patankar M: **Mesothelin-MUC16 binding is a high affinity, N-glycan dependent interaction that facilitates peritoneal metastasis of ovarian tumors.** *Mol Cancer* 2006, **5**:50.
 67. Belisle JA, Gubbels JA, Raphael CA, Migneault M, Rancourt C, Connor JP, Patankar MS: **Peritoneal natural killer cells from epithelial ovarian cancer patients show an altered phenotype and bind to the tumour marker MUC16 (CA125).** *Immunology* 2007, **122**:418-429.
 68. Wahrenbrock MG, Varki A: **Multiple hepatic receptors cooperate to eliminate secretory mucins aberrantly entering the bloodstream: are circulating cancer mucins the "tip of the iceberg"?** *Cancer Res* 2006, **66**:2433-2441.
 69. Bast RC Jr, Xu FJ, Yu YH, Barnhill S, Zhang Z, Mills GB: **CA 125: the past and the future.** *Int J Biol Markers* 1998, **13**:179-187.
 70. Bast RC Jr, Klug TL, St John E, Jenison E, Niloff JM, Lazarus H, Berkowitz RS, Leavitt T, Griffiths CT, Parker L, Zurawski V Jr, Knapp R: **A radioimmunoassay using a monoclonal antibody to monitor the course of epithelial ovarian cancer.** *N Engl J Med* 1983, **309**:883-887.

71. Bast RC Jr, Badgwell D, Lu Z, Marquez R, Rosen D, Liu J, Baggerly KA, Atkinson EN, Skates S, Zhang Z, Lokshin A, Menon U, Jacobs I, Lu KI: **New tumor markers: CA125 and beyond.** *Int J Gynecol Cancer* 2005, **15**(Suppl 3):274-281.
72. Rustin GJ, Bast RC Jr, Kelloff GJ, Barrett JC, Carter SK, Nisen PD, Sigman CC, Parkinson DR, Ruddon RW: **Use of CA-125 in clinical trial evaluation of new therapeutic drugs for ovarian cancer.** *Clin Cancer Res* 2004, **10**:3919-3926.
73. Kim YS, Gum J Jr, Brockhausen I: **Mucin glycoproteins in neoplasia.** *Glycoconj J* 1996, **13**:693-707.
74. Kim YS, Gum JR Jr, Crawley SC, Deng G, Ho JJ: **Mucin gene and antigen expression in biliopancreatic carcinogenesis.** *Ann Oncol* 1999, **10**(Suppl 4):51-55.
75. Robertson JF, Jaeger W, Szymendera JJ, Selby C, Coleman R, Howell A, Winstanley J, Jonssen PE, Bombardieri E, Sainsbury JR, Gronberg H, Kumpulainen E, Blamey RW: **The objective measurement of remission and progression in metastatic breast cancer by use of serum tumour markers. European Group for Serum Tumour Markers in Breast Cancer.** *Eur J Cancer* 1999, **35**:47-53.
76. Fritsche HA, Bast RC: **CA 125 in ovarian cancer: advances and controversy.** *Clin Chem* 1998, **44**:1379-1380.
77. Jacobs I, Bast RC Jr: **The CA 125 tumour-associated antigen: a review of the literature.** *Hum Reprod* 1989, **4**:1-12.
78. Jacobs IJ, Oram DH, Bast RC Jr: **Strategies for improving the specificity of screening for ovarian cancer with tumor-associated antigens CA 125, CA 15-3, and TAG 72.3.** *Obstet Gynecol* 1992, **80**:396-399.
79. Jacobs IJ, Rivera H, Oram DH, Bast RC Jr: **Differential diagnosis of ovarian cancer with tumour markers CA 125, CA 15-3 and TAG 72.3.** *Br J Obstet Gynaecol* 1993, **100**:1120-1124.
80. Davidson B, Baekelandt M, Shih le M: **MUC4 is upregulated in ovarian carcinoma effusions and differentiates carcinoma cells from mesothelial cells.** *Diagn Cytopathol* 2007, **35**:756-760.
81. Cramer DW, Titus-Ernstoff L, McKolanis JR, Welch WR, Vitonis AF, Berkowitz RS, Finn OJ: **Conditions associated with antibodies against the tumor-associated antigen MUC1 and their relationship to risk for ovarian cancer.** *Cancer Epidemiol Biomarkers Prev* 2005, **14**:1125-1131.
82. Hughes OD, Perkins AC, Frier M, Wastie ML, Denton G, Price MR, Denley H, Bishop MC: **Imaging for staging bladder cancer: a clinical study of intravenous 111 indium-labelled anti-MUC1 mucin monoclonal antibody C595.** *BJU Int* 2001, **87**:39-46.
83. Hughes OD, Bishop MC, Perkins AC, Frier M, Price MR, Denton G, Smith A, Rutherford R, Schubiger PA: **Preclinical evaluation of copper-67 labelled anti-MUC1 mucin antibody C595 for therapeutic use in bladder cancer.** *Eur J Nucl Med* 1997, **24**:439-443.
84. Hughes OD, Bishop MC, Perkins AC, Wastie ML, Denton G, Price MR, Frier M, Denley H, Rutherford R, Schubiger PA: **Targeting superficial bladder cancer by the intravesical administration of copper-67-labeled anti-MUC1 mucin monoclonal antibody C595.** *J Clin Oncol* 2000, **18**:363-370.
85. McQuarrie S, Mercer J, Syme A, Suresh M, Miller G: **Preliminary results of nanopharmaceuticals used in the radioimmunotherapy of ovarian cancer.** *J Pharm Pharm Sci* 2005, **7**:29-34.
86. Cirstoiu-Hapca A, Buchegger F, Bossy L, Kosinski M, Gurny R, Delie F: **Nanomedicines for active targeting: Physico-chemical characterization of paclitaxel-loaded anti-HER2 immunonanoparticles and in vitro functional studies on target cells.** *Eur J Pharm Sci* 2009, **38**(3):230-7.
87. Batra SK, Jain M, Wittel UA, Chauhan SC, Colcher D: **Pharmacokinetics and biodistribution of genetically engineered antibodies.** *Curr Opin Biotechnol* 2002, **13**:603-608.
88. Graham RA, Burchell JM, Taylor-Papadimitriou J: **The polymorphic epithelial mucin: potential as an immunogen for a cancer vaccine.** *Cancer Immunol Immunother* 1996, **42**:71-80.
89. Syrigos KN, Karayiannakis AJ, Zbar A: **Mucins as immunogenic targets in cancer.** *Anticancer Res* 1999, **19**:5239-5244.
90. Brossart P, Heinrich KS, Stuhler G, Behnke L, Reichardt VL, Stevanovic S, Muhm A, Rammensee HG, Kanz L, Brugger W: **Identification of HLA-A2-restricted T-cell epitopes derived from the MUC1 tumor antigen for broadly applicable vaccine therapies.** *Blood* 1999, **93**:4309-4317.
91. Goydos JS, Elder E, Whiteside TL, Finn OJ, Lotze MT: **A phase I trial of a synthetic mucin peptide vaccine. Induction of specific immune reactivity in patients with adenocarcinoma.** *J Surg Res* 1996, **63**:298-304.
92. Reddish MA, MacLean GD, Poppema S, Berg A, Longenecker BM: **Pre-immunotherapy serum CA27.29 (MUC-1) mucin level and CD69+ lymphocytes correlate with effects of Theratope sialyl-Tn-KLH cancer vaccine in active specific immunotherapy.** *Cancer Immunol Immunother* 1996, **42**:303-309.
93. Graham RA, Burchell JM, Beverley P, Taylor-Papadimitriou J: **Intramuscular immunisation with MUC1 cDNA can protect C57 mice challenged with MUC1-expressing syngeneic mouse tumour cells.** *Int J Cancer* 1996, **65**:664-670.
94. Johnen H, Kulbe H, Pecher G: **Long-term tumor growth suppression in mice immunized with naked DNA of the human tumor antigen mucin (MUC1).** *Cancer Immunol Immunother* 2001, **50**:356-360.
95. Lepisto AJ, Moser AJ, Zeh H, Lee K, Bartlett D, McKolanis JR, Geller BA, Schmotzer A, Potter DP, Whiteside T, Finn OJ, Ramanathan RK: **A phase I/II study of a MUC1 peptide pulsed autologous dendritic cell vaccine as adjuvant therapy in patients with resected pancreatic and biliary tumors.** *Cancer Ther* 2008, **6**:955-964.
96. Wierecky J, Mueller M, Brossart P: **Dendritic cell-based cancer immunotherapy targeting MUC-1.** *Cancer Immunol Immunother* 2006, **55**:63-67.
97. Heinzlmann-Schwarz VA, Gardiner-Garden M, Henshall SM, Scurry JP, Scolyer RA, Smith AN, Bali A, Bergh P, Vanden, Baron-Hay S, Scott C, Fink D, Hacker NF, Sutherland RL, O'Brien PM: **A distinct molecular profile associated with mucinous epithelial ovarian cancer.** *Br J Cancer* 2006, **94**:904-913.

Publish with **BioMed Central** and every scientist can read your work free of charge

"BioMed Central will be the most significant development for disseminating the results of biomedical research in our lifetime."

Sir Paul Nurse, Cancer Research UK

Your research papers will be:

- available free of charge to the entire biomedical community
- peer reviewed and published immediately upon acceptance
- cited in PubMed and archived on PubMed Central
- yours — you keep the copyright

Submit your manuscript here:
http://www.biomedcentral.com/info/publishing_adv.asp

